Prifysgol Cymru
Y Drindod Dewi Sant
University of Wales
Trinity Saint David

School of Engineering
MSc Mechanical Engineering

M7X01373 - Project
Dissertation - Final Report

Corrosion Under Insulation of Carbon Steel Pipework in the South Wales Coastal Region

James Milling
1503259
March 2021

Abstract

Corrosion under insulation of carbon steel pipework is a significant problem in thermal process industries. Review of literature has shown that corrosion under insulation is influenced by water ingress into insulation materials. This study analyses the effect of rainwater ingress into fibrous and closed cell elastomer insulation materials used in the insulation of small diameter carbon steel pipework in service applications in the South Wales coastal region. Building on previous studies it considers the effect that cyclic temperature service has on the water retention of insulation materials and the development of corrosion under insulation. An environmental test was conducted over a period of 12 weeks simulating insulated carbon steel pipework in both temperature cyclic and ambient conditions in the presence of rainwater. The analysis completed demonstrated that water retention within thermal insulation and the development of corrosion under insulation in cyclic temperature service was more severe than that in ambient conditions. The results indicated that the test insulation materials subject to temperature cyclic conditions see a reduction in hydrophobic properties, leading to an increase in water retention and development of corrosion under insulation. The integrity of weather barriers associated with insulation systems is considered of prime importance in mitigating against water ingress. Further research should be considered in analysing the degradation of thermal insulation hydrophobic properties in temperature cyclic service.

Acknowledgements

I would like to thank the following that have provided help, support and guidance throughout this study.

Andrew Thorn – University of Wales Trinty Saint David
For his guidance, support, encouragement and feedback as the authors project supervisor

Miles Gardner – Zurich Engineering
For facilitating laboratory resources from Zurich Engineering

Helen Burton
For providing support and encouragement

Declaration Statement

This dissertation has not previously been accepted in substance for any academic award and is not being concurrently submitted in candidature for any such award.

This dissertation is the result of my own independent work/investigation, except where otherwise stated. That explicit references are given, and a full bibliography is appended to the work.

Signed ……. (candidate)

Date March 2021 …….

Contents

Abstract i
Acknowledgements ii
Declaration Statement iii
List of Figures vii
List of Tables ix
1.0 Introduction 1
1.1 Problem Definition 2
1.2 Project Aim 2
1.3 Project Objectives 3
1.4 Research Question and Hypothesis 3
1.4.1 Research Question 3
1.4.2 Hypothesis 3
1.5 Background of problem (Reasons and Relevance of the project) 3
1.5.1 Reasons 3
1.5.2 Relevance 3
1.6 Project Plan 3
2.0 Literature Review 4
2.1 Corrosion Under Insulation 4
2.2 Mechanisms of Corrosion 7
2.2.1 Anodic Reaction 8
2.2.2 Cathodic Reaction 8
2.2.3 Redox Reaction 8
2.2.4 Conversion to Hydrated Ferric Oxide (Rust) 8
2.3 Other Parameters Influencing Corrosion 9
2.3.1 Relative Humidity 9
2.3.2 Time of Wetness 9
2.3.3 Chloride Content of the Electrolyte 9
3.0 Methodology 11
3.1 Experimentation Design 11
3.1.1 Dependant and Independent Variables 11
3.1.2 Confounding Variables 12
3.1.3 Duration and Condition of Experimentation 13
3.1.4 Pipe and Insulation Samples 14
3.2 Experimentation Preparation 15
3.2.1 Pipe Sample Preparation 15

3.2.2 Insulation Material Preparation 15
3.2.3 Experiment Test Environment Apparatus 17
3.2.3.1 Rainwater Catch Tank 17
3.2.3.2 Environmental Tank 17
3.2.3.3 Support Arrangement 17
3.2.3.4 Water Distribution System 18
3.2.5 Control and Monitoring - Cyclic Heating Unit 19
3.2.5.1 PTC Heating Element 19
3.2.5.2 Microcontroller – Temperature Control 20
3.2.5.3 Microcontroller - Datalogger 21
3.2.5.4 Cyclic Heating Pipe Sample Assembly 22
3.2.6 Other Instruments 23
3.3 Experimentation Monitoring 23
3.4 Conclusion of Experimentation Period 24
4.0 Results 25
4.1 Environmental and Rainwater Tanks 25
4.2 Cyclic Temperature Control and Datalogging 27
4.3 Mass of Pipe and Insulation Samples 29
4.3.1 Pipe Samples at Start of Experimentation 29
4.3.2 Insulation Samples at Start of Experimentation 29
4.3.3 Pipe Samples at End of Experimentation 29
4.3.4 Insulation Samples at End of Experimentation 30
4.4 Visual Macro Examination of Samples 30
4.4.1 Sample 1 – Cyclic - Rock Mineral Fibre Insulation 31
4.4.2 Sample 2 – Cyclic - Glass Wool Insulation 34
4.4.3 Sample 3 – Cyclic - Closed-Cell Elastomer Foam Insulation 37
4.4.4 Sample 4 – Ambient - Rock Mineral Fibre Insulation 41
4.4.5 Sample 5 – Ambient - Glass Wool Insulation 44
4.4.6 Sample 6 – Ambient - Closed-Cell Elastomer Foam Insulation 47
4.4.7 Sample 7 – Ambient - Uninsulated reference pipe 51
4.5 Metallographic Examination of Samples by Optical Microscopy 54
4.5.1 Sample 1 – Cyclic - Rock Mineral Fibre Insulation 55
4.5.2 Sample 2 – Cyclic - Glass Wool Insulation 57
4.5.3 Sample 3 – Cyclic - Closed-Cell Elastomer Foam Insulation 59
4.5.4 Sample 4 – Ambient - Rock Mineral Fibre Insulation 61
4.5.5 Sample 5 – Ambient - Glass Wool Insulation 63

4.5.6 Sample 6 – Ambient - Closed-Cell Elastomer Foam Insulation 65
4.5.7 Sample 7 – Ambient - Uninsulated reference pipe 67
4.6 Energy Dispersive X-Ray Spectroscopy 70
5.0 Discussion 72
5.1 Insulation Water Retention 72
5.2 Development of Corrosion 74
6.0 Conclusion 77
7.0 Recommendations and Further Work 78
8.0 References 79
9.0 Appendices 83
9.1 Appendix 1 – Project Plan (Gantt Chart) 84
9.2 Appendix 2 – Steel tube: Tata Steel Install Plus S235GT 85
9.3 Appendix 3 – Rock Mineral Fibre Insulation: Knauf HPS 035 AluR 87
9.4 Appendix 4 – Glass Wool Insulation: Isover CLIMPIPE Section Alu2 89
9.5 Appendix 5 – Closed-Cell Elastomer Foam Insulation: Union foam Eutobatex AT 91
9.6 Appendix 6 – Portable Water Quality Reference Readings 92
9.6.1 Portable Water Reference Tests during Experimentation 92
9.6.2 Published Portable Water Quality Data 93

List of Figures

Figure 1.1 Localised CUI on pipework (BoilerRock, 2017) 2
Figure 2.1 Depiction of aqueous Corrosion of Steel pipe surface 7
Figure 3.1 Pipe sample preparation 15
Figure 3.2 Insulation sample preparation, rock mineral fibre shown 16
Figure 3.3 Sectional view of pipe/insulation sample assembled. 16
Figure 3.4 Samples arranged in environmental tank. 17
Figure 3.5 Diagram of water distribution within environmental tank 18
Figure 3.6 Water distribution system in place within environmental tank. 19
Figure 3.7 PTC Heating element 19
Figure 3.8 PTC element and thermocouple assembly 20
Figure 3.9 Heat cycle controller operating (Units to left of image) 21
Figure 3.10 Datalogger in operation (Lower LCD) 21
Figure 3.11 Pipe sample assembled for cyclic heating. 22
Figure 3.12 Cyclic heating sample diagram 22
Figure 3.13 Weekly datalogger downloads and water quality measurement instruments 23
Figure 4.1 Rainwater Tank vs Environmental Tank tds Readings 26
Figure 4.2 Rainwater Tank vs Environmental Tank Conductivity Readings 27
Figure 4.3 Plot of sample heating cycles over 12-hour period 27
Figure 4.4 Plot of a heating cycles and normalization period at end of experimentation 28
Figure 4.5 Pipe Sample set at end of experimentation period 30
Figure 4.6 Pipe Sample 1 Cyclic – Rock mineral fibre insulation – Coating surface. 31
Figure 4.7 Pipe Sample 1 Cyclic – Rock mineral fibre insulation – Lower 180° 32
Figure 4.8 Pipe Sample 1 Cyclic – Rock mineral fibre insulation – Upper 0° 32
Figure 4.9 Pipe Sample 1 Cyclic - Rock mineral fibre insulation – Preparation surface. 33
Figure 4.10 Insulation Sample 1 Cyclic - Rock mineral fibre insulation – Inner surface. 33
Figure 4.11 Pipe Sample 2 Cyclic – Glass wool insulation – Coating surface. 34
Figure 4.12 Pipe Sample 2 Cyclic – Glass wool insulation - Lower 180° 35
Figure 4.13 Pipe Sample 2 Cyclic – Glass wool insulation - Upper 0° 35
Figure 4.14 Pipe Sample 2 Cyclic – Glass wool insulation - Preparation surface. 36
Figure 4.15 Insulation Sample 2 Cyclic – Glass wool insulation – Inner surface. 36
Figure 4.16 Pipe Sample 3 Cyclic – Closed-cell elastomer foam insulation – Coating surface. 37
Figure 4.17 Pipe Sample 3 Cyclic – Closed-cell elastomer foam insulation - Lower 180° 38
Figure 4.18 Pipe Sample 3 Cyclic – Closed-cell elastomer foam insulation – Upper 0° 38
Figure 4.19 Pipe Sample 3 Cyclic – Closed-cell elastomer foam insulation – Preparation surface. 39
Figure 4.20 Insulation Sample 3 Cyclic – Closed-cell elastomer foam insulation – Outer surface. 39
Figure 4.21 Insulation Sample 3 Cyclic – Closed-cell elastomer foam insulation – Inner surface. 40
Figure 4.22 Pipe Sample 4 Ambient - Rock Mineral Fibre Insulation – Coating surface. 41
Figure 4.23 Pipe Sample 4 Ambient - Rock Mineral Fibre Insulation - Lower 180° 42
Figure 4.24 Pipe Sample 4 Ambient - Rock Mineral Fibre Insulation - Upper 0° 42
Figure 4.25 Pipe Sample 4 Ambient - Rock Mineral Fibre Insulation – Preparation surface. 43
Figure 4.26 Insulation Sample 4 - Rock Mineral Fibre Insulation – Inner surface. 43
Figure 4.27 Pipe Sample 5 Ambient – Glass wool insulation – Coating surface. 44
Figure 4.28 Pipe Sample 5 Ambient – Glass wool insulation - Lower 180° 45
Figure 4.29 Pipe Sample 5 Ambient – Glass wool insulation - Upper 0° 45
Figure 4.30 Pipe Sample 5 Ambient – Glass wool insulation – Preparation surface. 46
Figure 4.31 Insulation Sample 5 Ambient - Glass wool insulation – Inner surface. 46

Figure 4.32 Pipe Sample 6 Ambient - Closed-cell elastomer foam insulation – Coating surface. 47
Figure 4.33 Pipe Sample 6 Ambient - Closed-cell elastomer foam insulation – Lower 180° 48
Figure 4.34 Pipe Sample 6 Ambient - Closed-cell elastomer foam insulation - Upper 0°..... 48
Figure 4.35 Pipe Sample 6 Ambient - Closed-cell elastomer foam insulation – Preparation surface. . 49
Figure 4.36 Insulation Sample 6 Ambient – Closed-cell elastomer foam insulation – Outer surface. . 49
Figure 4.37 Insulation Sample 6 Ambient – Closed-cell elastomer foam insulation – Inner surface. .. 50
Figure 4.38 Pipe Sample 7 Ambient – Uninsulated – Coating surface. 51
Figure 4.39 Pipe Sample 7 Ambient – Uninsulated - Lower 180° 52
Figure 4.40 Pipe Sample 7 Ambient – Uninsulated - Upper 0° 52
Figure 4.41 Pipe Sample 7 Ambient – Uninsulated – Preparation surface. 53
Figure 4.42 Position of metallographic test coupons within pipe sample 54
Figure 4.43 Pipe samples prepared for metallographic optical microscopy examination. 54
Figure 4.44 Pipe Sample 1 Cyclic – Rock mineral fibre insulation – 50x magnification. 55
Figure 4.45 Pipe Sample 1 Cyclic – Rock mineral fibre insulation – 200x magnification. 56
Figure 4.46 Pipe Sample 1 Cyclic – Rock mineral fibre insulation – 500x magnification. 56
Figure 4.47 Pipe Sample 2 Cyclic – Glass wool insulation – 50x magnification. 57
Figure 4.48 Pipe Sample 2 Cyclic – Glass wool insulation – 200x magnification. 58
Figure 4.49 Pipe Sample 2 Cyclic – Glass wool insulation – 500x magnification. 58
Figure 4.50 Pipe Sample 3 Cyclic – Closed-cell elastomer foam insulation – 50x magnification. 59
Figure 4.51 Pipe Sample 3 Cyclic – Closed-cell elastomer foam insulation – 200x magnification. 60
Figure 4.52 Pipe Sample 3 Cyclic – Closed-cell elastomer foam insulation – 500x magnification. 60
Figure 4.53 Pipe Sample 4 Ambient - Rock Mineral Fibre Insulation – 50x magnification. 61
Figure 4.54 Pipe Sample 4 Ambient - Rock Mineral Fibre Insulation – 200x magnification. 62
Figure 4.55 Pipe Sample 4 Ambient - Rock Mineral Fibre Insulation – 500x magnification. 62
Figure 4.56 Pipe Sample 5 Ambient – Glass wool insulation – 50x magnification. 63
Figure 4.57 Pipe Sample 5 Ambient – Glass wool insulation – 200x magnification. 64
Figure 4.58 Pipe Sample 5 Ambient – Glass wool insulation – 500x magnification. 64
Figure 4.59 Pipe Sample 6 Ambient - Closed-cell elastomer foam insulation – 50x magnification. 65
Figure 4.60 Pipe Sample 6 Ambient - Closed-cell elastomer foam insulation – 200x magnification. .. 66
Figure 4.61 Pipe Sample 6 Ambient - Closed-cell elastomer foam insulation – 500x magnification. .. 66
Figure 4.62 Pipe Sample 7 Ambient – Uninsulated – 50x magnification. 67
Figure 4.63 Pipe Sample 7 Ambient – Uninsulated – 200x magnification. 68
Figure 4.64 Pipe Sample 7 Ambient – Uninsulated – 5000x magnification. 68
Figure 4.65 Pipe Sample 7 Ambient – Uninsulated – Inner wall 50x magnification. 69
Figure 4.66 Pipe Sample 7 Ambient – Uninsulated – Inner wall 200x magnification. 69
Figure 4.67 SEM and EDX sample chamber 70
Figure 4.68 Sample preparation for EDX 71

List of Tables

Table 2.1 Coastal and inland comparison of rainwater chloride content and conductivity 10
Table 3.1 Independent and dependant variables 11
Table 3.2 Confounding Variables and Control Measures 13
Table 4.1 Rainwater tank – Water Quality Readings 25
Table 4.2 Environmental Tank – Water Quality and Makeup Readings 26
Table 4.3 Datalogger – 12-week period average readings 28
Table 4.4 Pipe samples measured mass at start of experimentation. 29
Table 4.5 Insulation samples measured mass at start of experimentation. 29
Table 4.6 Pipe samples measured mass at end of experimentation. 29
Table 4.7 Insulation samples measured mass at end of experimentation. 30
Table 9.1 Portable Water Reference Tests 92

1.0 Introduction

Carbon steel pipework is used extensively within manufacturing facilities for the transfer of process fluids between process stages or for the provision of thermal fluids for heating or cooling of the process as necessary. Where a temperature differential exists between the fluid conveyed within the pipe and the ambient environment, energy losses occur, such energy losses increase significantly with an increase in temperature differential and the area of pipe exposed. To improve efficiency insulation is typically fitted to the external surfaces of pipe, which can reduce energy losses by 90% (U.S. Department of Energy , 2012). However, the fitting of insulation frequently presents another problem in form of localised corrosion referred to as Corrosion Under Insulation (CUI).

Corrosion Under Insulation (CUI) occurs as a result of water penetrating insulation material and migrating towards the pipe surface. The water in conjunction with oxygen and other compounds within the insulation material such as water-soluble chloride salts form an electrolyte allowing corrosion to take place, the rate of corrosion being influenced by the temperature of the pipe system and the process is cyclic in nature.

The global costs associated with loss due to corrosion in general are significant and have been subject of many investigations and studies. A study undertaken in 1949 suggested that the annual cost due to corrosion at that time were US$5.5 Billion equivalent to 2.5% of US GPD, which was made of direct losses due to providing protection to metal surfaces and the cost of replacement, and indirect losses such as loss of production (Uhlig, 1949). More recently a report published by the National Association of Corrosion Engineers (NACE) estimates the global cost of corrosion to be US $2.5 trillion, equivalent to 3.4% of global GPD in 2013 (NACE, 2016). A study undertaken in China in 2017 suggested that the cost of corrosion in China was in the region of US $310 Billion, equivalent to 3.3% of China's GDP (Baorong, et al., 2017).

The understanding and assessment of the causes and effects of corrosion is an important part of the role of a pressure system engineer with responsibility for the assessment and examination of in-service pressure systems in varied industrial and manufacturing sector across the UK. CUI that effects low pressure service steam pipework in process installations is of particular interest due to the intermittent and cyclic nature of operation, such service pipework often goes overlooked where planned preventative maintenance schedules focus on the larger process system vessels and pipework during planned maintenance outages. The study focuses on the development of CUI in thermally insulated service pipework in the South Wales coastal region.

1.1 Problem Definition

Corrosion Under Insulation (CUI) occurs on steels when covered by insultation in the presences of water, it exhibits itself as a server form of localised corrosion, which if left uncorrected often results in loss of containment, unscheduled plant shutdown, and ongoing preventative maintenance costs (Winnik, 2008). The severity of corrosion is influenced by environmental and operating conditions, with the introduction of chlorides in coastal areas and cyclic operating temperatures exacerbating the problem. (HSE, 2013). Water and other contaminants such as chlorides primarily enter the insulation material due to a failure in the outer environmental barrier, caused by incorrect installation and maintenance procedures, or inadequacies in design (NACE, 2010).

Figure 1.1 Localised CUI on pipework (BoilerRock, 2017)

1.2 Project Aim

The effect of rainwater ingress on thermal insulation associated with process service pipework in cyclic temperature applications where CUI is present as a degradation mechanism in manufacturing facilities in the South Wales coastal region has not been widely reported.

The intention of this research project is to contribute to the understanding of the effect of rainwater ingress and retention on thermal insulation materials in cyclic temperature applications and the effect on the development of CUI on carbon steel pipework located in manufacturing facilities in the South Wales coastal region. Carbon steel pipework is routinely specified as process service pipework in the diameter range of 12mm – 50mm and is used for the distribution of low-pressure steam and hot water for process heating and cleaning applications.

The research project investigates a range of factors to ascertain if the specification of thermal insulation materials in cyclic temperature applications where rainwater ingress is present has an influence on water retention and the development of CUI.

1.3 Project Objectives

The objectives of this research project are defined as:

1. Evaluate the effect of cyclic temperature change within thermal insulation and water retention where water is introduced into the insulation material.
2. Evaluate the effect of cyclic temperature change and the development of CUI on thermally insulated carbon steel pipework where water is introduced into the insulation material.
3. Draw conclusions and make recommendations based on the findings of the investigation.

1.4 Research Question and Hypothesis

From the project aim and objectives the following research question and hypothesis is developed

1.4.1 Research Question

What effect does cyclic temperature change have on the water retention of thermal insulation material and the development of CUI on thermally insulated carbon steel pipework where water is introduced into the insulation material?

1.4.2 Hypothesis

Cyclic temperature change will increase the water retention of thermal insulation material and development of CUI on thermally insulated carbon steel pipework where water is introduced into the insulation material.

1.5 Background of problem (Reasons and Relevance of the project)

1.5.1 Reasons

The condition of the insulation system and the associated environment barrier are of critical importance in mitigating against the onset of CUI. However, in practice this proves difficult to manage effectively due the very nature of pipe system geometry, associated supports, valves, and other components which form part of a typical service pipe system. The potential for water ingress is high due to poor installation and maintenance practices. The extent of CUI within petrochemical refineries has been estimated to cost as much as 40 to 60% of pipework maintenance, which in turn accounts for 10% of a typical refinery maintenance budget (Fitzgerald & Winnik, 2005).

1.5.2 Relevance

Undetected corrosion can lead to a loss of containment and the uncontrolled release of hazardous fluids, a study undertaken by ExxonMobile found that in 80% of incidents in pipe systems CUI was identified as a contributory factor (Fitzgerald, et al., 2003). Such failures can result in much larger loses where the process fluid is flammable, and the pipe system forms part of a larger refining unit. One such example occurred in 2006, at an established petrochemical refinery on the US Gulf coast. A leaking 100mm diameter process line containing hydrocarbon fluids was identified as the cause of a major fire within the refining complex, destroying half of the unit in which the pipe was located, the cost of replacement was in the region of US$50 million (Anderson, 2010).

1.6 Project Plan

The project is scheduled in accordance with a Gantt chart project plan, a copy of the plan is included within Appendix 1 for reference.

2.0 Literature Review

2.1 Corrosion Under Insulation

Corrosion Under Insulation (CUI) is a serious problem affecting process piping within refineries and other industries conveying process fluids, due to the significance of the problem both the American Petroleum Institute (API) and the National Association of Corrosion Engineers (NACE) outline causes and methods of mitigation, which are detailed within the following respective publications; API 570 Piping Inspection Code: In-service Inspection, Rating, Repair, and Alteration of Piping Systems. API 571 Damage Mechanisms Affecting Fixed Equipment in the Refining Industry, and NACE Corrosion control in the refining industry. Both organisations confirm the temperature range over which CUI is likely to occur in carbon steel as between -12°C and 175°C, and highlight contributing causes as water ingress through the insulation external weather cladding, and cyclic temperature operation. The rate of corrosion being significant where the surface metal temperature is between 100°C and 121°C (API, 2016), (API, 2011), (NACE, 2010).

Whilst the position on general corrosion and degradation mechanism of both API and NACE align with respect to CUI, the position taken by API alters when addressing CUI specifically in API 583 Corrosion Under Insulation and Fireproofing. A lower range of between 77°C and 110°C is stated, API cite the reason being due to the process temperature being stated in many cases, rather the actual metal temperature at the pipe/insulation interface. API point out that a critical factor in CUI is the presence of an aqueous layer on the metal surface covered by insulation, which can occur during a period of operation, either on or offline (API, 2019). The contradiction in positions of recognised authorities in asset integrity management suggest there is wider misconceptions with respect to the conditions under which CUI is likely to occur. A review of published experimental reports cites the simulated temperatures as process temperatures, not actual surface metal/insulation interface temperature.

Failures in pipework can be attributed to failure in a corrosion control system, Cosham, et al. describe a system combining the environment, coating condition and rapid corrosion which ultimately lead to corrosion failure, importantly the failure is not due to corrosion alone, but a failure in the corrosion control system. (Cosham, et al., 2007).

The application of suitable coating systems to process pipework as a barrier between the metal pipe and insulation is considered as an effective means of managing CUI, with Thermal Spray Aluminium (TSA) and organic coatings finding application in both process pipe and vessel protection throughout the petrochemical industries (Bahadori, 2014). A laboratory investigation comparing the corrosion resistance of a unprotected steel pipe section and a section where protected by TSA in a cyclic environment insulated with mineral wool confirms the effectiveness of TSA, the results indicating that the corrosion rate of pipe protected with TSA are reduced to 0.003 mm/year, a significant improvement over the unprotected pipe in the same environment where a corrosion rate of 1.0 mm/year was observed (Kane, et al., 2008). However, whilst there are significant gains in utilising TSA, the preparation, application and protection against damage of the coating system requires careful control to avoid localised corrosion rates of up to 0.03 mm/year.

TSA also has practical limitations with respect to pipe diameter and the effective coating using manual application methods, with some systems limited to diameters above 75mm (Praxair, 2010). Pipe diameters associated with low pressure service steam distribution are typically in the range of 12mm – 50mm and are also subject to installation in restricted areas often routed around main process pipe

and vessel systems. This restricted access can potentially cause set up problems for manual TSA application (Ashrafizadeh, et al., 2016), and the level of surface preparation required before application of TSA (Bock, 2015). In most cases the manufactures applied coating in relied on for corrosion protection.

A case study undertaken on the failure of a refinery carbon steel process line due to CUI operating at 90°C supports the view of failure being attributed to a failure in the corrosion control system. The failure resulting due to aggressive localised corrosion where water had collected at the lowest point due to inadequate installation techniques, the remainder of the pipe system inclusive of coating and insulation system being in good order. The plant was located in a coastal area, on close examination of the corroded pipe evidence of chloride and sodium contamination was evident (Geary, 2013). An estimated corrosion rate of 0.6mm/year was suggested, correlating with figures published by NACE indicating temperatures over 80dec can result in corrosion rates of 0.75mm/y and above (NACE, 2010). The introduction of drainage openings within the outer insulation casing allowing the insulation to drain of water was shown to have a limited influence on CUI, and possible could accelerate the effect (Pojtanabuntoeng, et al., 2015).

Whilst corrosion in open systems decreases with an increase in temperature, the same is not true of corrosion which takes place under insulation, an increase in temperature correlates to an increase in corrosion, behaving in the same way corrosion would be expected within a closed system (Reichert, 1998).

Several published papers describe testing in accordance with the ASTM standard ASTM G189 – Standard Guide for Laboratory Simulation of Corrosion Under Insulation, which describes a laboratory test cell set up to simulate a temperature cyclic environment which cycles between a wet period of 20 hours at 60°C, and a dry period of 4 hours at 150°C, which runs over a period of 72 hours. Where water is introduced as the test fluid into the area between the pipe wall and thermal insulation. However, ASTM cautions against standard laboratory tests not considering actual service conditions, often presenting an inaccurate representation of the development of CUI where actual rates of corrosion are in excess of those developed in laboratory conditions (ASTM, 2013). This position is shared by Begg (2016), who proposed an alternative corrosion test which reflects field conditions with respect to geometry and wet/dry temperature cycles over a period of 60 days (Begg, 2018).

Burhani, et al. (2016) supports the position suggesting that the most influential factors in CUI are cyclic operating conditions with temperatures up to 120°C from ambient, where the most sever corrosion takes place at temperatures between 100°C and 120°C, their study also suggests that water retention within the insulation material is greater in this temperature range as it is less likely to dry completely (Burhani, et al., 2016).

Field tests undertaken in Norway during 2010 and 2015 assessing mineral wool and cellular glass insulation with seawater used as the wetting medium identified that the test samples subject to cyclic changes in temperature exhibited significant CUI compared to the samples which remained at ambient temperatures. Both tests were run over a three-month period with the earlier test focusing on insulated pipe subject to an operational temperature of 105°C and immersion for 30 minutes in seawater (NACE-Jubail, 2015). And the later subjecting insulated pipe to cyclic heating and cooling between ambient and 150°C, and intermittent wetting by sea (Haraldsen, 2010). A further study suggests the rate of corrosion increased with an increase of seawater introduced to the insulation

material (Eltai, et al., 2016). The findings of both studies which utilised seawater as the fluid medium are supported by the results of a simulation where an increase in the rate of CUI in carbon steel was found where the test solution contained an increasing concentration of NaCl (Tang, et al., 2012). The area of CUI in marine environments appears to be well reported with a further investigation setting out an experimental design and proposed predictive model to study CUI in harsh marine environments (Caines, et al., 2015).

An investigation into the failure of a section of 50mm diameter process pipework due to corrosion under insulation in cyclic temperature service operating between ambient and 240°C for a period of 5 hours per month found that the rate of corrosion was significant at 3mm/year. The root cause analysis conducted found that the breakdown in the insulation weather barrier was a significant contributory factor in addition to the cyclic service and cited a failure in the risk-based inspection process as the reason the corrosion remaining undetected, the pipework was replaced with a personal protective mesh as opposed to thermal insulation (Ifezue, et al., 2014). The investigation supports the positions of Burhani, et al, regarding temperature cyclic operation, and Cosham, et al, with respect to a failure in the maintenance system.

A study undertaken of pipework totalling 11km in length within major gas processing plants in Malaysia identified that in 60% of cases where CUI had occurred the pipework was less than 50mm in diameter (Burhani, et al., 2019), the study supports the position that smaller diameter pipework is often overlooked when specifying protective coatings such as TSA due to the difficulties of application to smaller diameter pipework.

Water vapour diffusion was analysed in a study of water permeability in semi-closed and closed cell insulation and the effect on corrosion rates attributed to CUI in a cyclic system in line with laboratory simulation described in ASTM G189. The study found that water permeable material which was able to dry where water could escape had low corrosion rates compared to those of semi-closed and closed cell construction (Rasmussen, 2017). However, the advantage may be lost when considered in actual operating environments as external temperatures below freezing can damage the structure of thermal insulation which contains water (Bahadori, 2014).

Fibre insulation materials such as mineral wool are water repellent, however water can be held within the spaces between the fibres, resulting in water migration towards the pipe surface. This is overcome by using additives within the insulation binder which repel water from between the fibres giving the finished insulation product hydrophobic properties. Oil based additives begin to lose effectiveness above 150°C and silicone based above 250°C (DuBose, 2020). Inorganic resin additives are also used which have effective working temperatures up to 250°C. Whilst manufactures tests support the effectiveness of the additives discussed with respect to water repellent properties (Zwaag & Rasmussen, 2018), caution is clearly required in the specification of insulation material in addition to that of the installation and maintenance requirements with respect to water ingress.

The external influence of marine and near coastal atmospheres and the effect of chloride and dissolved solids is well reported in the earlier literature with respect to CUI. However, chlorides can also be found within mineral derived insulation material along with other dissolvable solids which are able to leach out when the insulation material becomes wet (Ahluwalia, 2006), this in turn increases corrosive attack in areas remote from coastal regions.

2.2 Mechanisms of Corrosion

Corrosion Under Insulation is a severe localised form of atmospheric corrosion which takes place due to an electrochemical reaction that occurs in the presence of water and contaminants forming an electrolyte in an aqueous solution. Water which passes through the weather barrier of a thermal insulation material migrates inwards towards the metallic pipe surface, through the joins and penetrations in material of closed cell construction, and additionally between the fibres of glass and rock wool materials. If the surface temperature of the pipe is such that the water remains in its vapour phase, corrosion is significantly reduced as an electrode potential cannot form on the metallic surface. However, where the surface temperature of the pipe is such that the water condenses allowing water to collect on the pipe surface in its liquid phase an electrode potential can form, which in turn presents the conditions under which electrochemical corrosion will occur (Groysman, 2010).

As the water forms an electrolyte on the metallic pipe surface the electrochemical corrosion that takes place is described as aqueous corrosion. Aqueous corrosion consists of four component parts (Edwards, 2013).

1. An electrolyte which consists of cations and anions.
2. A metallic material through which electrons pass.
3. The anode where corrosion and rust occur.
4. The cathode where oxygen is reduced.

The mechanism of aqueous corrosion which takes place on a steel pipe surface is described in figure 2.1 below.

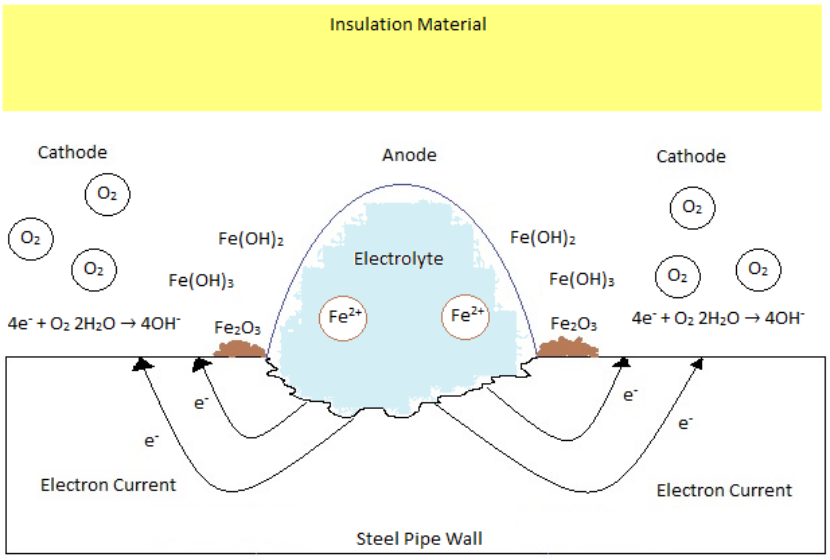

Figure 2.1 Depiction of aqueous Corrosion of Steel pipe surface

The corrosion of the steel pipe surface is described by the following equations.

2.2.1 Anodic Reaction

The corrosion of the pipe wall takes place at the anodic sites where in contact with the electrolyte as described by reaction (2.1).

$$\mathrm{Fe} \rightarrow \mathrm{Fe}^{2+} + 2\mathrm{e} \qquad (2.1)$$

The iron (Fe) within the steel is oxidized producing ferrous ions (Fe^{2+}) which transfer into the electrolyte solution, and electrons which flow through the pipe wall to the cathodic sites which has a greater electrical potential. To maintain an equilibrium, and for further corrosion of the pipe wall to take place, the electrons which are produced as part of the anodic reaction are consumed as part of another reaction which occurs simultaneously at the cathode.

2.2.2 Cathodic Reaction

The simultaneous reaction which occurs at the cathodic sites of the pipe wall are described by reaction (2.2).

$$O_2 + 2H_2O + 4e \rightarrow 4OH^- \qquad (2.2)$$

Oxygen molecules within the space between the insulation and pipe surfaces which is present within the cathodic areas react with the electrons discarded as part of the anodic reaction and water to produce hydroxyl anions (OH^-) during a reduction process.

2.2.3 Redox Reaction

Reactions that take place simultaneously at both the anodic and cathodic areas are known as a redox reaction. Where each reaction is either a reduction where electrons are gained, or oxidation where electrons are lost (Schmitz, 2017). The anodic reaction (2.1) and cathodic reaction (2.2) can be combined to form a balanced equation (2.3), as the electrons are lost as part of the anodic reaction and gained by the cathodic reaction. Corrosion of the pipe wall cannot take place unless both reactions occur.

$$2Fe + O_2 + 2H_2O \rightarrow 2Fe^{2+} + 4OH^- \qquad (2.3)$$

2.2.4 Conversion to Hydrated Ferric Oxide (Rust)

As the anodic and cathodic areas are separated by negligible distances and further abundant Oxygen molecules remain present in the area of the anode, the ferrous ions (Fe^{2+}) precipitate out of the electrolyte solution and form hydrated ferric oxide (Ahmad, 2006) through the series of reactions described below.

The hydroxyl anions (OH^-) produced by the cathodic reaction (2.2) and the ferrous ions (Fe^{2+}) of the anodic reaction (2.1) react to form ferrous (II) hydroxide as described by reaction (2.4).

$$2Fe^{2+} + 4OH^- \rightarrow 2\mathrm{Fe(OH)}_2 \quad (2.4)$$

The ferrous (II) hydroxide from reaction (2.4) reacts with further Oxygen and water molecules present to form ferrous (III) hydroxide as described by reaction (2.5).

$$4\mathrm{Fe(OH)}_2 + O_2 + 2H_2O \rightarrow 4\mathrm{Fe(OH)}_3 \qquad (2.5)$$

Hydrated ferric oxide ($Fe_2O_3.H_2O$) is formed by the reaction between ferrous (III) hydroxide from reaction (2.5) and further Oxygen molecules present and is described by reaction (2.6).

$$4\mathrm{Fe(OH)}_3 + O_2 \rightarrow 2\mathrm{Fe}_2\mathrm{O}_3 \,.\, H_2O + 2H_2O \qquad (2.6)$$

The resulting hydrated ferric oxide ($Fe_2O_3.H_2O$) is commonly referred to as rust with a distinctive reddish-brown colour.

2.3 Other Parameters Influencing Corrosion

Whilst section 2.2 sets out the mechanism of corrosion under insulation due to water ingress other parameters influences the rate at which that corrosion occurs and are considered as follows

2.3.1 Relative Humidity

For aqueous atmospheric corrosion to occur water must be present for an electrolyte to form on a metallic pipe surface. Water is present in air, which can condense on the pipe surface, the amount of water present is described by the relative humidity, the ratio between the actual vapour pressure and saturation pressure of water in air (Ahmad, 2006). The rate of corrosion increasing significantly from 80%, however in marine environments this can be lower at around 35%.

2.3.2 Time of Wetness

The time during which the metallic pipe surface is wet is considered as the main factor which influences both the corrosion mechanism and rate of corrosion (Groysman, 2010), if water cannot collect on the pipe surface an electrochemical cell cannot form without a suitable electrolyte. This is most critical where the relative humidity is greater than 80% at temperatures of 0°C and above. The corrosion rate during dry periods being of one to two orders of magnitudes lower (Landolt, 2007).

2.3.3 Chloride Content of the Electrolyte

Chlorides present within the electrolyte increase the ionic conductivity of the aqueous solution present on the pipe surface, which in turn increases the rate of corrosion (Ahmad, 2006). The increase in chloride content of both rainwater and atmospheric air that is blown in land from the sea represents a significant source of chlorides that influences corrosion under insulation. The location where corrosion is present in proximity to the cost has a significant effect, Ahmad suggests that the additional chloride present can be seen up to 10km inland.

The study focuses on the effect of corrosion under insulation in the South Wales coastal region, no direct data was available from accessible sources with respect to chloride content and conductivity of rainwater in this region within the 10km zone from the shoreline. However, to form a relative comparison for information in support of the literature review table 2.1 describes data retrieved during 2020 from the Department for Environment Food and Rural Affairs UKEAP: Precip-Net monitoring network, which monitors the composition of rainwater from 38 sites across the UK (Department for Environment Food & Rural Affairs, 2020). The comparison being drawn between the coastal monitoring station at Goonhilly, located on the southern coast of Cornwall, which is located geographically in a similar position to Swansea on the South Wales coast, both being exposed to the prevailing winds from the north Atlantic, generally from the South West to South South West (Department of Enery and Climate Change, 2009) and within 10km of the shore. And the nearest Precip-Net monitoring station inland to Swansea located at Crai in the upper Swansea valley.

Precip-Net Station	Location	Closest point to coast (km)	Bearing	Average Conductivity	Average Chloride
Yes	Goonhilly	4.9 km	159°	45.7µS/cm	13.4mg/l
No	Test site (Swansea)	2.4 km	169°	----------	----------
Yes	Crai Reservoir 2	34 km	208°	20.4 µS/cm	4.5mg/l

Table 2.1 Coastal and inland comparison of rainwater chloride content and conductivity

An increase in chloride concentration within the aqueous solution is shown to increase the formation of pitting during corrosion (Ahmad, 2006), also chloride salts which are left present on metal surface during the dry phase reduce the saturation pressure of air containing moisture, which in turn reduces the relative humidity at which corrosion occurs (Landolt, 2007).

3.0 Methodology

3.1 Experimentation Design

The social and travel restrictions in place due to the current Covid-19 pandemic have significantly impacted on the design of the experimentation. It has not been possible to utilise the university laboratory facilities to run a laboratory experiment. The instrumentation which has been sourced independently to measure variables during the experimentation period is not of laboratory standard or calibrated to a known traceable nation standard, to provide a level of credibility to readings obtained the instruments have been refenced against known conditions where possible.

Therefore, due to the constrains a cross sectional quasi-experimental approach is applied to the study with the intention of undertaking an explanatory analysis, it is acknowledged that the sample size is limited.

3.1.1 Dependant and Independent Variables

As the research investigates the cause-and-effect relationship between rainwater and the development of CUI, and the water retention of insulation materials, in temperature dependant conditions the dependant and independent variables are identified and considered to ensure appropriate controls are in place, detailed in Table 3.1.

Question	Independent Variable	Dependent Variable
Effect of cyclic temperature change and the development of CUI on thermally insulated carbon steel pipework where water is introduced into the insulation material.	Cyclic temperature change between ambient conditions and 140°C	Development of CUI
Effect of cyclic temperature change within thermal insulation and water retention where water is introduced into the insulation material.	Cyclic temperature change between ambient conditions and 140°C	Volume of water retention within insulation material

Table 3.1 Independent and dependant variables

3.1.2 Confounding Variables

The confounding variables which are identified and potentially influence the research cause-and-effect relationship, and the respective control measures put in place to support validity in the findings of the analysis are set out in Table 3.2.

Question	Confounding Variable	Control Measure
Effect of cyclic temperature change and the development of CUI, and water retention of insulation material, on thermally insulated carbon steel pipework where water is introduced into the insulation material.	Variation in volume of water which enters the insulation material. An increase or decrease in the volume of water entering the insulation material influences the development of CUI.	Control experimentally: Volume of water is monitored and introduced at a controlled rate, 3 drops/minute. Water enters the insulation via a 6mm diameter hole made in each of the samples at the longitudinal central point of the top dead center position. Monitored daily by manually observation and adjustment of flow control, as necessary.
	Variation in volume of water which drains naturally from the insulation material. An increase or decrease in the volume of water draining naturally from the insulation material influences the development of CUI.	Control experimentally: The insulation samples are prepared so that the cut ends have no environmental barrier in place, allowing water to drain naturally. Monitored daily by manually observation.
	Variation in upper temperature limit. Temperature in excess of 140°C would not be expected in process service pipework in cyclic temperature applications. Excess temperature will result in unexpected drying of insulation material. An increase or decrease in the volume of water entering the insulation material influences the development of CUI.	Control experimentally: Heating module controlled by PID controller. Controller set point and process variable monitored daily. Process variable temperature verified weekly against temperature measurements record by datalogger.

	Variation in heating cycle time. The experiment simulates process service pipework in cyclic temperature applications where the heating service is applied for two periods of 3 hours, equally separated in a 24-hour period. Heating periods in excess of those defined will result in unexpected drying of insulation material. An increase or decrease in the volume of water within the insulation material influences the development of CUI.	Control experimentally: Heating cycle time controlled by microcontroller. Heating cycle time observed daily. The heating cycle period verified weekly against temperature measurements record by datalogger.

Table 3.2 Confounding Variables and Control Measures

3.1.3 Duration and Condition of Experimentation

The duration of the experimentation, 12 weeks, aligns with studies discussed within the reviewed literature suggesting that laboratory tests do not simulate service conditions and expected development of CUI in such applications.

The 12-week experimentation simulates insulated carbon steel pipe exposed to ingress of rainwater both in ambient and temperature cyclic conditions.

The temperature and duration of the heat cycle, temperature cyclic condition, is based on a typical batch process application where a service, steam at 140°C (Saturated steam at 2.6 barg), is required on a cyclic basis, 3 hours, for heating and cleaning purposes.

A test environment is set up consisting of an environmental tank where test samples of insulted pipe subject to ambient and cyclic conditions are exposed to a controlled volume of applied rainwater. The coastal city of Swansea receives an average rainfall of 1321mm/year, the average ambient air temperature being 10.1°C (Climate-Data.org, 2020), the experimentation reflecting the average rainfall. The environmental tank also ensures that each sample is exposed to the same external conditions.

Both qualitative and quantitative methods are proposed in testing the hypothesis and observations and data is recorded accordingly.

3.1.4 Pipe and Insulation Samples

The pipe and insulation material selected align with that commonly specified for service applications in process industries and are set out as defined below, the datasheets are contained within the respective appendices for information as listed. No external weather cladding or protection is specified as part of the experimentation, which would normally be fitted over the insulation material facing the external environment, as external weather cladding or protection is not considered as part of the study.

Samples

- Carbon Steel pipe: Tata Install Plus S235GT hot finished tube 48.3mm OD (Appendix 2)
- Rock Mineral Fibre Insulation: Knauf HPS 035 AluR (Appendix 3)
- Glass Wool Insulation: Isover CLIMPIPE Section Alu2 (Appendix 4)
- Closed-Cell Elastomer Foam Insulation: Union foam Eutobatex AT (Appendix 5)

The test samples are set up within the environmental tank with the cyclic samples positioned above the ambient samples so as to mitigate against the effect of heat lost from the cyclic samples being gained by the ambient samples.

Top row of samples

- Sample 1 – Cyclic - Rock Mineral Fibre Insulation
- Sample 2 – Cyclic - Glass Wool Insulation
- Sample 3 – Cyclic - Closed-Cell Elastomer Foam Insulation

Bottom row of samples

- Sample 4 – Ambient - Rock Mineral Fibre Insulation
- Sample 5 – Ambient - Glass Wool Insulation
- Sample 6 – Ambient - Closed-Cell Elastomer Foam Insulation
- Sample 7 – Ambient – Uninsulated reference pipe

3.2 Experimentation Preparation

3.2.1 Pipe Sample Preparation

The carbon steel pipe samples are sourced from the same supplied length of stock material to ensure the consistency of the material grade, the stock material being supplied with an external standard protective coating of *Tata Steel red paint.*

Each of the pipe samples are cut to a length of 60mm, half of the external protective coating as supplied is removed (180-0°) to expose the bare parent pipe material using a 120-grit abrasive flap sanding disc, ASTM G4 suggests that 120-grit abrasive will produce an acceptable finish (ASTM, 1995). The top position (0°) is marked on each end of the cut sample in addition to a sample reference using a paint marker pen.

The samples are placed in an oven at 120°C for 1 hour before the mass is recorded.

Figure 3.1 Pipe sample preparation

3.2.2 Insulation Material Preparation

The insulation material samples are sourced from the same supplied length of stock insulation to ensure consistency, the diameter of the insulation corresponds with manufactures specification for 48.3mm OD tube.

Each of the insulation material samples are cut to a length of 150mm. A 6mm diameter hole is formed centrally through the insulation material at the top position (0°), where the bottom position (180°) is taken as the formed longitudinal split which facilitates fitting.

The samples are placed in an oven at 120°C for 1 hour before the mass is recorded.

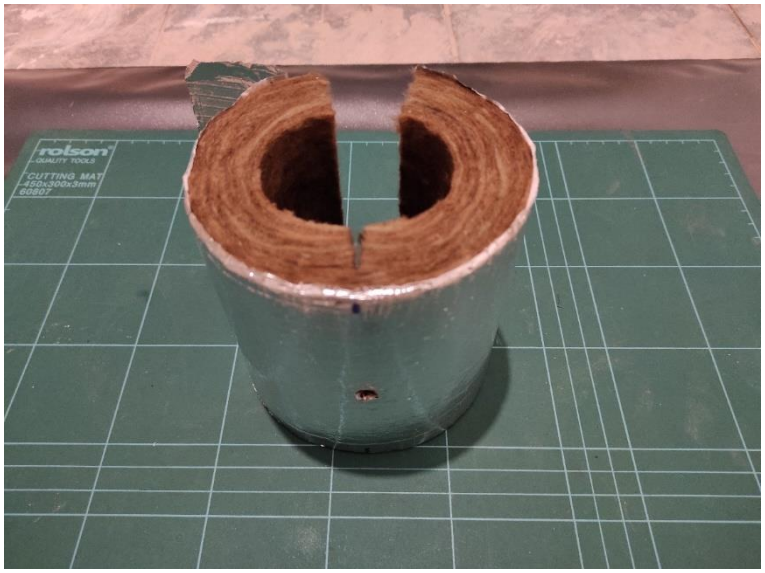

Figure 3.2 Insulation sample preparation, rock mineral fibre shown.

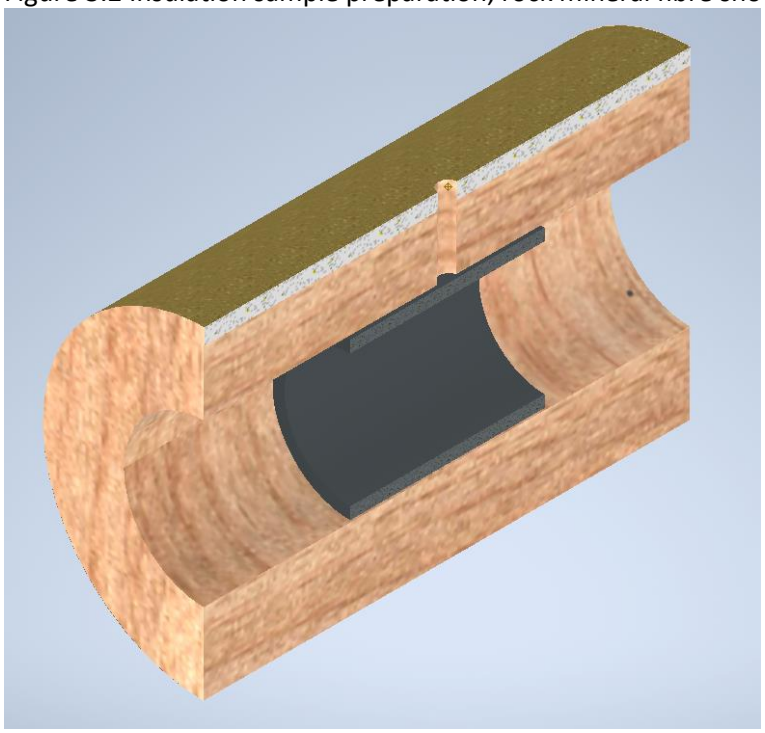
Figure 3.3 Sectional view of pipe/insulation sample assembled.

3.2.3 Experiment Test Environment Apparatus

The experiment is undertaken at a location 2.5km from the coastline in a northerly direction from the coastal city of Swansea. The experimental environment consists of the following apparatus.

3.2.3.1 Rainwater Catch Tank

The rainwater catch tank is located externally; rainwater is collected directly into the tank through a perforated cover. The capacity of the catch tank is 40 litres and is manufactured from polypropylene.

3.2.3.2 Environmental Tank

The environmental tank is located within an uninsulated and unheated external outbuilding which has open ventilation allowing the free circulation of external air at ambient temperature and humidity. The capacity of the catch tank is 80 litres and is manufactured from polypropylene.

3.2.3.3 Support Arrangement

The samples are support above the environmental tank water level by stainless steel wire. The samples being arranged in two rows, the top row is heated cyclically, the bottom row is unheated and remain at ambient conditions. The pipe sample and insulation are retained in position using a plastic retaining clip. Figure 3.4 shows samples placed in environmental tank prior to filling with water. The orientation of the uninsulated sample is just visible in the lower left of the image.

Figure 3.4 Samples arranged in environmental tank.

3.2.3.4 Water Distribution System

The rainwater collected within the rainwater catch tank is transferred into the environmental tank to establish a working volume of 20 litres at the start of the experimentation.

A small centrifugal fish tank pump (300litres/hour) is submersed below the water level of the environmental tank and distributes water through 4mm diameter PVC tubing to each of the suspended samples. The flow of water is controlled by a nylon needle valve so that each sample receives water at the rate of 2 drops/minute, a plastic funnel being partially inserted into the hole formed in the insulation material allows the drop rate to be monitored daily. The volume of each water droplet was estimated as ≈ 0.06ml. To establish an estimation of the water volume droplet an average was taken over 3 sperate mass measurements where 30 drops were collected into a beaker from the outlet of a needle valve. Over a 24-hour period each sample receives ≈ 173 ml of water which is able to drain out of the bottom of the insulation material where the split is present at the 180° position and is recirculated within the environmental tank. The water distribution system is described in figures 3.5 and 3.6.

The recirculation of rainwater contained within the environmental tank aligns with studies discussed within the literature review, the working volume is manually observed on a weekly basis and maintained at 20 litres by transferring rainwater from the rainwater catch tank to allow for water loss due to evaporation.

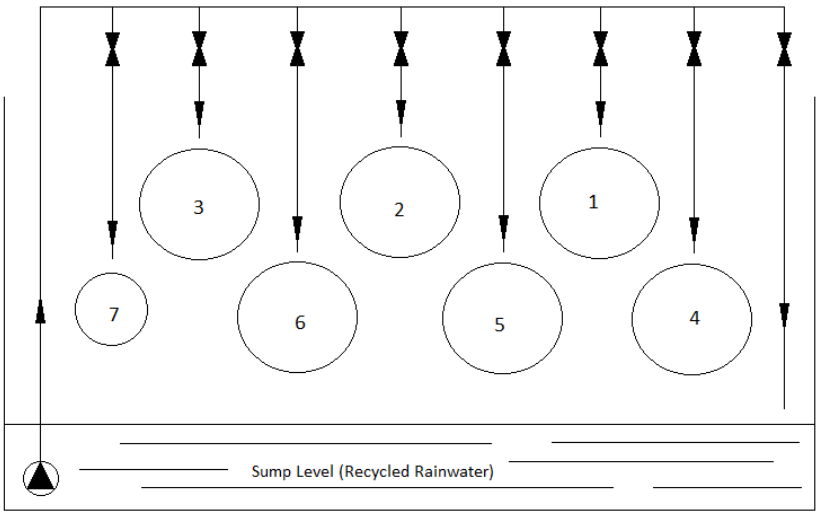

Figure 3.5 Diagram of water distribution within environmental tank

The volume of rainwater which each sample is exposed to over the period of experimentation is 14.5 litres, this being greater than would be expected to fall on the surface area of the insulation sample over a period of an average year under normal rainfall conditions at 13.2 litres over an area of 100mm^2.

Figure 3.6 Water distribution system in place within environmental tank.

3.2.5 Control and Monitoring - Cyclic Heating Unit

The top row of pipe samples within the environmental tank are subject to a periodic heating cycle which mimics a typical service application in a process environment. The duration of each heat cycle is 3 hours, on completion of the heat cycle the pipe sample cools naturally to ambient conditions.

The cyclic heating unit consist of the following components, which operate at 12 volts and below. The Arduino microcontroller was specified as it allows the development of bespoke code scripts which meet the requirements of sample heating control and data logging within the experiment (Arduino, 2020).

3.2.5.1 PTC Heating Element

The internal volume of pipe sample contains air as the heat transfer fluid and is heated by a 12-volt 22w PTC (Positive Temperature Coefficient) heating element rated at 220°C. A PTC heating element is specific as it is considered safer than other electrical heating methods due to the self-regulating nature of PTC. The maximum temperature cannot be exceeded as the resistance of the heating element increases with temperature to the point where it acts as an insulator (DBK, 2020).

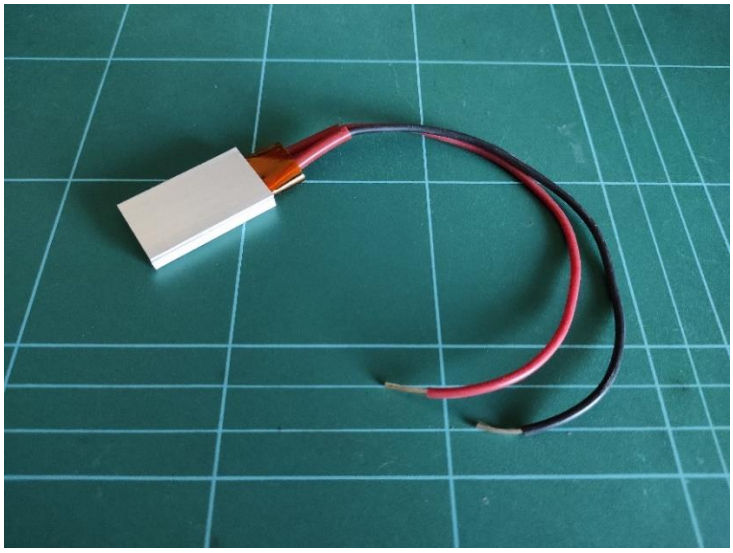

Figure 3.7 PTC Heating element

3.2.5.2 Microcontroller – Temperature Control

An Arduino Uno microcontroller is used to control the duration of the heating period of each pipe sample subject to cyclic heating within a 24-hour period and the setpoint temperature at 140°C. A real time clock (DS3231) provides the reference for each of the heating cycles within a 24-hour period and are defined as follows with each of the pipe samples being subject to two heating periods of three hours.

- Channel A – 0900-1200hrs (Sample 1 - Rock Mineral Fibre Insulation)
- Channel B – 1300-1600hrs (Sample 2 - Glass Wool Insulation)
- Channel C – 1700-2000hrs (Sample 3 - Closed-Cell Elastomer Foam Insulation)
- Channel A – 2100-0000hrs (Sample 1 - Rock Mineral Fibre Insulation)
- Channel B – 0100-0400hrs (Sample 2 - Glass Wool Insulation)
- Channel C – 0500-0800hrs (Sample 3 - Closed-Cell Elastomer Foam Insulation)

A simple PID (Proportional, Integral and Derivative) control script runs during each of the periods defined above, the setpoint temperature of the internal fluid of the pipe and PTC heating element is monitored by a thermocouple and provides feedback to the PID control loop via a thermocouple amplifier (MAX6675). The PTC heating element is controlled by a relay unit which receives its control signal from the microcontroller.

The assembled PTC heating element and thermocouple are detailed in figure 3.8, where both parts are fixed to the stainless-steel support rod. The heating unit in operation is detailed in figure 3.9, the LCD screen to the right shows Channel A on a heat cycle. The units to the lower left are the thermocouple amplifiers, lower right relay unit.

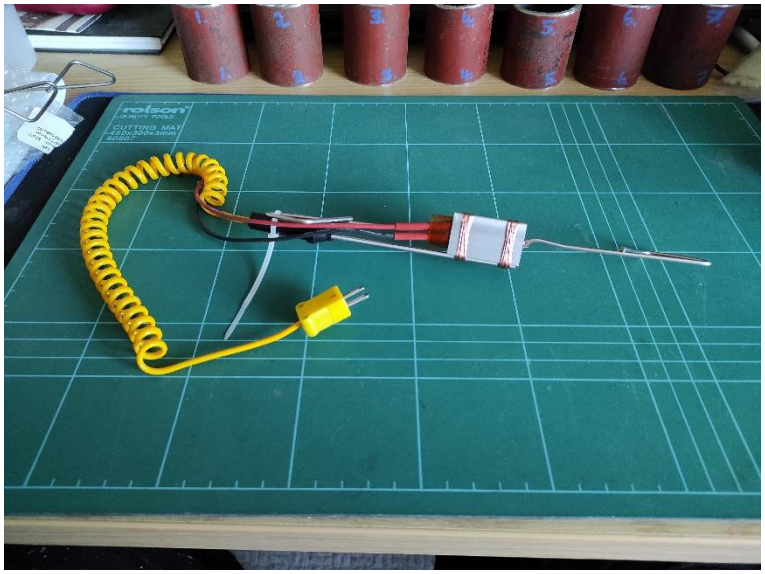

Figure 3.8 PTC element and thermocouple assembly

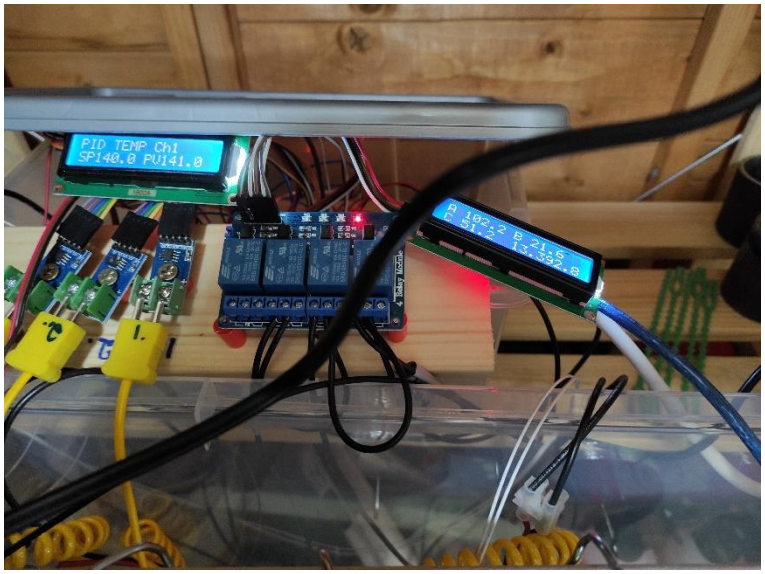

Figure 3.9 Heat cycle controller operating (Units to left of image)

3.2.5.3 Microcontroller - Datalogger

An Arduino Nano microcontroller is used to control the datalogger with an output to an LCD display and SD card. The environmental tank ambient air temperature and relative humidity is established using a combined temperature and humidity sensor (DHT22). The external surface temperature of the pipe sample insulation interface is established using a NTC 100k thermistor, the thermistor is foil wrapped to provide protection from the corrosive environment present at the interface between the pipe surface and insulation. The values record for the ambient air temperature and humidity and the respective cyclically heated pipe samples is written to the SD card at one-minute intervals.

The datalogger is independent of the microcontroller used for the cyclic heating unit.

Figure 3.10 details the LCD output of the datalogger (Lower LCD), the white wires to the left are the leads associated with the thermistors, the white unit in the lower left is the ambient temperature and humidity sensor.

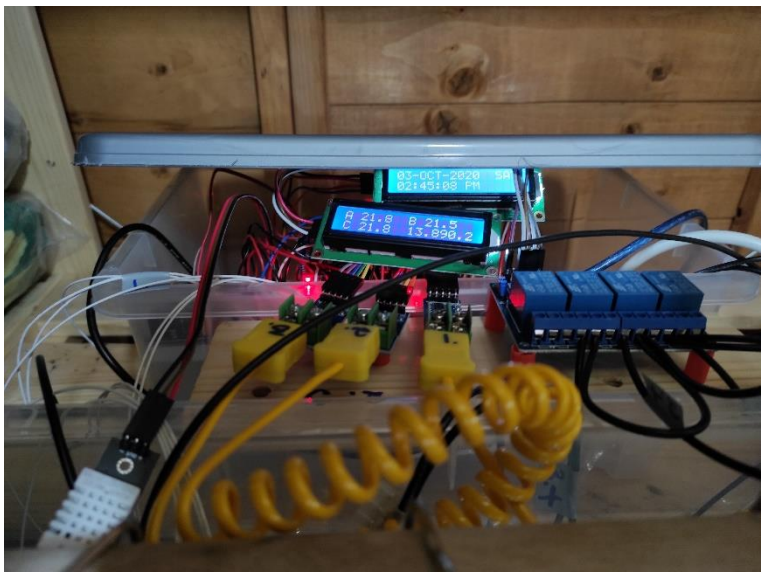

Figure 3.10 Datalogger in operation (Lower LCD)

3.2.5.4 Cyclic Heating Pipe Sample Assembly

The assembled cyclic heating sample with PID feedback thermocouple, datalogger thermistor and PTC element leads visible are detailed in figure 3.11 below. The void space between the pipe sample and each end of insulation sample and respective clip supports is filled with thermal insulation to improve thermal efficiency during the period of experimentation.

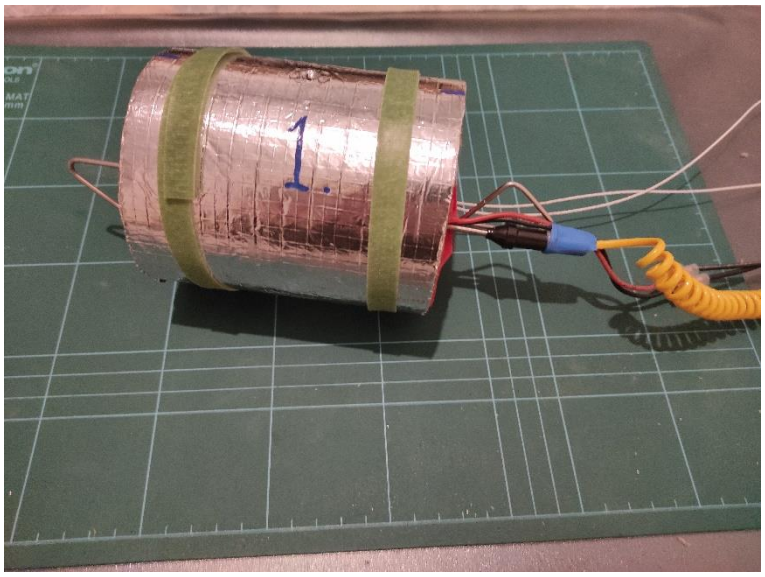

Figure 3.11 Pipe sample assembled for cyclic heating.

The sectional diagram in figure 3.12 details the position of the respective parts that make up the cyclic heating pipe samples. The respective items being: 1. Support rod, 2. PID feedback thermocouple, 3. Datalogger thermistor, 4. PTC heating element, 5. Pipe sample, 6. Insulation sample. The datalogger thermistor is located at the midpoint 90° position on the coating pipe surface to insulation interface.

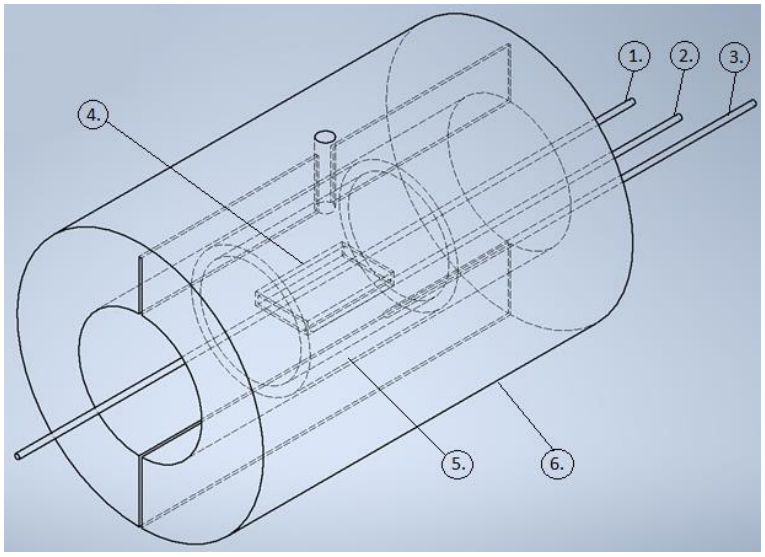

Figure 3.12 Cyclic heating sample diagram.

3.2.6 Other Instruments

The following instruments are used to record observations undertaken during the duration of experimentation.

- Portable pH, conductivity, temperature and dissolved solids meters. Utilised for monitoring the water quality within the environmental and rainwater catch tanks on a weekly basis.
- Electronic scales – resolution 0.1g. Utilised for establishing the mass of pipe and insulation samples at the start and end of experimentation.

3.3 Experimentation Monitoring

During the 12-week period over which the corrosion experiment is conducted (5th October – 28th December) the following observation are made and recorded.

- Daily – Water drop rate from flow control valves (2 drops/minute)
- Weekly – Data download from datalogger SD card (Environment Tank)
    - Ambient air temperature
    - Ambient air relative humidity
    - Channel A – Pipe/insulation interface temperature (Sample 1)
    - Channel B – Pipe/insulation interface temperature (Sample 2)
    - Channel C – Pipe/insulation interface temperature (Sample 3)
- Weekly – Environmental and rainwater catch tanks
    - pH
    - Total dissolved solids
    - Conductivity
    - Temperature
    - Volume of rainwater made up in environmental tank
- Start/Finish
    - Mass – Pipe sample
    - Mass – Insulation sample

The weekly datalogger download and portable instruments used for water quality reading is described in figure 3.13.

Figure 3.13 Weekly datalogger downloads and water quality measurement instruments

3.4 Conclusion of Experimentation Period

At the end of the 12-week duration on the 28th of December the cyclic heating controller is switched off and the water circulation pump left running for a further 24-hour period to allow all samples to normalise to ambient conditions and allow for the uptake of any water into the insulation material which may have been displaced from the insulation samples subject to cyclic heating.

On conclusion of the 24-hour period under ambient conditions all sample assemblies are removed from the environmental tank and disassembled into component parts of insulation and pipe for macro analysis as described in section 4.3.

The metallographic analysis and associated preparation of samples described in section 4.5 is undertaken at the Zurich Engineering laboratory in Wolverhampton. Zurich Engineering made the facilities available to the author to undertake both visual microscopic examination and energy dispersive x-ray spectroscopy as part of the study.

4.0 Results

The following results section sets out the data recorded, and observations made over the duration of the 12-week experimentation, and of the individual samples at the start and end of the period.

4.1 Environmental and Rainwater Tanks

Tables 4.1 and 4.2 describe the respective weekly monitoring readings taken for water quality within the environmental and rainwater tanks. As the measuring instruments used were supplied un-calibrated a reference test was made at the time of the weekly measurement against a portable water supply and the readings compared to that published by the local water supply company in Swansea (Welsh Water, 2020), the reference test results, and published data are provided in Appendix 2 within tables 9.1 and 9.2 for information.

Date	pH	Temperature (°C)	tds (mg/l)	Conductivity (µS/cm)
04/10/2020	7	12.4	14	14
11/10/2020	7	10.8	15	16
18/10/2020	7	6.2	13	12
25/10/2020	7	6.5	15	14
01/11/2020	7	10.8	17	34
08/11/2020	7	10.1	17	34
15/11/2020	7	9	18	36
22/11/2020	7	5.8	16	32
29/11/2020	7	4.2	15	30
06/12/2020	7	2.2	14	24
13/12/2020	7	4.4	12	24
20/12/2020	7	4.4	10	20
27/12/2020	7	2	11	22
Average	7	6.83	14.38	24
Median	7	6.2	15	24

Table 4.1 Rainwater tank – Water Quality Readings

The rainwater quality readings observed during the period of experimentation remained within expected values and consistent with published data reviewed.

Date	pH	Temperature (°C)	tds (mg/l)	Conductivity (µS/cm)	Makeup water (l)
04/10/2020	7	12.8	14	14	0
11/10/2020	7	11.4	15	22	2
18/10/2020	7	6.2	15	26	1
25/10/2020	7	8.4	15	30	1
01/11/2020	7	11.8	36	72	2
08/11/2020	7	10.6	42	84	1
15/11/2020	7	10	49	98	2
22/11/2020	7	7.8	51	102	1
29/11/2020	7	6	54	110	1
06/12/2020	7	3.4	51	102	1
13/12/2020	7	4.4	54	108	2
20/12/2020	7	5.8	58	116	1
27/12/2020	7	5	64	126	1
Average	7	7.97	39.85	77.69	Total
Median	7	7.8	49	98	16

Table 4.2 Environmental Tank – Water Quality and Makeup Readings

The reading taken for the total dissolved solids and conductivity within the environmental tank are seen to increase throughout the duration of the experimentation in relation to the rainwater tank and are described in a graphical format in figures 4.1 and 4.2. No change was noted in pH in any of the readings taken across both tanks within the accuracy of the instrument used.

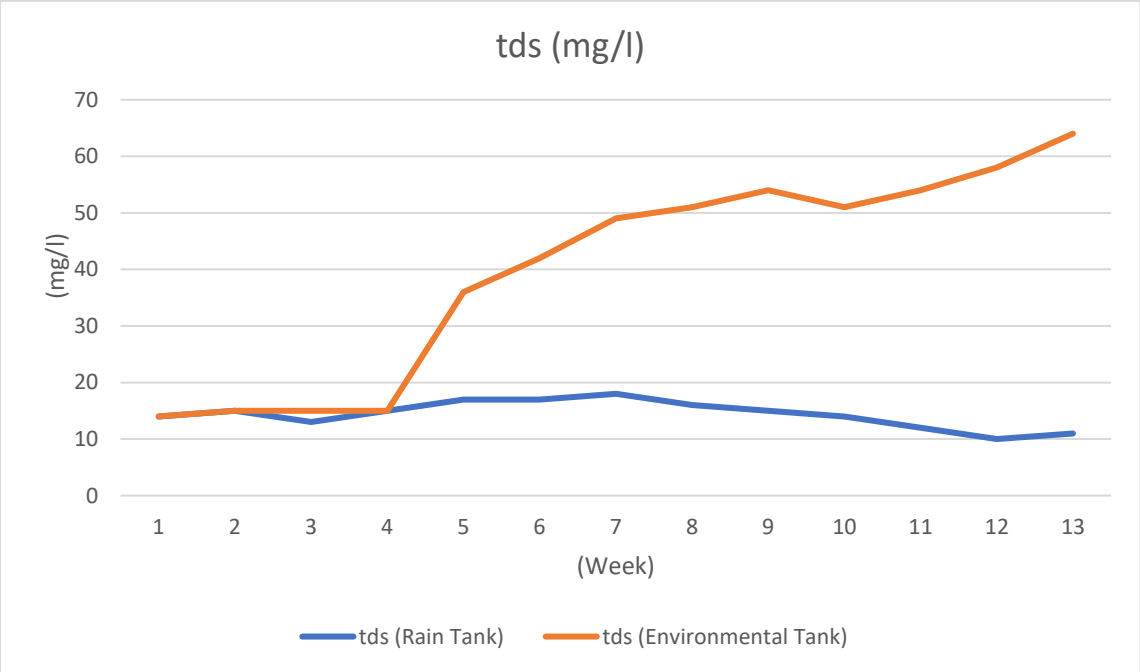

Figure 4.1 Rainwater Tank vs Environmental Tank tds Readings

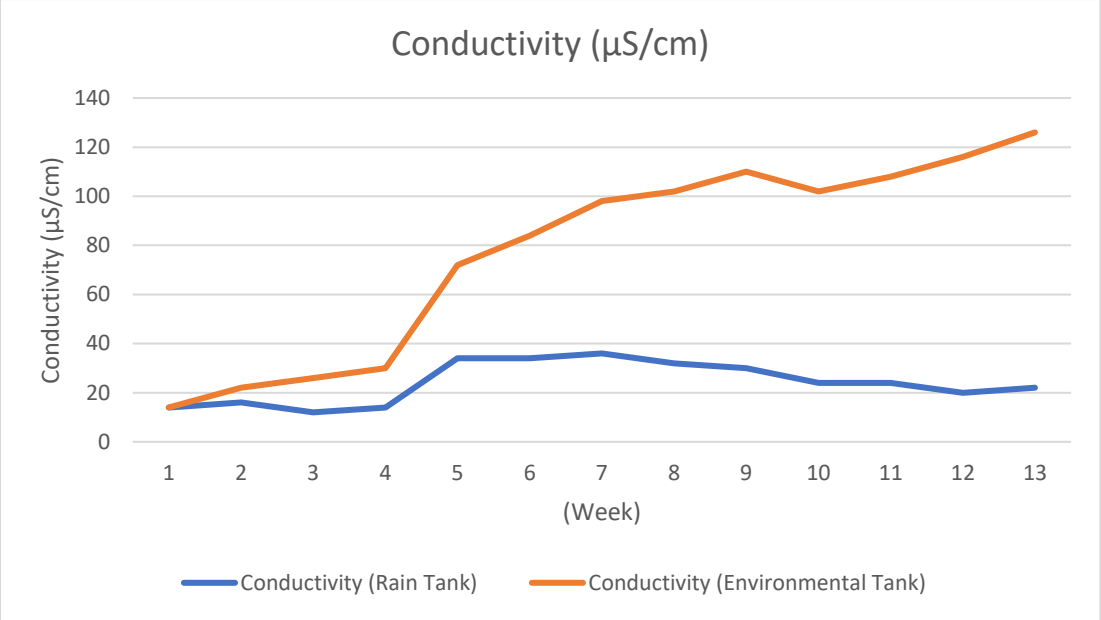

Figure 4.2 Rainwater Tank vs Environmental Tank Conductivity Readings

4.2 Cyclic Temperature Control and Datalogging

The datalogger output was reviewed weekly over the 12-week experimentation period to ensure that the duration and temperature of the heating cycle for the cyclic temperature test samples remained within the desired range, the set point of the temperature controller being 140°C, the measured values from the datalogger recorded the interface temperature between the pipe surface and insulation material and can be seen to trend at temperatures below the controller set point across the three cyclic channels, A, B and C in figure 4.3 which is a random sample of a 12-hour period over which the heating cycle occurs.

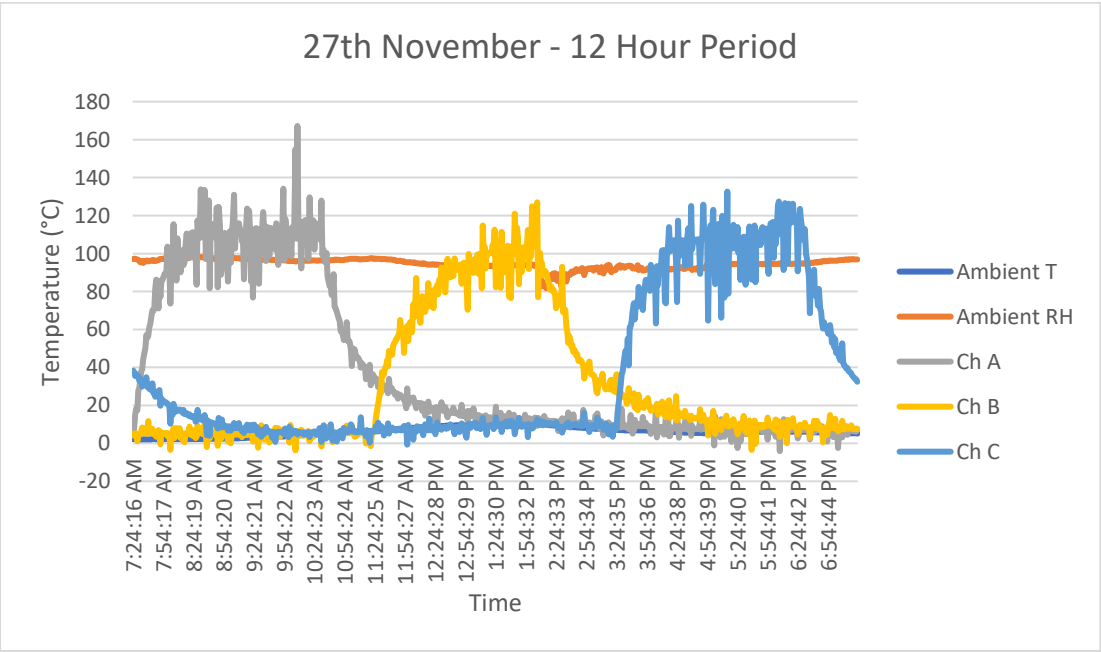

Figure 4.3 Plot of sample heating cycles over 12-hour period

The range of variation within the recorded values of temperature was anticipated due to the simplistic nature of the both the electronic components and temperature monitoring script written for the Arduino microcontroller allowing for available memory to process readings taken across 3 channels, however it clearly demonstrates the duration and profile of the temperature cycle for each of the samples subject to cyclic heating and cooling. The normalisation period at the end of the 12-week cyclic experimentation period is described in figure 4.4.

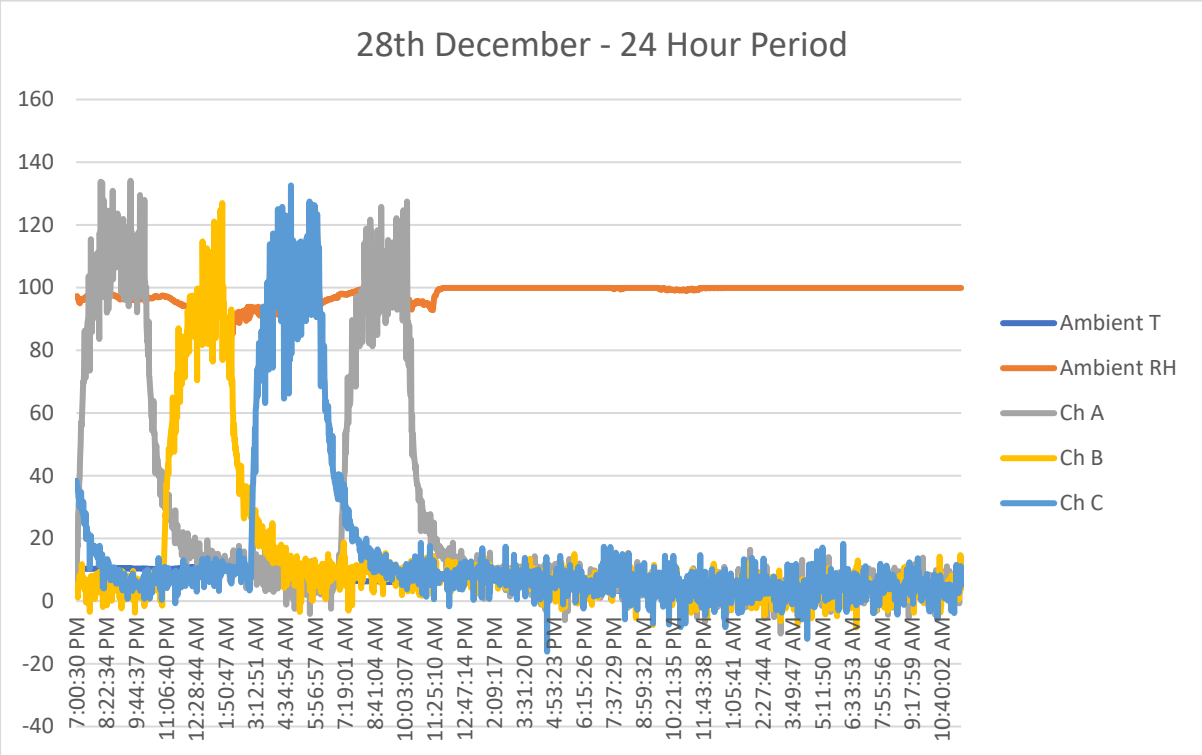

Figure 4.4 Plot of a heating cycles and normalization period at end of experimentation

The full dataset from the datalogger download was analysed in excel and the average readings taken over the 12-week experimentation period are set out below in table 4.3. The average figures for both ambient temperature and relative humidity consider the full recoded data range for the respective channels. The average figures for each of the cyclic channel's A, B and C considers the recorded data during the soak period of the heating cycle. The ambient and ramp temperature figures are omitted from the average calculation.

Datalogger - 12 Week Period Average				
Ambient Temperature (°C)	Relative Humidity (%)	Channel A (°C)	Channel B (°C)	Channel C (°C)
9.6	95.9	112.3	105.8	118.7

Table 4.3 Datalogger – 12-week period average readings

None of the measured cyclic channels recorded an interface temperature which aligned with the heating controller set point for any significant period over the period of experimentation. Both the fibre-based samples interface temperatures, Sample 1 – Rock fibre (Channel A), and Sample 2 – Glass fibre (Channel B), consistently registering lower interface temperatures than Sample 3 – Closed cell elastomer (Channel C) over the period of experimentation.

4.3 Mass of Pipe and Insulation Samples

The scales used to measure the mass of the samples was supplied un-calibrated, a test mass of known value was used as a test reference. The samples are placed in an oven 120°C for 1 hour and 130°C for 4 hours respectively at the start and end of the experimentation period where dry measurements are recorded. Differences in measured starting mass for same material type is due to samples being rough sawn from stock material to the specified length.

4.3.1 Pipe Samples at Start of Experimentation

Pipe Measured Mass (g) - Start of Experimentation						
Sample 1	Sample 2	Sample 3	Sample 4	Sample 5	Sample 6	Sample 7
238.8	246.1	249.1	247.5	234	246.3	253

Table 4.4 Pipe samples measured mass at start of experimentation.

4.3.2 Insulation Samples at Start of Experimentation

Insulation Measured Mass (g) - Start of Experimentation						
Sample 1	Sample 2	Sample 3	Sample 4	Sample 5	Sample 6	Sample 7
86.2	100.5	43.8	102.1	78.7	39.8	***

Table 4.5 Insulation samples measured mass at start of experimentation.

4.3.3 Pipe Samples at End of Experimentation

The figures presented in table 4.6 are in relation to the starting mass from table 4.4. The figure for gain between dry and wet conditions is where the sample mass is measured in the as removed condition from the environmental tank before being drying. The pipe sample mass after drying was recoded before and after the removal of loose material by vacuuming and light brushing.

	Pipe Measured Mass (g) - End of Experimentation						
	Sample 1	Sample 2	Sample 3	Sample 4	Sample 5	Sample 6	Sample 7
Mass (Start) table 4.4	238.8	246.1	249.1	247.5	234	246.3	253
Mass (Wet)	242.4	252.4	252.2	250.5	236.5	247	253
Mass (Dry)	240.2	248.7	251.4	248.3	234.8	246.4	253
Mass (Dry – vacuumed)	239.2	246.9	250	246.8	233.7	246.1	253
Gain (Dry - Wet)	3.6	6.3	3.1	3	2.5	0.7	0
Gain (Dry)	1.4	2.6	2.3	0.8	0.8	0.1	0
Gain (Dry - Vacuumed)	0.4	0.8	0.9	-0.7	-0.3	-0.2	0

Table 4.6 Pipe samples measured mass at end of experimentation.

The samples have seen an increase in mass in all cases except for sample 7 (taking the accuracy of the scale used into account), this is expected as the oxide (rust) produced during the corrosion process gains mass, due to the reaction of iron with both oxygen and water forming the oxide of iron as described by the equations in section 2.2.5.

Where the samples are dried the increased mass is seen to reduce as the residual water held on the surfaces of the formed oxide and metal surfaces is driven off. Where the loose oxide is brushed off

the mass gain is further reduced, where hard oxide remains, or the sample is shown to have lost mass where only loose oxide was present, and the corroded metal surface is exposed.

4.3.4 Insulation Samples at End of Experimentation

The figures presented in table 4.7 are in relation to the starting mass from table 4.5. The figure for gain being where the sample is removed in the wet condition. The figure for loss being on completion of the drying period.

	Insulation Measured Mass (g) - End of Experimentation						
	Sample 1	Sample 2	Sample 3	Sample 4	Sample 5	Sample 6	Sample 7
Mass (Start) table 4.5	86.2	100.5	43.8	102.1	78.7	39.8	***
Mass (Wet)	199.2	248.2	64.2	193.6	134	47.1	***
Mass (Dry)	84.7	95.4	43.4	101.9	78.5	39.8	***
Gain (Dry - Wet)	113	147.7	20.4	91.5	55.3	7.3	***
Loss (Dry)	-1.5	-5.1	-0.4	-0.2	-0.2	0	***

Table 4.7 Insulation samples measured mass at end of experimentation.

The samples in all cases see an increase in mass due to water retention during the period of experimentation. The samples subject to cyclic heating conditions have retained a greater volume of water over the period. Some loss of the fibrous insulation material was expected due to handling and binding with the oxide formed on the pipe surface which was removed at the time of cleaning the pipe sample as described in section 4.3.3.

4.4 Visual Macro Examination of Samples

The following images depict the samples after removal from the environmental tank and drying. The lighting, camera exposure and position is consistent for all images. Figure 4.5 depicts all samples after completion of experimentation period.

Figure 4.5 Pipe Sample set at end of experimentation period

The following sections describe the visual observations made on the pipe and insulation samples on completion of the experimentation period.

4.4.1 Sample 1 – Cyclic - Rock Mineral Fibre Insulation

Localised areas of slight surface corrosion and deposits of attached oxide is seen on the sample pipe coating surface where breakage of the manufacturers surface coating is breached exposing the metallic surface as seen in figure 4.6, the areas where the coating is breached is consistent with the as supplied condition of the sample pipe. The preparation surface is subject to moderate uniform corrosion over all the prepared surface, with areas of attached oxide and scale still present to a moderate thickness which was not able to be removed by light mechanical cleaning, as seen in figure 4.9. A clear termination between the coating and preparation surfaces is visible in figures 4.7 and 4.8. The insulation material is found in a condition consistent with its as new application, with minor de-bonding of fibres due to attachment to surface, oxide and scale formed, and where the insulation is layered up, and handling as detailed in figure 4.10.

Figure 4.6 Pipe Sample 1 Cyclic – Rock mineral fibre insulation – Coating surface.

Figure 4.7 Pipe Sample 1 Cyclic – Rock mineral fibre insulation – Lower 180°

Figure 4.8 Pipe Sample 1 Cyclic – Rock mineral fibre insulation – Upper 0°

Figure 4.9 Pipe Sample 1 Cyclic - Rock mineral fibre insulation – Preparation surface.

Figure 4.10 Insulation Sample 1 Cyclic - Rock mineral fibre insulation – Inner surface.

4.4.2 Sample 2 – Cyclic - Glass Wool Insulation

The coating face of the pipe sample has significant areas of localised corrosion and attached oxide where the manufacturers surface coating is breached, further corrosion is noted where the protective surface coating has broken down during the period of experimentation as seen in figure 4.11. The preparation surface is subject to significant unform corrosion over all the prepared surface, with significant areas of attached oxide and scale present to a significant thickness which was not able to be removed by light mechanical cleaning as seen in figure 4.14. A termination between the coating and preparation surfaces is visible in figures 4.12 and 4.13. The insulation material is generally found in a condition consistent with its as new application, with some de-bonding of fibres due to attachment to surface and where oxide and scale formed, also where water was noted to have collected between the layup of the insulation, and on removal and handling as detailed in figure 4.15. Areas of deposited dissolved solids are noted on all surfaces and are visible as white deposits on the respective pipe sample images.

Figure 4.11 Pipe Sample 2 Cyclic – Glass wool insulation – Coating surface.

Figure 4.12 Pipe Sample 2 Cyclic – Glass wool insulation - Lower 180°

Figure 4.13 Pipe Sample 2 Cyclic – Glass wool insulation - Upper 0°

Figure 4.14 Pipe Sample 2 Cyclic – Glass wool insulation - Preparation surface.

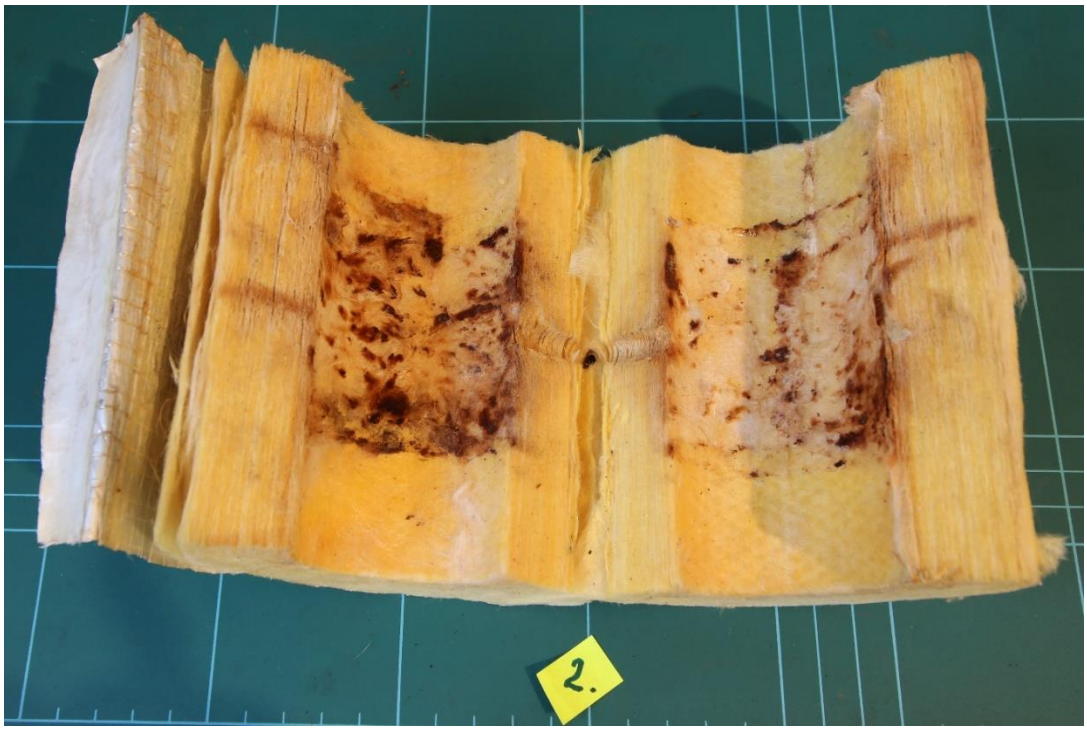

Figure 4.15 Insulation Sample 2 Cyclic – Glass wool insulation – Inner surface.

4.4.3 Sample 3 – Cyclic - Closed-Cell Elastomer Foam Insulation

Localised areas of slight surface staining, corrosion and deposits of attached oxide is seen on the sample pipe coating surface where breakage of the manufacturers surface coating is breached as seen in figure 4.16, the areas where the coating is breached is consistent with the as supplied condition of the sample pipe, with additional corrosion noted where further parts of the protective coating have broken down during the period of experimentation. The preparation surface is subject to moderate uniform corrosion over all the prepared surface, with isolated visible large shallow pitting, with areas of attached oxide and scale still present to a minimal thickness which was generally able to be removed by light mechanical cleaning, as seen in figure 4.19. The termination between the coating and preparation surfaces is not clearly visible in figures 4.17 and 4.18. The insulation material is found to have deteriorated significantly on both the outer and inner surfaces as depicted in figures 4.20 and 4.21 respectively from the as new application condition, with significant shrinkage and contraction noted to the cellular structure.

Figure 4.16 Pipe Sample 3 Cyclic – Closed-cell elastomer foam insulation – Coating surface.

Figure 4.17 Pipe Sample 3 Cyclic – Closed-cell elastomer foam insulation - Lower 180°

Figure 4.18 Pipe Sample 3 Cyclic – Closed-cell elastomer foam insulation – Upper 0°

Figure 4.19 Pipe Sample 3 Cyclic – Closed-cell elastomer foam insulation – Preparation surface.

Figure 4.20 Insulation Sample 3 Cyclic – Closed-cell elastomer foam insulation – Outer surface.

Figure 4.21 Insulation Sample 3 Cyclic – Closed-cell elastomer foam insulation – Inner surface.

4.4.4 Sample 4 – Ambient - Rock Mineral Fibre Insulation

Some isolated areas of slight surface corrosion on the sample pipe surface where breakage of the manufacturers surface coating is breached exposing the metallic surface, however other parts where surface breakage of the protective coating has occurred has not been subject to visually observed corrosion, as seen in figure 4.22. The preparation surface has areas of both superficial surface corrosion, and localised uniform corrosion with slight deposits of attached oxide and scale which was not able to be removed by light mechanical cleaning, interspaced between areas where no visible surface corrosion is present as seen in figure 4.25. A clear termination between the coating and preparation surfaces is visible in figures 4.23 and 4.24. The insulation material is found in a condition consistent with its as new application, with minor de-bonding of fibres due to attachment to surface, oxide and scale formed, and handling as detailed in figure 4.26, staining of the surfaces in contact with the metallic pipe surface is also noted.

Figure 4.22 Pipe Sample 4 Ambient - Rock Mineral Fibre Insulation – Coating surface.

Figure 4.23 Pipe Sample 4 Ambient - Rock Mineral Fibre Insulation - Lower 180°

Figure 4.24 Pipe Sample 4 Ambient - Rock Mineral Fibre Insulation - Upper 0°

Figure 4.25 Pipe Sample 4 Ambient - Rock Mineral Fibre Insulation – Preparation surface.

Figure 4.26 Insulation Sample 4 - Rock Mineral Fibre Insulation – Inner surface.

4.4.5 Sample 5 – Ambient - Glass Wool Insulation

Isolated areas of slight surface corrosion on the sample pipe surface where breakage of the manufacturers surface coating is breached exposing the metallic surface, other areas where surface breakage of the protective coating has occurred has not been subject to visually observable corrosion, as seen in figure 4.27. The preparation surface has areas of localised uniform corrosion with deposits of attached oxide and scale which was not able to be removed by light mechanical cleaning where there is contact with the insulation material, as seen by the pattern of visible corrosion mirroring the insulation surface in contact with the pipe, areas interspaced between corrosion have no visible surface corrosion present as seen in figure 4.30. A clear termination between the coating and preparation surfaces is visible in figures 4.28 and 4.29. The insulation material is found in a condition consistent with its as new application, with minor de-bonding of fibres due to attachment to surface, oxide and scale formed, and handling as detailed in figure 4.31.

Figure 4.27 Pipe Sample 5 Ambient – Glass wool insulation – Coating surface.

Figure 4.28 Pipe Sample 5 Ambient – Glass wool insulation - Lower 180°

Figure 4.29 Pipe Sample 5 Ambient – Glass wool insulation - Upper 0°

Figure 4.30 Pipe Sample 5 Ambient – Glass wool insulation – Preparation surface.

Figure 4.31 Insulation Sample 5 Ambient - Glass wool insulation – Inner surface.

4.4.6 Sample 6 – Ambient - Closed-Cell Elastomer Foam Insulation

Localised areas of slight surface staining, corrosion and deposits of attached oxide is seen on the sample pipe coating surface where breakage of the manufacturers surface coating is breached as seen in figure 4.32, with isolated areas of additional corrosion noted where further parts of the protective coating have broken down during the period of experimentation. The preparation surface is subject to moderate uniform corrosion over the prepared surface where in contact with the insulation material, with isolated visible large shallow pitting, areas of attached oxide and scale still present to a minimal thickness which was generally able to be removed by light mechanical cleaning, as seen in figure 4.35. Other parts not in contact with the insulation material are affected by isolated areas of superficial surface corrosion. The termination between the coating and preparation surfaces is visible in figures 4.33 and 4.34. The insulation material is found to have deteriorated slightly on the inner surfaces as depicted in figures 4.37 where the pipe has been in close contact. Externally the insulation is found in a condition consistent with its as new application as detailed in figure 4.36.

Figure 4.32 Pipe Sample 6 Ambient - Closed-cell elastomer foam insulation – Coating surface.

Figure 4.33 Pipe Sample 6 Ambient - Closed-cell elastomer foam insulation – Lower 180°

Figure 4.34 Pipe Sample 6 Ambient - Closed-cell elastomer foam insulation - Upper 0°

Figure 4.35 Pipe Sample 6 Ambient - Closed-cell elastomer foam insulation – Preparation surface.

Figure 4.36 Insulation Sample 6 Ambient – Closed-cell elastomer foam insulation – Outer surface.

Figure 4.37 Insulation Sample 6 Ambient – Closed-cell elastomer foam insulation – Inner surface.

4.4.7 Sample 7 – Ambient - Uninsulated reference pipe

Sample 7 was not covered with thermal insulation; the sample being exposed to ambient conditions within the environmental tank and subject to the same volume of recirculated rainwater as the insulated pipe samples. Some isolated areas of slight surface corrosion are noted on the sample pipe surface where breakage of the manufacturers surface coating is breached exposing the metallic surface, however other parts where surface breakage of the protective coating has occurred has not been subject to visually observed corrosion, as seen in figure 4.38. The preparation surface has areas of both superficial surface corrosion, and localised pitting corrosion with slight deposits of attached oxide and scale which was not able to be removed by light mechanical cleaning, the axial extremities of the pipe sample where no visible surface corrosion is present is generally in areas where recirculated rainwater was not in contact with the pipe surface as seen in figure 4.41. A clear termination between the coating and preparation surfaces is visible in figures 4.40, whilst a clear termination is also noted in figure 4.39 further localised general surface corrosion, oxide and scaling is found where the surface water applied forms into droplets before returning to the environmental test tank sump.

Figure 4.38 Pipe Sample 7 Ambient – Uninsulated – Coating surface.

Figure 4.39 Pipe Sample 7 Ambient – Uninsulated - Lower 180°

Figure 4.40 Pipe Sample 7 Ambient – Uninsulated - Upper 0°

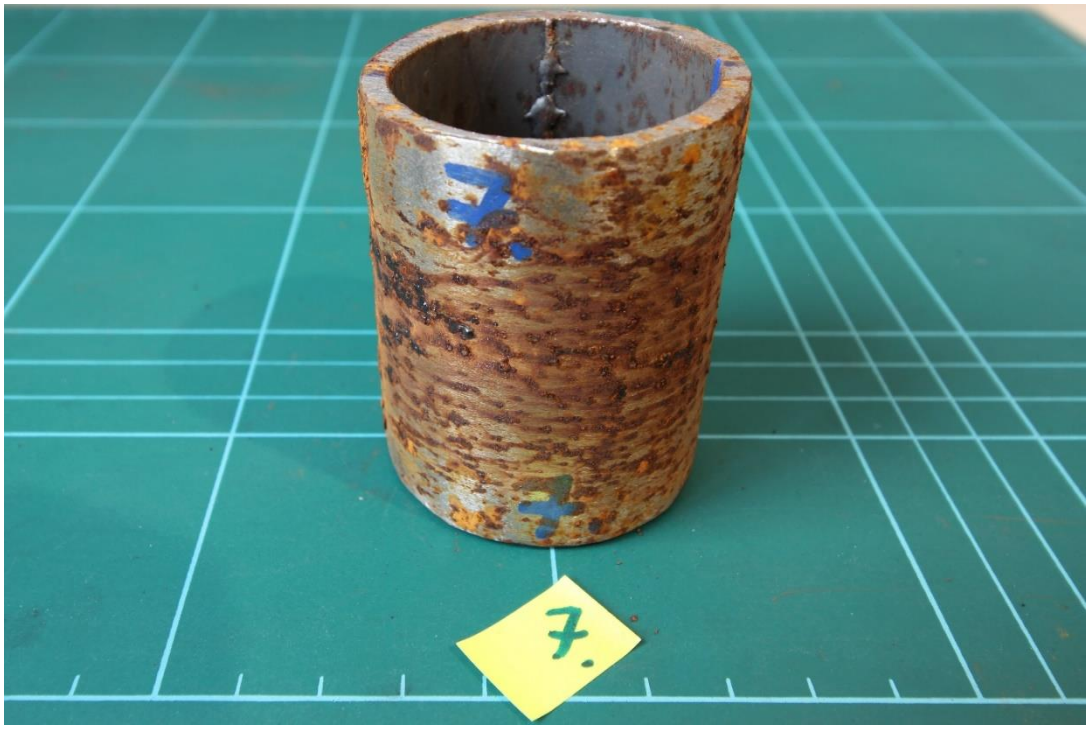

Figure 4.41 Pipe Sample 7 Ambient – Uninsulated – Preparation surface.

4.5 Metallographic Examination of Samples by Optical Microscopy

Each of the samples is sectioned for metallographic examination by removing a test coupon from the preparation surface at the midpoint of the 270° position as detailed in figure 4.42.

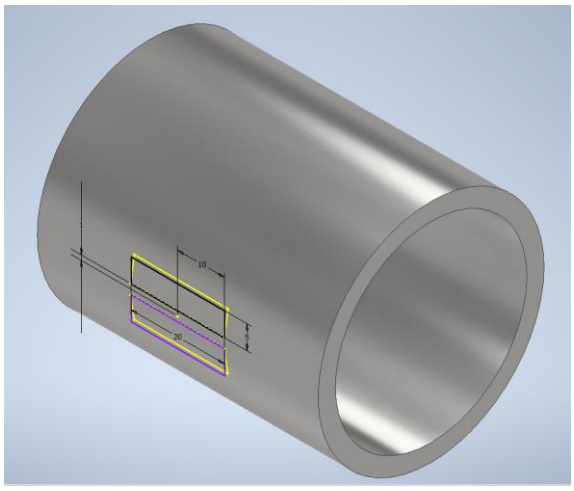

Figure 4.42 Position of metallographic test coupons within pipe sample

The test coupon (20mm x 5mm) is mounted in a Bakelite puck, each of the pucks holding two samples, except for sample 7 which is mounted exclusively. The samples are polished through successive steps to a 1-micron mirror finish. Figure 4.43 describes the samples mounted in bakerite pucks in preparation for metallographic examination by optical microscopy.

Each of the samples is viewed at 50x and 200x magnification in the unetched condition, the samples are then subject to etchant (5% nitric acid) before viewing at x500 magnification.

The etchant is used on the samples at 500x magnification to highlight the grain boundaries within the metal sample to aid in the identification of any intergranular and/or transgranular corrosion. The darker bulk area in the image is Bakelite puck material. The products of corrosion appearing in the interface between the puck material and steel, note that the un-etched metal surface appears white to grey in the images due to the mirror finish, the etched images clearly showing the grain structure of the steel.

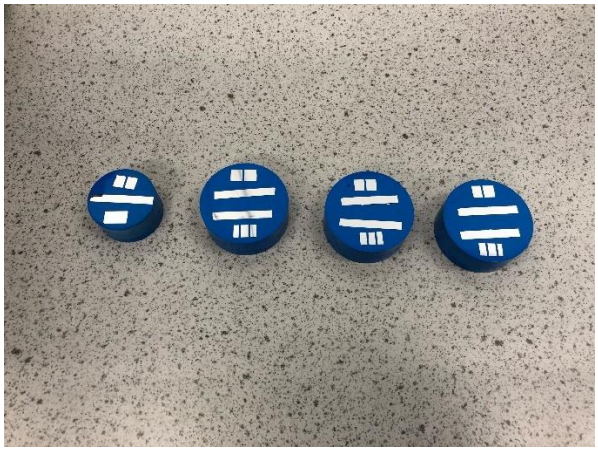

Figure 4.43 Pipe samples prepared for metallographic optical microscopy examination.

The following sections describe the visual observations during the optical microscopy examination on the pipe samples on completion of the experimentation period.

4.5.1 Sample 1 – Cyclic - Rock Mineral Fibre Insulation

The preparation surface is subject to regular aggressive pitting corrosion, which occurs consistently over the sample as described in the 50x image detailed in figure 4.44, the products of corrosion forming a continuous oxide layer up to 50-70 microns in places, the oxide layer is found with multiply fractures which propagating to the exposed steel surface as seen in figures 4.44 and 4.45. No intergranular or transgranular corrosion is seen to originate from the corrosion pits into the grain boundaries of the exposed steel as detailed in figure 4.46.

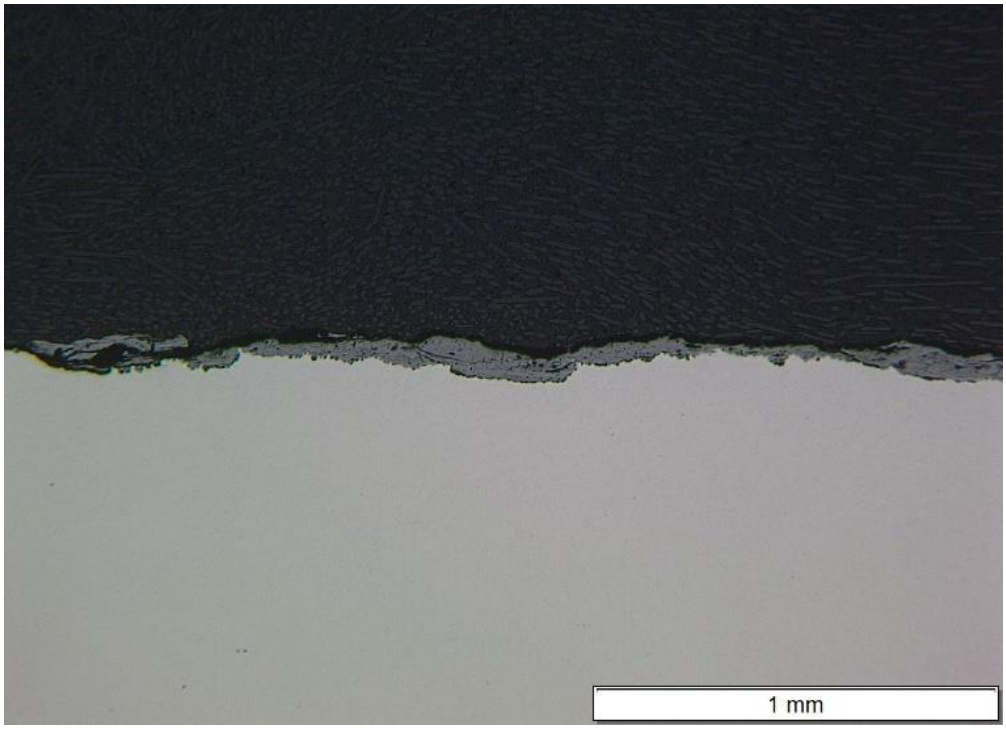

Figure 4.44 Pipe Sample 1 Cyclic – Rock mineral fibre insulation – 50x magnification.

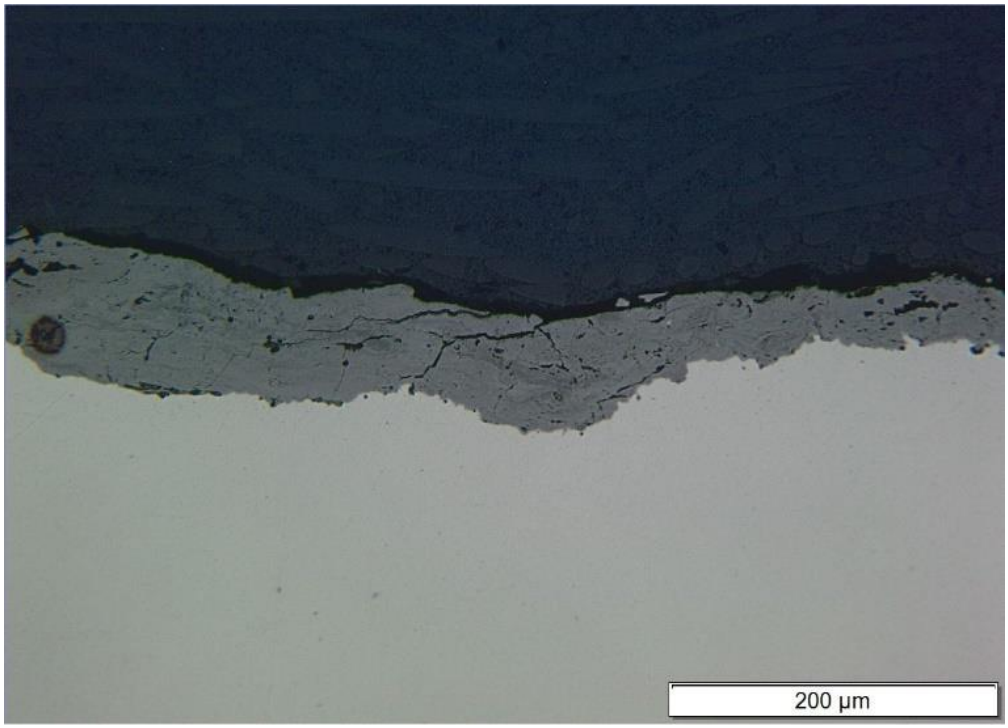

Figure 4.45 Pipe Sample 1 Cyclic – Rock mineral fibre insulation – 200x magnification.

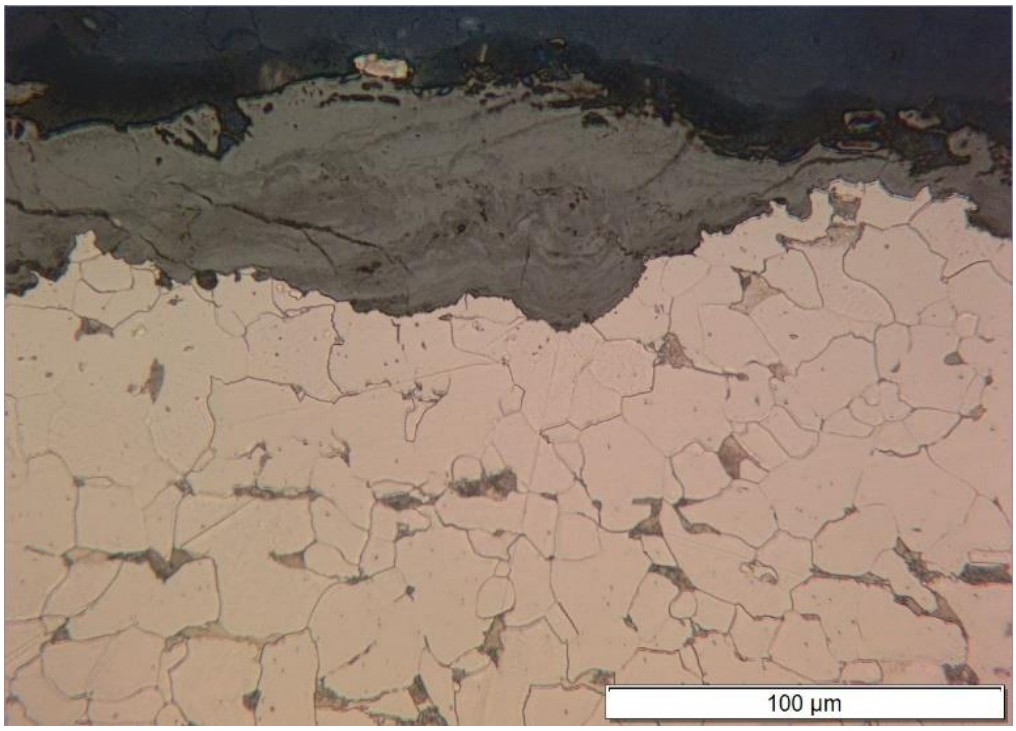

Figure 4.46 Pipe Sample 1 Cyclic – Rock mineral fibre insulation – 500x magnification.

4.5.2 Sample 2 – Cyclic - Glass Wool Insulation

The preparation surface is subject to regular aggressive pitting corrosion, which occurs consistently over the sample as described in the 50x image detailed in figure 4.47, the products of corrosion forming a continuous oxide layer up to 80-120 microns in places, the oxide layer is found with multiply fractures which propagating to the exposed steel surface as seen in figures 4.48 and 4.49. No intergranular or transgranular corrosion is seen to originate from the corrosion pits into the grain boundaries of the exposed steel as detailed in figure 4.49.

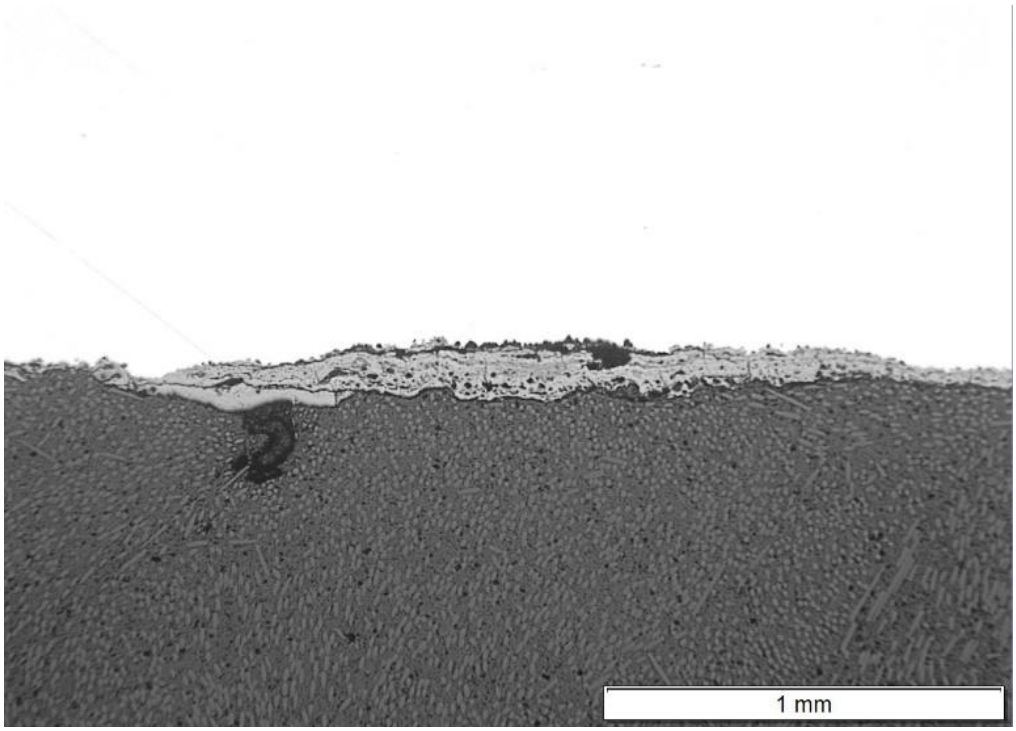

Figure 4.47 Pipe Sample 2 Cyclic – Glass wool insulation – 50x magnification.

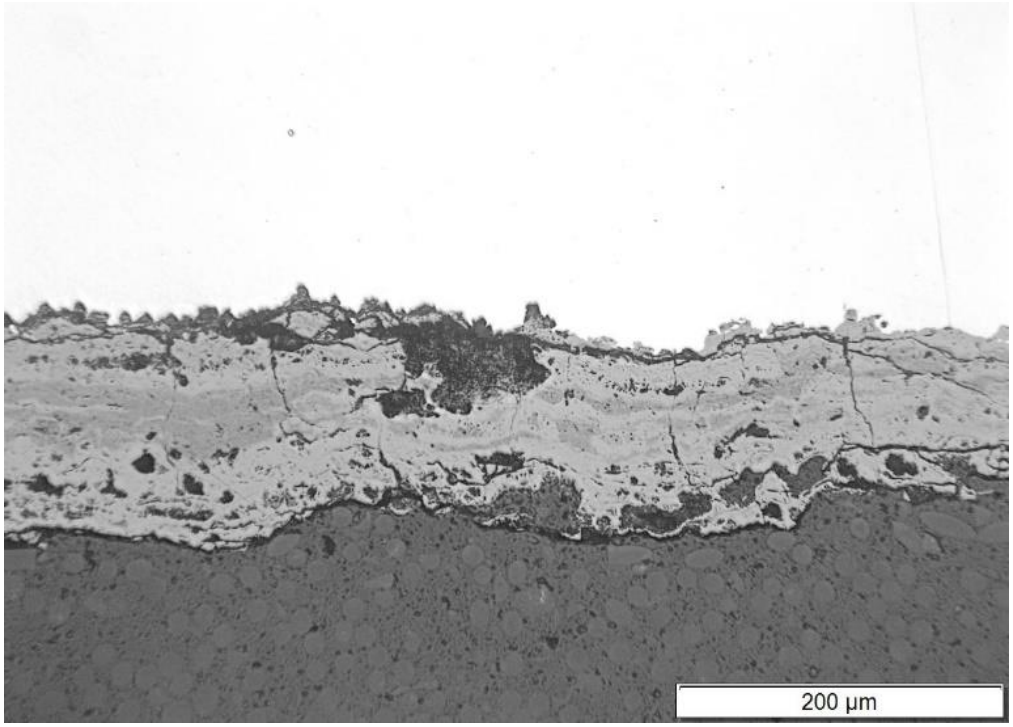

Figure 4.48 Pipe Sample 2 Cyclic – Glass wool insulation – 200x magnification.

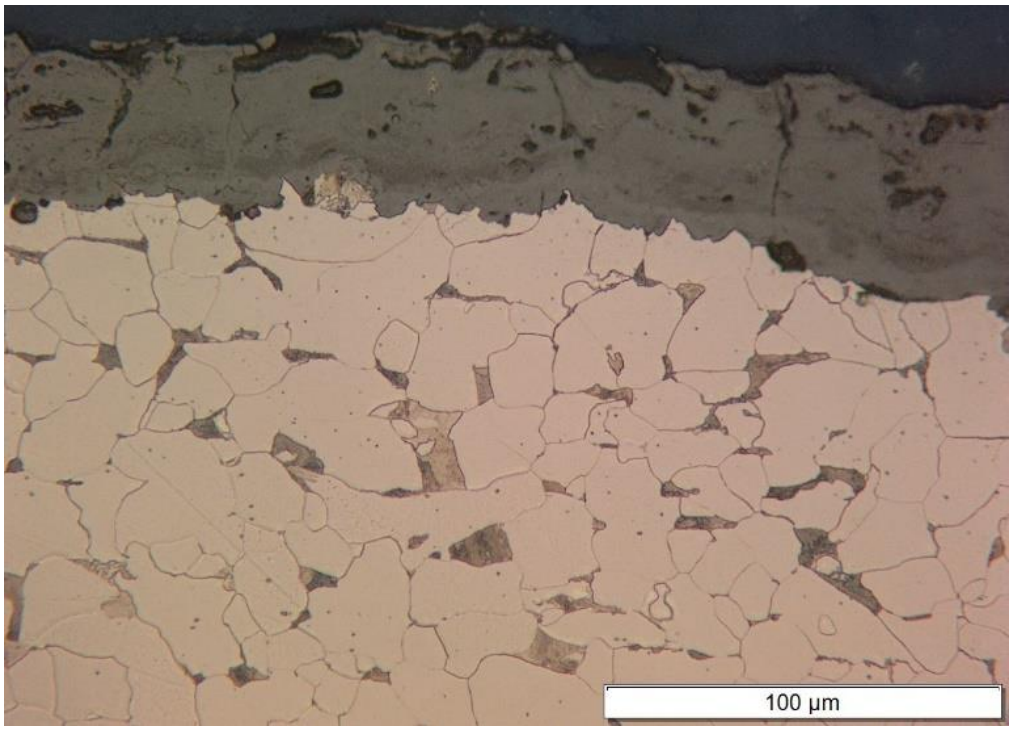

Figure 4.49 Pipe Sample 2 Cyclic – Glass wool insulation – 500x magnification.

4.5.3 Sample 3 – Cyclic - Closed-Cell Elastomer Foam Insulation

The preparation surface is subject to regular pitting corrosion, which occurs consistently over the sample as described in the 50x image detailed in figure 4.50, the products of corrosion forming a continuous oxide layer up to 40-60 microns in places, the oxide layer is found with multiple fractures which propagating to the exposed steel surface as seen in figures 4.51 and 4.52. No intergranular or transgranular corrosion is seen to originate from the corrosion pits into the grain boundaries of the exposed steel as detailed in figure 4.52.

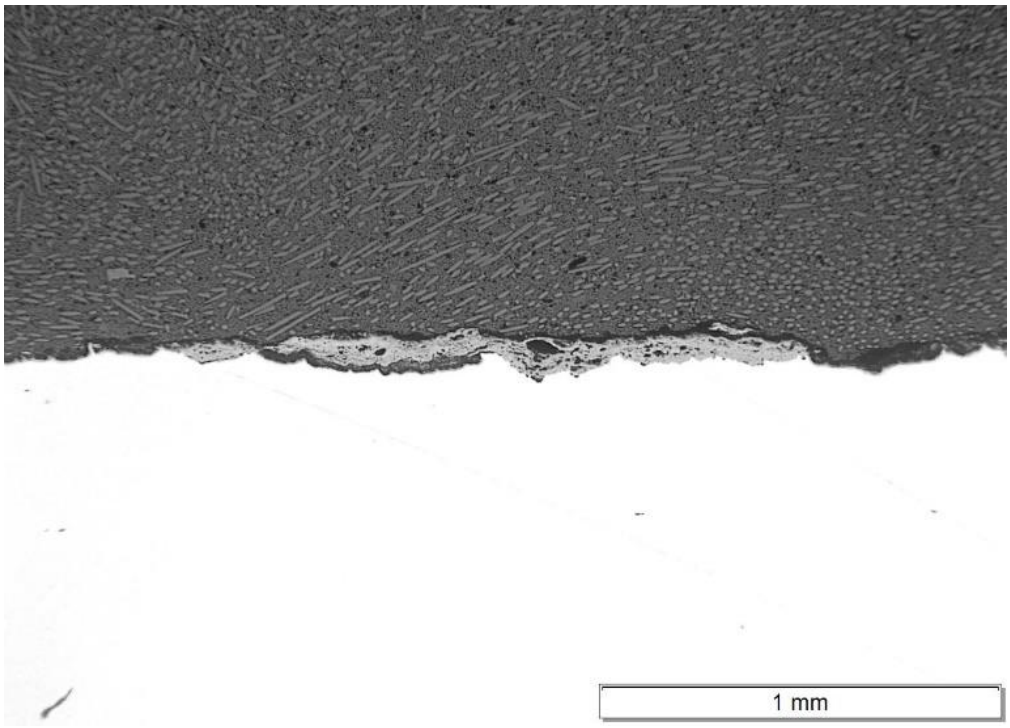

Figure 4.50 Pipe Sample 3 Cyclic – Closed-cell elastomer foam insulation – 50x magnification.

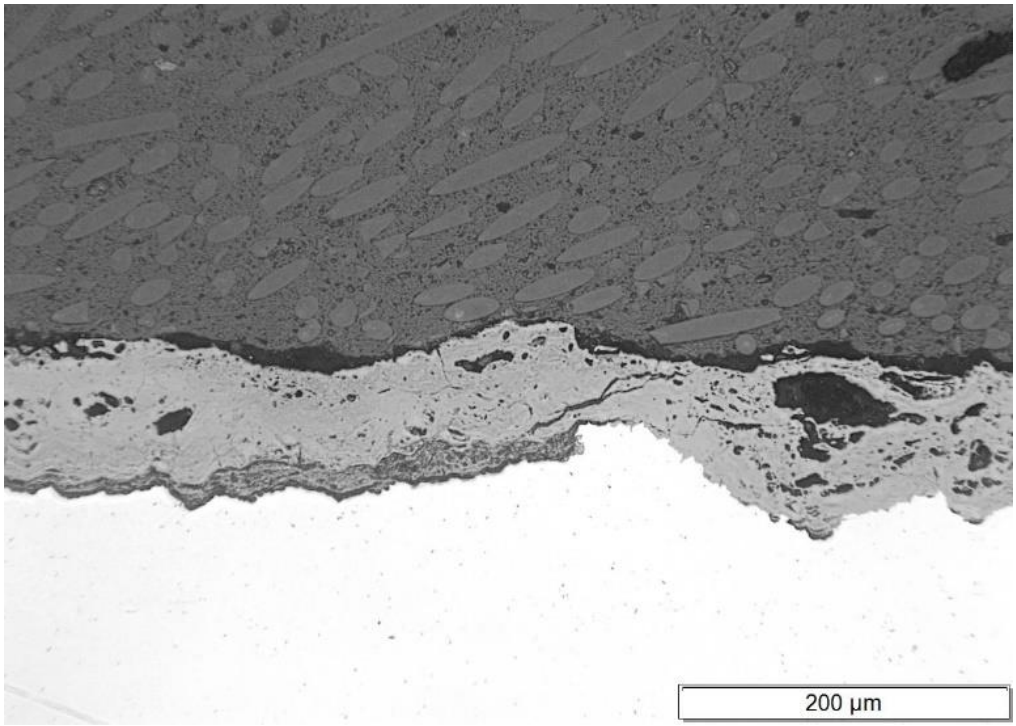

Figure 4.51 Pipe Sample 3 Cyclic – Closed-cell elastomer foam insulation – 200x magnification.

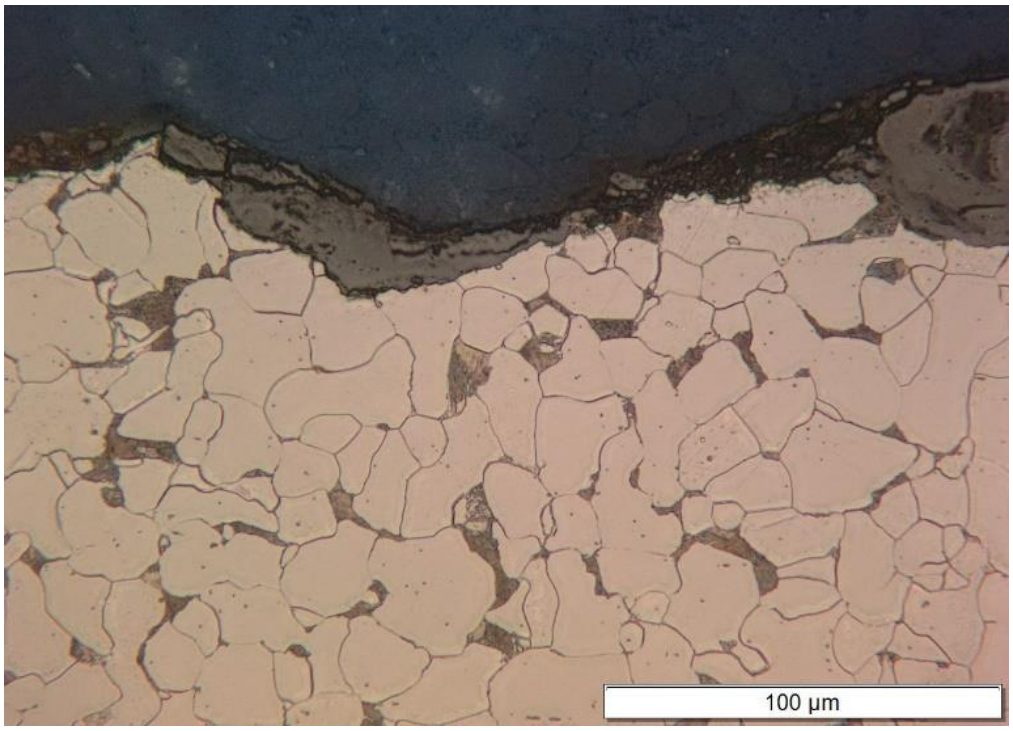

Figure 4.52 Pipe Sample 3 Cyclic – Closed-cell elastomer foam insulation – 500x magnification.

4.5.4 Sample 4 – Ambient - Rock Mineral Fibre Insulation

The preparation surface is subject to regular minor pitting corrosion, which occurs consistently over the sample as described in the 50x image detailed in figure 4.53, the products of corrosion forming a continuous oxide layer up to 10-20 microns in places, the oxide layer is found generally intact with no fractures propagating to the exposed steel surface as seen in figures 4.54 and 4.55. No intergranular or transgranular corrosion is seen to originate from the corrosion pits into the grain boundaries of the exposed steel as detailed in figure 4.55.

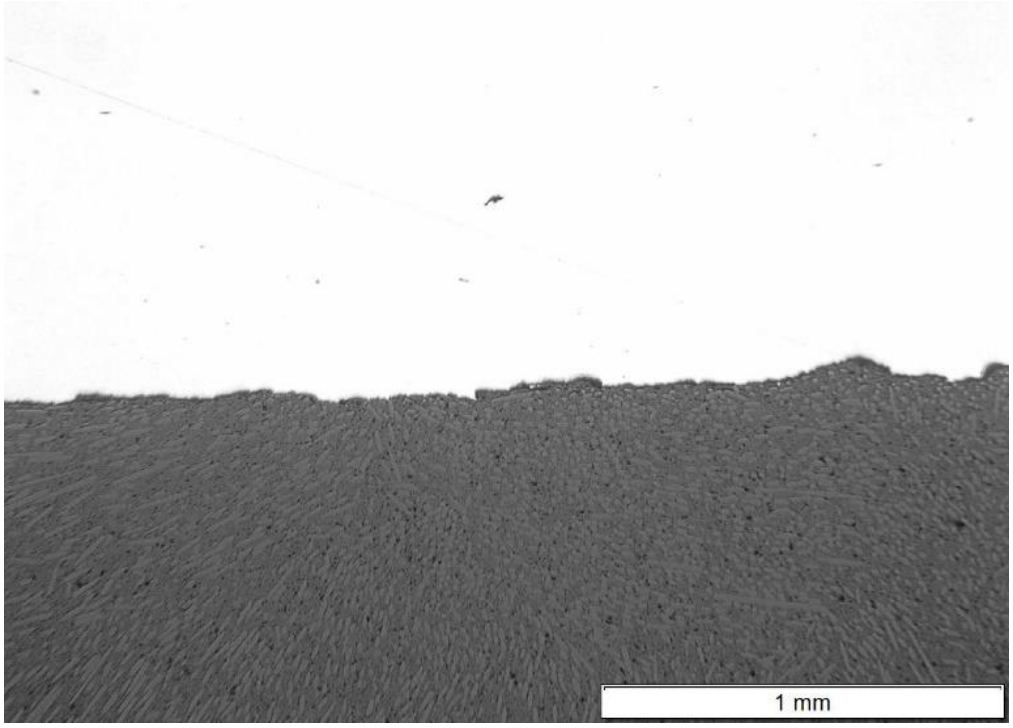

Figure 4.53 Pipe Sample 4 Ambient - Rock Mineral Fibre Insulation – 50x magnification.

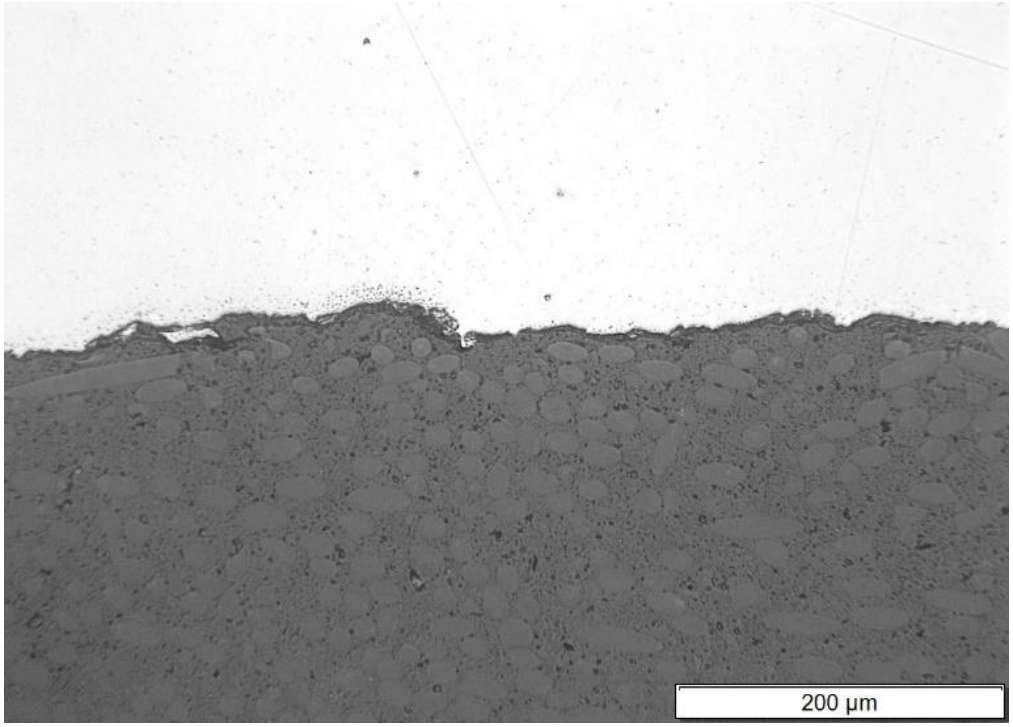

Figure 4.54 Pipe Sample 4 Ambient - Rock Mineral Fibre Insulation – 200x magnification.

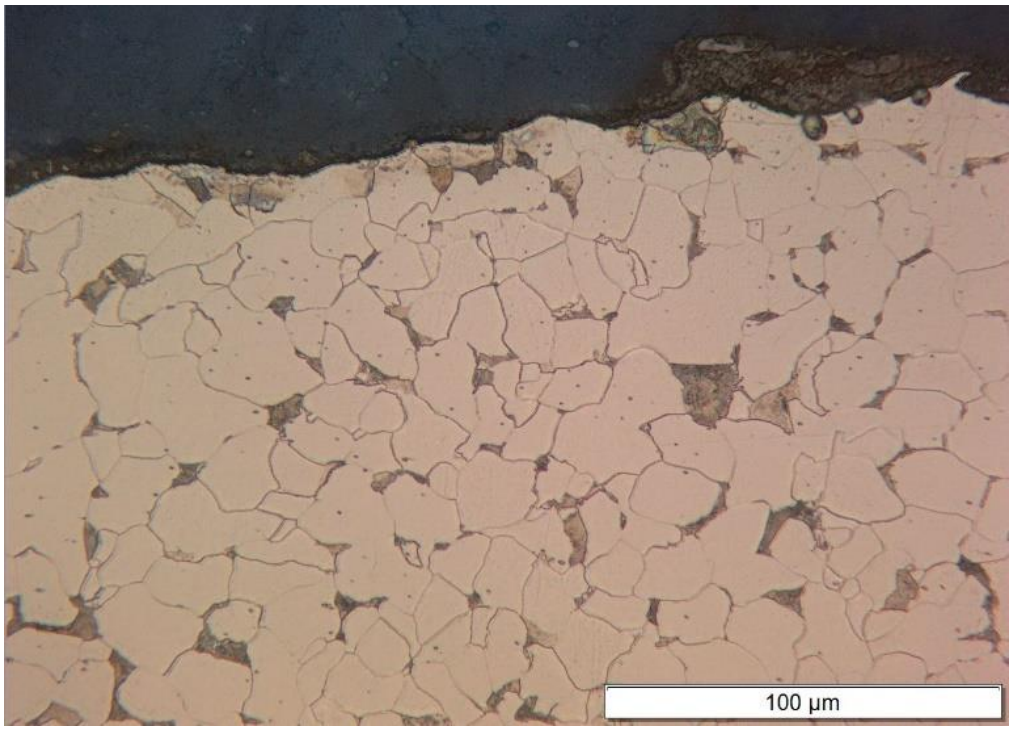

Figure 4.55 Pipe Sample 4 Ambient - Rock Mineral Fibre Insulation – 500x magnification.

4.5.5 Sample 5 – Ambient - Glass Wool Insulation

The preparation surface is subject to regular moderate pitting corrosion, with isolated areas of aggressive pitting corrosion, both occurring consistently over the sample as described in the 50x image detailed in figure 4.56, the products of corrosion forming a continuous oxide layer up to 5-10 microns, increasing to 20-40 microns in places, the oxide layer is found generally intact with no fractures propagating to the exposed steel surface as seen in figures 4.57 and 4.58. No intergranular or transgranular corrosion is seen to originate from the corrosion pits into the grain boundaries of the exposed steel as detailed in figure 4.55.

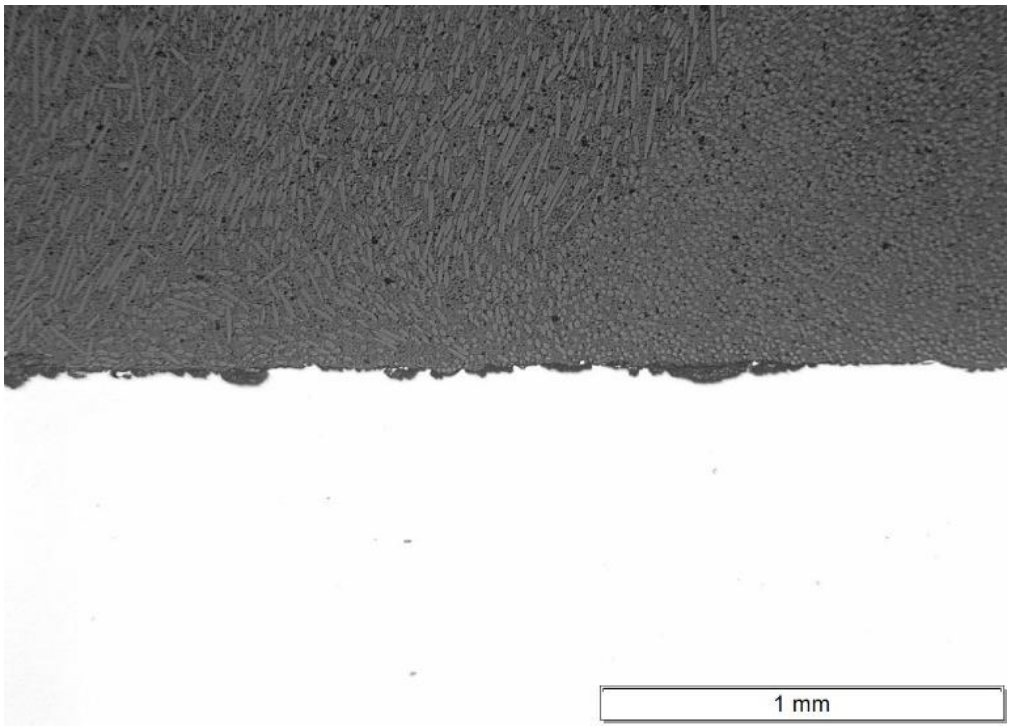

Figure 4.56 Pipe Sample 5 Ambient – Glass wool insulation – 50x magnification.

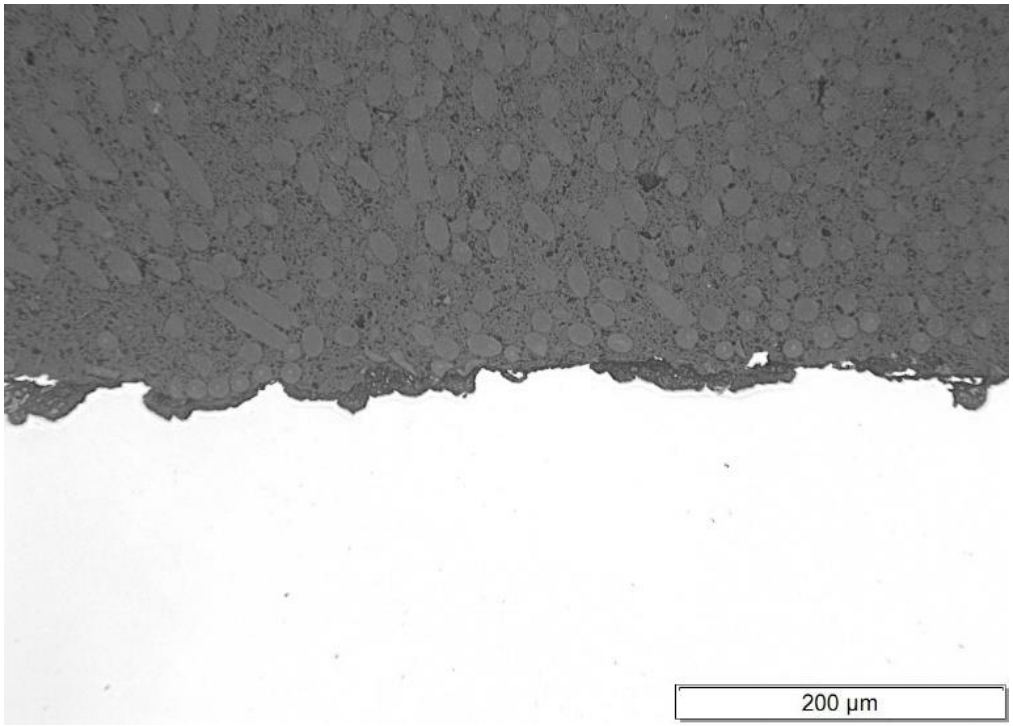

Figure 4.57 Pipe Sample 5 Ambient – Glass wool insulation – 200x magnification.

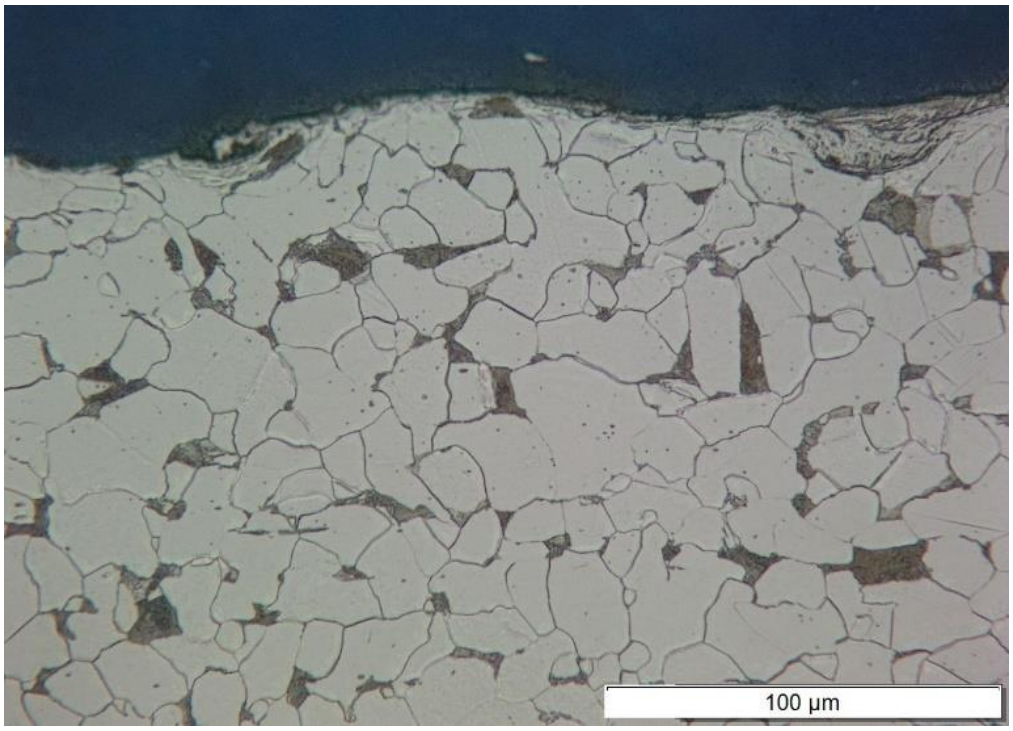

Figure 4.58 Pipe Sample 5 Ambient – Glass wool insulation – 500x magnification.

4.5.6 Sample 6 – Ambient - Closed-Cell Elastomer Foam Insulation

The preparation surface is subject to regular minor pitting corrosion, with isolated areas of aggressive pitting corrosion, both occurring consistently over the sample as described in the 50x image detailed in figure 4.59, the products of corrosion forming a continuous oxide layer up to 5-10 microns, increasing to 20-40 microns in places, the oxide layer is found generally intact with no fractures propagating to the exposed steel surface as seen in figures 4.60 and 4.61. No intergranular or transgranular corrosion is seen to originate from the corrosion pits into the grain boundaries of the exposed steel as detailed in figure 4.61.

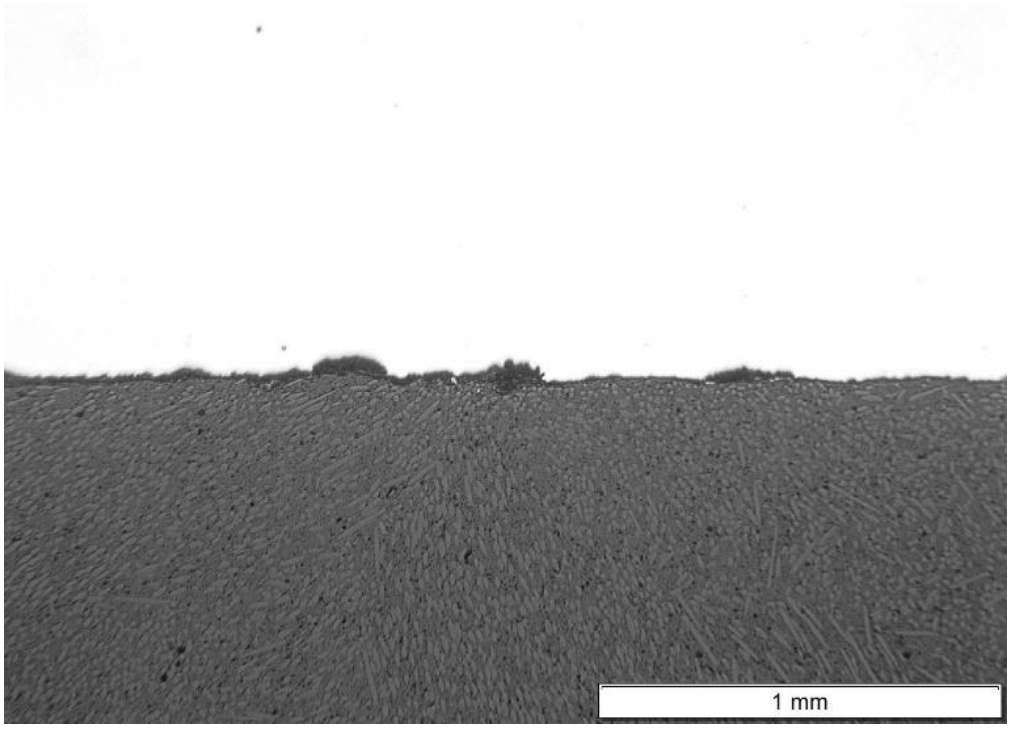

Figure 4.59 Pipe Sample 6 Ambient - Closed-cell elastomer foam insulation – 50x magnification.

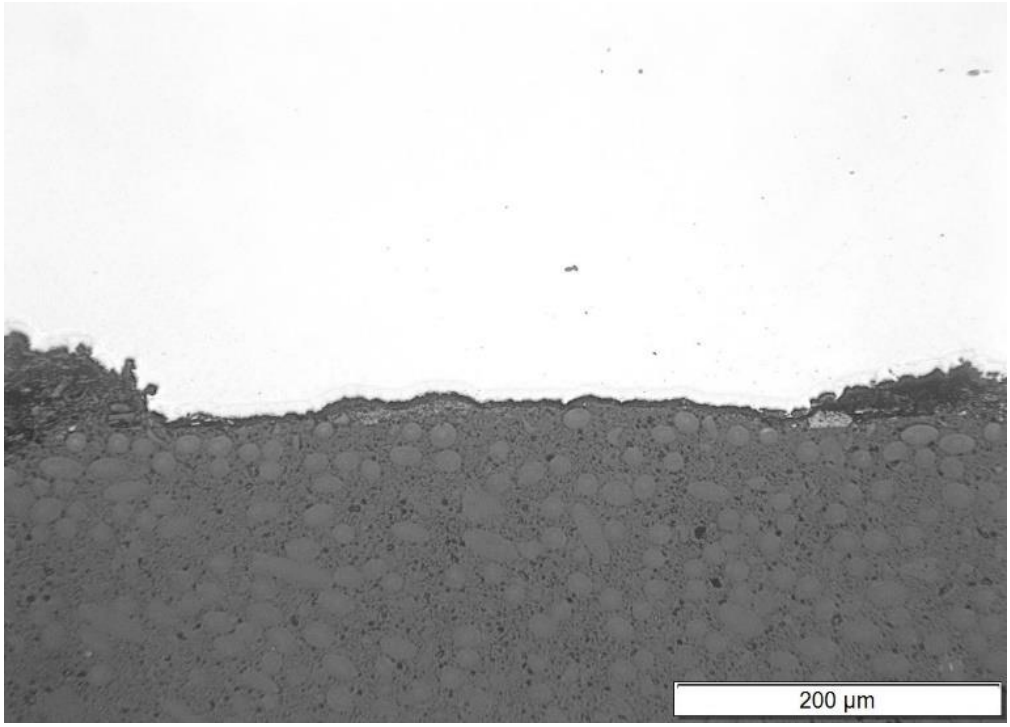

Figure 4.60 Pipe Sample 6 Ambient - Closed-cell elastomer foam insulation – 200x magnification.

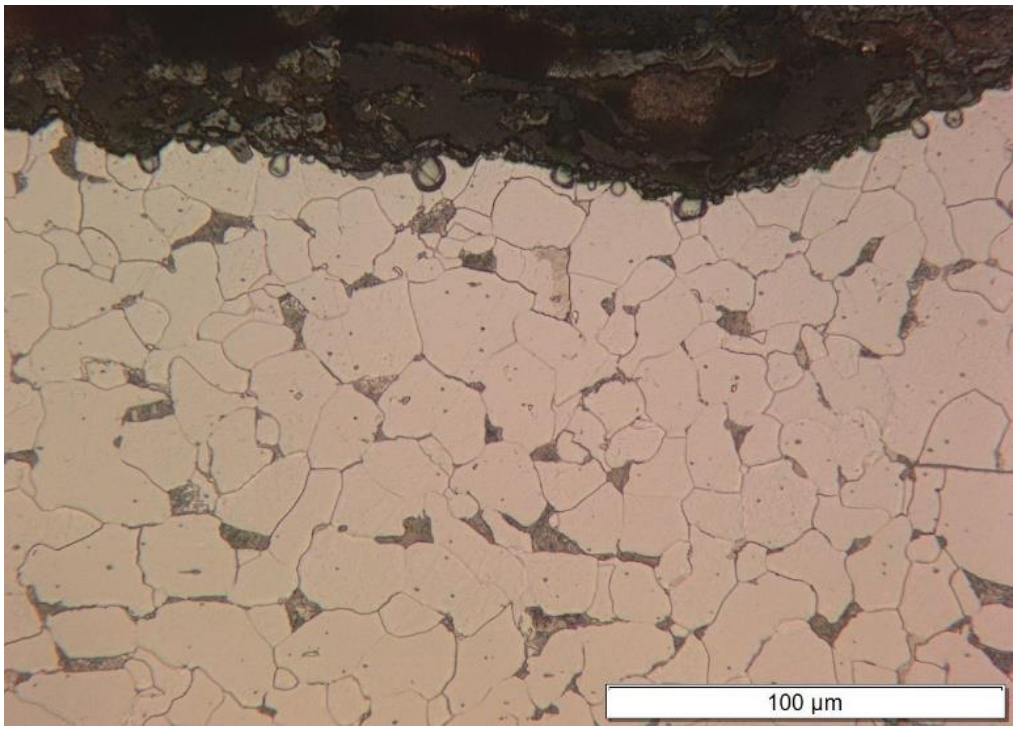

Figure 4.61 Pipe Sample 6 Ambient - Closed-cell elastomer foam insulation – 500x magnification.

4.5.7 Sample 7 – Ambient - Uninsulated reference pipe

The preparation surface is subject to isolated areas of aggressive pitting corrosion occurring consistently over the sample as described in the 50x image detailed in figure 4.62, the products of corrosion forming oxide layers up to 50 microns within the formed pits, the oxide layer is found generally intact with isolated fractures propagating to the exposed steel surface in places as seen in figures 4.63. No intergranular or transgranular corrosion is seen to originate from the corrosion pits into the grain boundaries of the exposed steel as detailed in figure 4.64.

Figures 4.65 and 4.66 detail the inner surface of the pipe wall, mill scale present for manufacture is seen uniformly up to 5 microns.

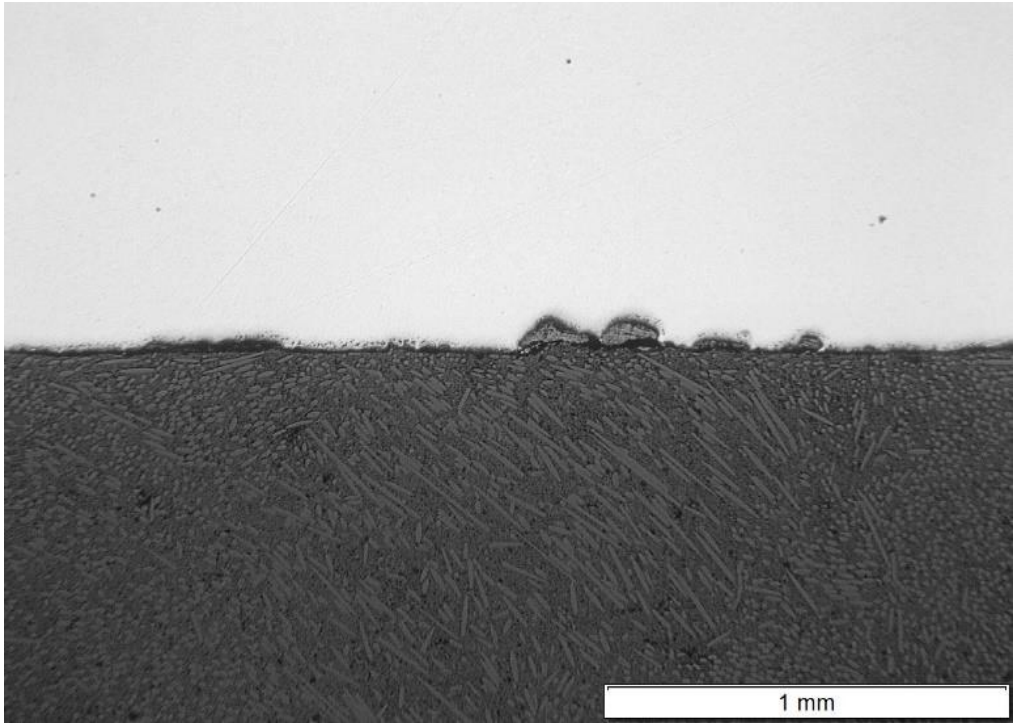

Figure 4.62 Pipe Sample 7 Ambient – Uninsulated – 50x magnification.

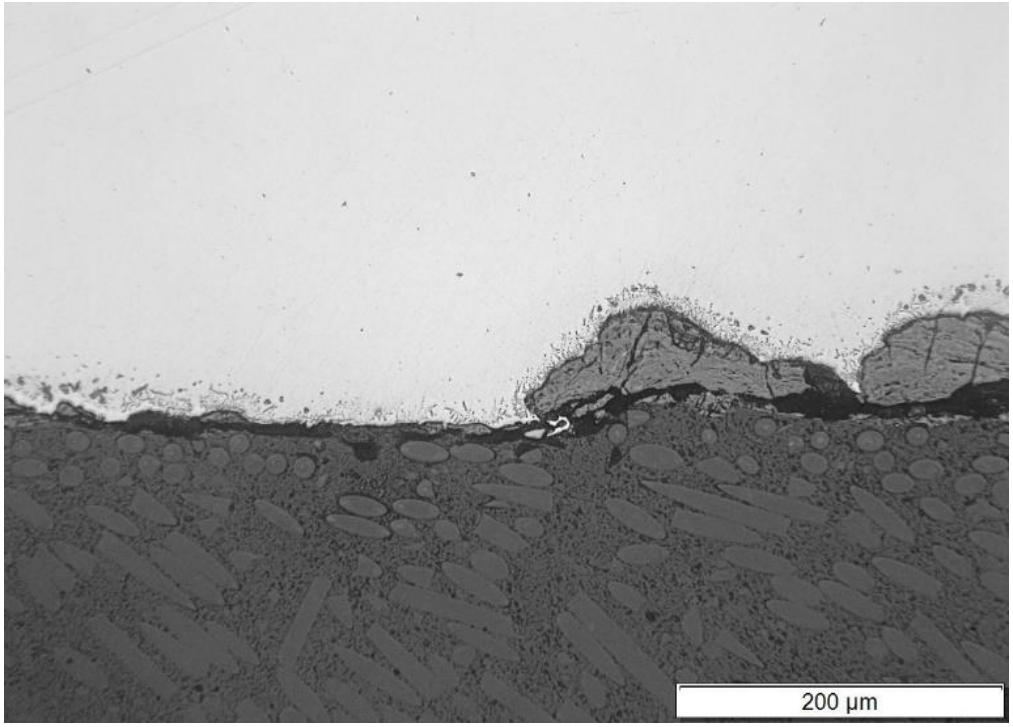

Figure 4.63 Pipe Sample 7 Ambient – Uninsulated – 200x magnification.

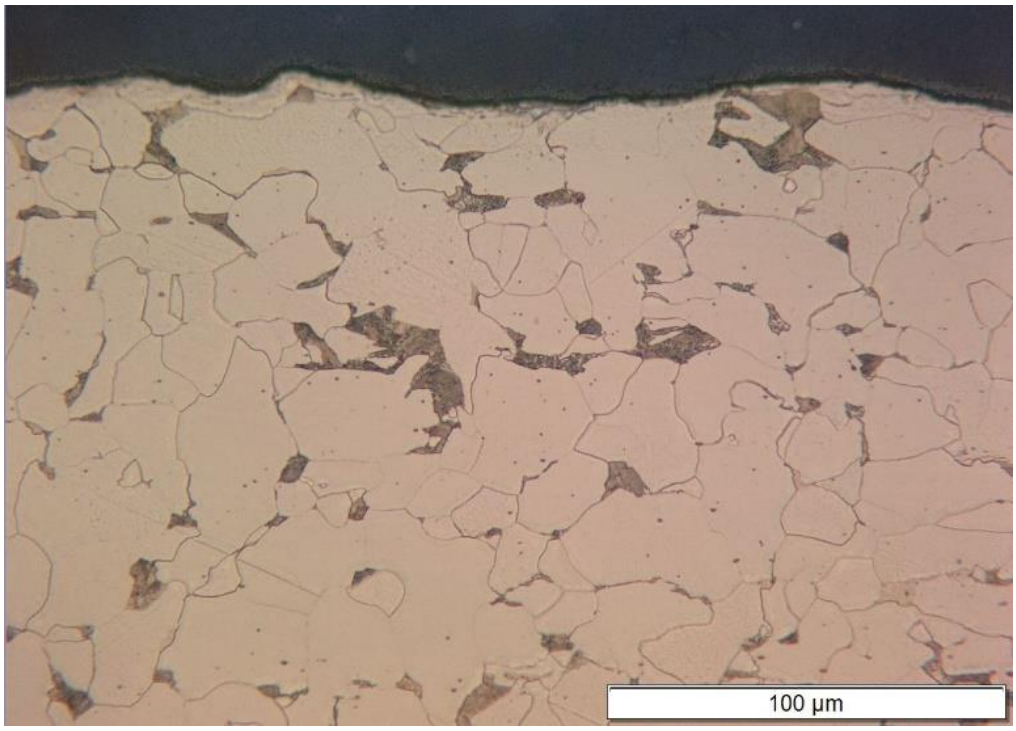

Figure 4.64 Pipe Sample 7 Ambient – Uninsulated – 5000x magnification.

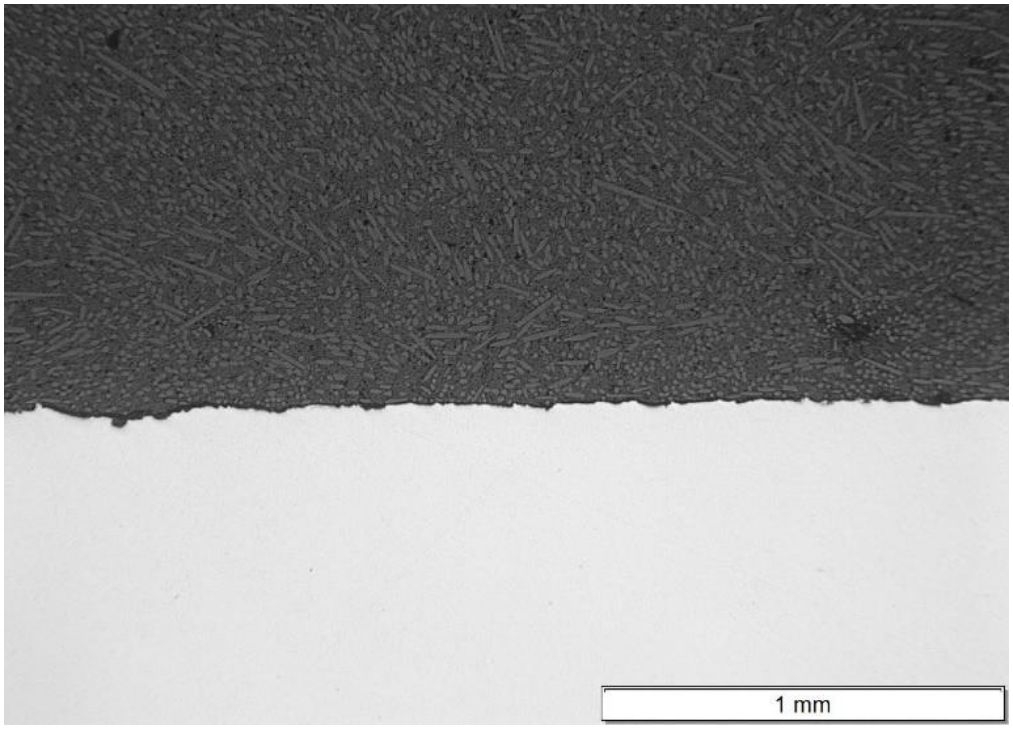

Figure 4.65 Pipe Sample 7 Ambient – Uninsulated – Inner wall 50x magnification.

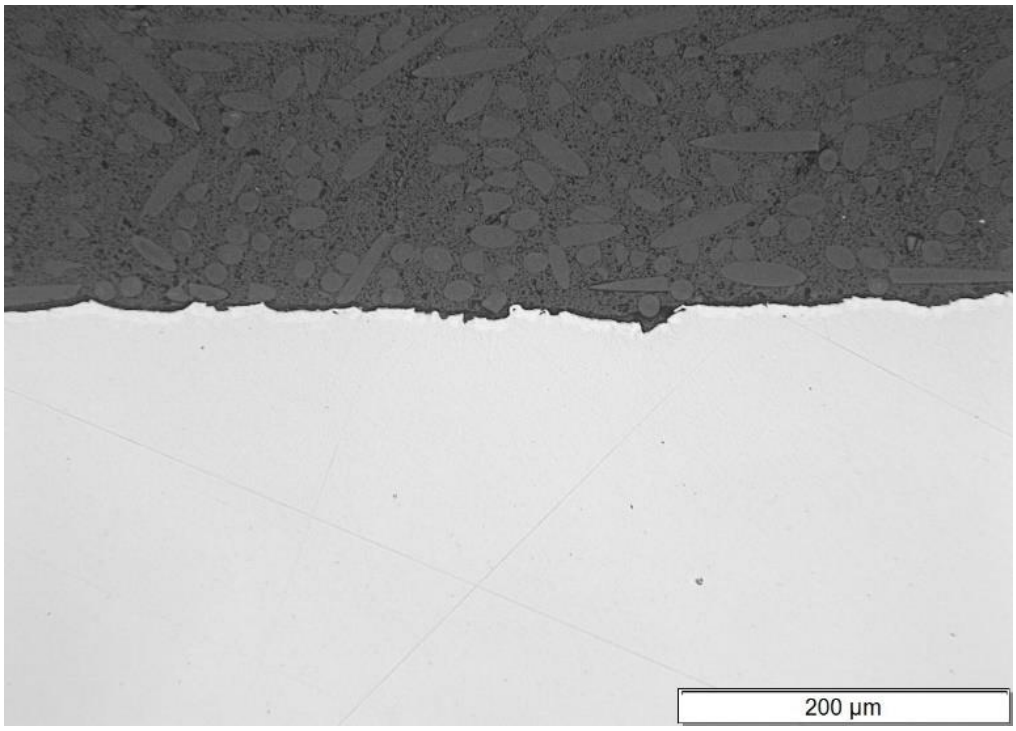

Figure 4.66 Pipe Sample 7 Ambient – Uninsulated – Inner wall 200x magnification.

4.6 Energy Dispersive X-Ray Spectroscopy

A further set of test coupons extracted from the preparation surface as described in figure 4.42 of section 4.5 is prepared for energy dispersive x-ray spectroscopy (EDX) analysis.

The EDX analysis is undertaken using a scanning electron microscope (SEM) with an EDX function. As the samples have already been examined using conventional optical microscopy the higher magnification available with SEM was not considered necessary as part of this study, and only the EDX function is utilised. Figure 4.67 describes the SEM and EDX sample chamber.

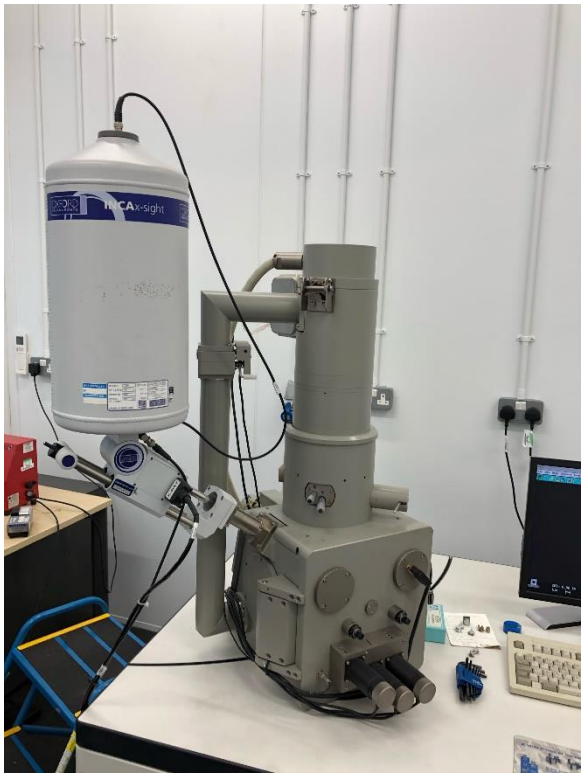

Figure 4.67 SEM and EDX sample chamber

EXD allows the elemental composition analysis of a materials surface to be undertaken and provides a spectrum of the elements present within the sample area. Whilst the technique can be used to determine the presence of elements, the results are relative to all elements present on the sample.

The individual pipe samples are shown in figure 4.68 in preparation for analysis, the samples number 1 through to 7 in a clockwise rotation from the zero position. The samples are not subject to any surface preparation after the test coupon is removed from the pipe sample.

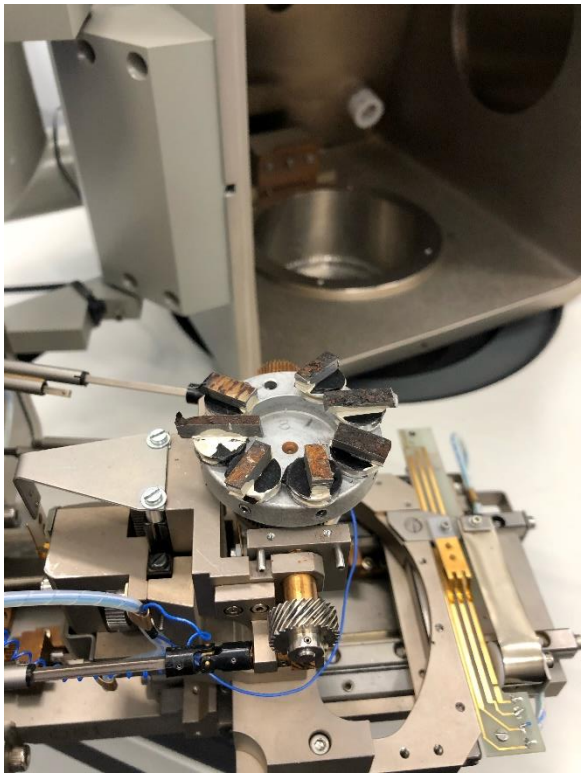
Figure 4.68 Sample preparation for EDX

The results of the EDX analysis were consistent across all samples, with trace elemental indications of silica, sodium, calcium, magnesium and chlorine at comparable levels in relation the iron and carbon of the pipe material. The trace elements being consistent with dissolved minerals found in rainwater, and also mineral derived insulation materials.

5.0 Discussion

Corrosion under insulation of carbon steel pipework in process manufacturing system presents a significant problem for operators, where left unmanaged it often results in significant maintenance costs, and wider environmental implications due to loss of containment.

This study considered the effect that cyclic temperature change, typical of service pipework associated with process systems, has on the water retention of thermal insulation material and the development of corrosion under insulation on thermally insulated carbon steel pipe where rainwater in the South Wales coastal region was introduced into fibrous and closed cell elastomer insulation materials.

The hypothesis of the study proposed that cyclic temperature change will increase the water retention of thermal insulation material and development of corrosion under insulation on thermally insulated carbon steel pipework where water is introduced into the insulation material.

The study demonstrates a correlation between both the development of corrosion under insulation of carbon steel and the water retention of insulation material where subject to cyclic temperature conditions in the presence of introduced rainwater. The results indicate that both the development of corrosion and water retention of insulation increase when subject to cyclic temperature conditions. However due to the small sample size and specific insulation material types the generalisability is limited.

5.1 Insulation Water Retention

Over the 12-week period of experimentation all the insulation samples displayed an increase in water retention, with those subject to cyclic heating and cooling displaying further increase in water retention as described in table 4.7 of section 4.3.4

The fibre insulation materials, rock mineral wool and glass wool, in both the case of cyclic heating and ambient conditions, retained a significant amount of water, with cyclic samples able to retain water equivalent in excess of its starting mass, and those subject to ambient conditions below its starting mass. The closed cell elastomer material following the same pattern, however with a reduced water retention.

Whist manufacturers of fibrous insulation materials promote the hydrophobic properties and the ability to repel water at ambient and elevated temperatures, the results of the study confirm that in the case of the insulation materials tested water retention is still present where free drainage from the insulation is provided. DuBose (2019), suggests that water repellent additives combined with insulation materials start to lose their hydrophobic properties and effectiveness above 150°C for oil based, and 250°C for silicon-based additives. Considering the pipe/insulation interface temperatures recorded over the duration of the experimentation as set out in table 4.3 of section 4.2 the average interface temperatures for the rock mineral wool and glass wool, 112.3°C and 105°C respectively, are considerably lower than those put forward by Dubose (2019), and therefore would suggest that water repellent additives start to lose their hydrophobic properties at much lower temperatures.

Debonding of the insulation material in both rock mineral wool and glass wool can be clearly seen in the cyclic sample images described in figures 4.10 and 4.15 of sections 4.4.1 and 4.4.2 respectively. Which is not present to the same extent as seen in the ambient sample images of figures 4.26 and 4.31 of sections 4.4.4 and 4.4.5. The debonding confirms the breakdown of the insulation binder and water repellent additive. The spaces created by the debonding of the insulation fibres allowing

additional water to be retained in the cyclic samples over that of the ambient samples, accounting for the increase in wet mass as described in table 4. Previous research completed by Burhani, et al (2016) suggest that water retention is greater in insulation materials at temperatures between 100°C and 120°C as its less likely to dry completely in cyclic service, this study supports the position of Burhani, et al, and additionally provides an explanation for additional water retention which affects drying time in that the breakdown of the insulation creates voids for water retention. The cyclic rock mineral wool and glass wool samples were observed to hold 41% and 76% more water respectively than the corresponding ambient sample at the end of the experimentation period.

While previous research conducted by Pojtanabuntoeng, et al (2015) point out that drain holes may have a limited influence on corrosion under insulation, the results demonstrate that water retention in insulation material influences the rate of corrosion, rather than the ability of water to drain away freely due to lack of adequate drainage provisions during the installation process. During the period of experimentation the water was observed to drain freely, however importantly the water that did drain away was that which could not be held once the insulation had become saturated.

The closed cell elastomer insulation whilst holding less water than both the rock mineral wool and glass wool in both cyclic and ambient conditions as described in table 4.7 did not meet with the manufacturers stated performance criteria for temperature. The insulation having a rated upper temperature limit of 150°C, in excess of the cyclic experimental internal pipe temperature at 140°C, and the measured average pipe/insulation interface temperature at 118.7°C. The deterioration noted on both the external and internal surfaces of the cyclic insulation sample being significant as detailed in figures 4.20 and 4.21 of section 4.4.3, when compared to the ambient sample detailed in figures 4.36 and 4.37 of section 4.4.6. The close cell construction being severally affected during the cyclic heating cycles, the cyclic sample retaining 28% more water than the ambient sample.

The integrity of the closed cell structure of elastomer insulation materials has a significant effect on its ability to mitigate against water ingress and retention. Earlier observation by Bahadori (2014), regarding low temperature damage to the insulation structure and its effectiveness against water retention highlight the weaknesses of such materials in certain applications, this study demonstrates that there are limitations at higher operating temperatures. This would certainly question the performance ability of such materials in extreme applications.

An increase in dissolved solids and conductivity was seen in the recirculated rainwater of the environmental test tank, which was in excess of that recorded over the same period within the rainwater tank as illustrated in table 4.1 of section 4.1. Whilst the dissolved solids and conductivity for the collected rainwater at the location of the experimentation in Swansea South Wales generally agreed with the relative comparison of UKEAP:Precip-Net data, it was not possible to clearly establish which insulation materials had contributed to the increase in dissolved solids and conductivity within the environmental tank and confirm the observation of Ahlumalia (2006).

The energy dispersive x-ray spectroscopy undertaken on the pipe sample test coupons was inconclusive and indicated comparable levels of silica, sodium, calcium, magnesium and chlorine across all the test samples. This highlighted a limitation in the design of the experimentation, specifically in that the recirculated rainwater within the environmental tank is common to all samples and in turn invalidated the energy dispersive x-ray spectroscopy analysis. Whilst this ruled out any further understanding of the effect of rainwater contamination and insulation leeching with respect

to individual samples within the environmental tank, the overall experimentation with respect to water retention remains valid across the sample group, with a caveat that the increase in concentration of dissolved solids is likely to accelerate the rate of corrosion across the sample set during the period of experimentation.

The mass analysis undertaken at the end of experimentation indicated that sample 2, cyclic glass wool, had lost 5.1g during the period, while the others had lost between 0.2 and 1.5g which could be attributed to mechanical cleaning as part of sample preparation. Whilst sample 2 had lost the greatest mass to the recirculating rainwater it was not clear if this sample was solely responsible for the increase in dissolved solids and conductivity within the environmental tank.

5.2 Development of Corrosion

All of the steel pipe samples were seen to develop corrosion on the bare metal preparation surfaces over the 12-week period of experimentation, the pipe samples which were subject to cyclic heating and cooling were found to have more advanced corrosion over a greater surface area than the pipe samples subject to ambient conditions only, the mass gain and loss of each sample being described in table 4.6 of section 4.3.3.

The samples subject to cyclic heating and cooling were found have active corrosion over all of the bare metal preparation surface covered by insulation, the ambient samples however displayed areas both affected and not affect by corrosion. On microscopic examination the areas of corrosion of the cyclic samples were found to have highly developed corrosion pitting with an oxide covering three to four times thicker than the ambient sample, the oxide was found to have multiple fractures which were observed to run to the exposed metal surface, the fracturing of the oxide was not observed on the samples covered by insulation remaining at ambient temperatures.

The repeated heating and cooling of the cyclic samples results in a fracture of the oxide layer allowing fresh electrolyte to enter the pit, and corrosion to continue. Importantly this is not corrosion fatigue of the steel pipe material, which would have been evident as a crack propagating into the steel from the surface, containing corrosion products. No evidence is seen during the microscopic analysis as detailed in section 4.5 of intergranular or transgranular corrosion and fatigue cracking. The fractures within the oxide layer providing space for the electrolyte to be retained during the heating cycle, which would increase the time of wetness, a factor which Groysman (2010) describes as the main factor in influencing the corrosion mechanism and rate of corrosion.

The widespread corrosion over the preparation surfaces which are subject to cyclic heating would suggest that during the heating phase the water is driven away from the surface to be replaced again on cooling, the cyclic nature of the process and wicking effect of the fibrous material drawing more water into the body of the insulation sample, and diffusion through the material to all of the surface in contact with the steel pipe material. The breakdown of the closed cell elastomer insulation during the cyclic process similarly allowing water retention in the same way within the body of the material. The increased corrosion activity in the cyclic samples confirm the position of Burhani, et al (2016). The observations do not fit in with the theory of Rasmussen (2017), who suggest that the corrosion rate would be lower where permeable material could dry. In line with the hypothesis there is a clear increase in the development of corrosion under insulation where the sample is subject to cyclic temperature change. The source of available water and likelihood of incomplete drying between heating cycles is only exacerbated by the deterioration of the insulation material discussed previously.

The change in mass observed between the cyclic an ambient sample as set out in table 4.6 of section 4.3.3 suggests that all insulated pipe samples gained mass during the corrosion process as expected and indicated a loss of parent material where the product of corrosion was easily removed. However, it was not possible to determine the rate of corrosion of individual samples or draw a comparison between samples, this is due to the nature of sample preparation and means of measurement available during the experimentation. The rate of corrosion would also likely be effected by the common nature of rainwater recirculation discussed with respect to the insulation materials, and it is therefore considered that the experimentation design as applied during this study would not give a true representation of the rate of corrosion over the period of experimentation.

While some of the previous research reviewed within literature describe corrosion taking place at higher temperatures due to the quotation of system temperature set points, this investigation additionally monitored the pipe/insulation interface temperature, the findings confirm the position of API (2019) with respect to significant corrosion occurring at lower temperatures, quoting the range of 77-110°C. Considering table 4.3 in section 4.2, the average surface interface temperate for channel B, which monitored sample 2 (Cyclic - glass wool) was 105.8°C during the heating soak period, sample 2 was found to be the most effected during the period of experimentation, with significant corrosion taking place over all parts of the exposed preparation surface. While samples 1, channel A, and 3, channel C, having higher surface interface temperatures, 112.3°C and 118.7°C respectively, displayed less aggressive corrosion over the exposed preparation surface. However, the findings contradict the claims of Landolt (2007), who suggest that the rate of corrosion is lower during periods of dryness. During the period of experimentation each cyclic sample experienced a two dry periods of 3 hours in a 24-hour cycle, and in all cases the sample was observed to have developed more severe corrosion than the ambient non-cyclic sample.

The observed results of the study confirm that cyclic temperature change between ambient conditions and a pipe/insulation interface temperature up to 120°C have a significant influence on the development of corrosion under insulation on carbon steel pipework where fibrous insulation materials are specified. This aligns with claims of both Burhani, et al (2016) and Nace-Jubail (2015), where previous studies have drawn the same conclusion. However, whilst previous research has focus on fibrous rock and glass wool insulation materials, the results of this study demonstrate the unsuitability of certain closed cell insulation materials in temperature cyclic service where significant corrosion is also likely in applications reflecting the experimentation design.

It was not possible to determine the effect of increased chloride concentration on each of the individual samples as discuss previously due to the limitation of the common recirculation of rainwater within the environmental test tank, and that the energy dispersive x-ray spectroscopy undertaken on the pipe sample test coupons was inconclusive in that chloride was present in the spectrum of all test coupons analysed. However, the results have confirmed that chlorides were present in the test environment and increased over the duration of experimentation by way of the weekly monitoring as described in section 4.1. From the visual macro-observations undertaken on sample 2 it was noted that dissolved solids had collected on the pipe surface during the cyclic heating and cooling, which would have contributed to increasing the ionic activity within the electrolyte present on the pipe surface and pipe/insulation interface. The increase in ionic activity within the electrolyte leading to an increase in corrosion as described by Ahmad (2006), this supports the visual findings with respect to sample 2 being subject to the most aggressive corrosion within the sample set. The period of

corrosion on sample 2 during the wet phase of the cycle is likely to be extended when consideration is given to the position of Landolt (2007) with respect to relative humidity, the concentration of dissolved solids present on the metallic surface reducing the point at which corrosion occurs due to relative humidity.

The importance of the protective coating applied to the steel pipe surface during manufacture is demonstrated during the period of experimentation. With the exception of sample 2 which has been subject to further breakdown, the protective coating is generally in good order for the other samples with only superficial corrosion present where the coating is breached before the start of experimentation. Whilst the literature review discussed the benefits of thermal spray aluminium as a protective coating for larger diameter process pipe, its application is limited in smaller diameter service pipework, this study focusing on service pipework of 50mm diameter. The results of the study therefore confirm the importance of maintaining the integrity of the manufacture applied protective coating system during installation where the pipe is overlaid with insulation material, and at further points where maintenance is completed which may cause a breach in the coating system.

Sample 7 was included within the experimentation as an uninsulated reference to compare effects of corrosion under ambient conditions. Whilst isolated pitting corrosion has taken place over the upper parts, and was significantly less than all other samples where covered by insulation, the observations would confirm the position of Ahmad (2006) regarding an increase in corrosion where the relative humidity is greater than 80% at temperatures 0°C and above, as the environmental tank ambient conditions where averaged over duration of experimentation were observed as 95.9% and 9.6°C respectively as detailed in table 4.3 of section 4.2. This would confirm the importance of maintaining a protective coating on the metallic pipe surface in cases where breaks in the application of insulation are present, or where the insulation has been removed to mitigate against corrosion. The localised corrosion over the lower part where water formed into droplets algins with the statement made by Groysman (2016) regarding the time of wetness influencing the rate of corrosion. The observations strengthen the finding of this study with respect to water retention at the metallic pipe surface/insulation interface influencing the development of corrosion under insulation.

The introduction of an air gap at the pipe surface to insulation interface would likely contribute to reducing the extent of the development of corrosion as the rainwater which forms the electrolyte on the metallic pipe surface is held within the thermal insulation material, rather than the insulation material holding the rainwater against the metallic pipe surface. This is clearly seen in the macro comparison of the cyclic and ambient sample corrosion, where the wicking that has occurred in the cyclic samples has drawn the rainwater further over the pipe sample. An air gap would facilitate faster drying times due to an increase in the pipe surface temperature, thereby reducing the time of wetness and relative humidity at pipe/insulation interface. Potentially an air gap may also aid in reducing the thermal insulation material temperature and mitigating against the reduction in the hydrophobic properties.

6.0 Conclusion

This research study aimed to identify the effect cyclic temperature change has on the water retention of thermal insulation material and the development of corrosion under insulation on thermally insulated carbon steel pipework where rainwater from the South Wales coastal region is introduced into the insulation material.

Due to the unprecedented disruption caused by the Covid-19 pandemic and the uncertainty caused by restrictions in travel and attending university as normal, the design of the research study and experimentation was developed around facilities and materials available remote from the university laboratory setting. Due to the limitations on apparatus and sample size an explanatory analysis was undertaken applying a cross sectional quasi-experimental design to test the study hypothesis and provide an answer to the research question.

Based on the empirical evidence gathered during the period of experimentation it can be concluded that cyclic temperature change in small diameter carbon steel process pipework affects both the water retention of insulation materials and the development of corrosion under insulation, where rainwater in the South Wales coastal region is introduced into the insulation material.

The experimentation method attempted to simulate a meaningful test environment further to the observations raised in previous work discussed within the literature review with respect to the duration of the experimentation period. The results of the research clearly confirmed the proposed hypothesis, but also raises the question of the suitability of recirculating the test medium within the environmental test tank. Whilst the recirculated rainwater confirmed that corrosion would take place, the limitation of isolating the effect on individual samples was exposed.

While the quasi-experimental design limits the generalisability of the results due to the limited sample size and common rainwater re-circulation, the method provides a clear insight into the effect that cyclic temperature operation and rainwater ingress have on both fibre and closed elastomer insulation and water retention and the development of corrosion under insulation.

The results of this study confirm the findings of other studies considered as part of the literature review with respect to corrosion under insulation being more aggressive at temperatures between 70-120°C, and additionally identify a weakness in the suitability of the sample insulation materials in temperature cyclic service consistent with process service applications and their stated hydrophobic properties.

From an in-service operational and maintenance perspective the findings of the study highlight the importance of the views of Cosham, et al. (2007) with respect to a failure in the corrosion control system. Whilst the study purposely set out to understand the effect of rainwater ingress, the importance of mitigating against ingress to the metallic pipe surface in the first place cannot be overstated. Both the pipe coating system and insulation weather barrier playing a key part in reducing the development and onset of corrosion under insulation.

7.0 Recommendations and Further Work

Based on the conclusion drawn from the study undertaken and to aid in the further understanding of the effect of rainwater ingress into insulation materials future studies may wish to consider the following identified during the study

Limitations

1. The sample size should be increased to support confidence in the findings and generalisability.
2. To better understand the effect of rainwater on individual samples the influence of common rainwater recirculation should be considered as a confounding variable.
3. The rate of corrosion should be considered as dependant variable.

Building on findings

1. Both the fibre-based insulation materials, rock mineral wool and glass wool, and the closed cell elastomer insulation material were observed to start to break down in temperature cyclic service at temperatures lower that the maximum operating temperature stated by the manufacture. Further study may wish to consider the suitability of insulation materials in temperature cyclic service.
2. An air gap introduced at the interface between the metallic pipe surface and insulation material may reduce the impact of corrosion under insulation. Further study may wish to consider the effect the introduction of an air gap at the metallic pipe surface to insulation material interface has on the development of corrosion under insulation.

From an operational perspective the following recommendations are made with respect to small diameter thermally insulated service pipework and mitigation against corrosion under insulation

1. The outer weather barrier/membrane associated with a thermal insulation system is of critical importance in stopping water entering insulation material. The integrity of such systems should be maintained to the highest standard both during installation and maintenance to prevent water ingress. This study has demonstrated that insulation in both cyclic and ambient conditions retains water even when drainage facilities are provided, and that corrosion under insulation develops in both cases.
2. Pipe sections specified for small bore service application are typically supplied with an external protective coating that is effective in delaying and reducing the effect of corrosion under insulation. However, where the coating system is breached or removed as part of installation, maintenance or modification suitable precautions should be taken to identify the breached areas and apply a further layer of protective coating before application of insulation and return to service. The study has demonstrated that corrosion under insulation can develop significantly under certain conditions over a relativity short period of time where the protective coating is removed.
3. Where thermal insulation is specified for personnel protection over thermal efficiency consideration should be given to protection by other means, such as barrier or caging.
4. To mitigate against the wicking of water through insulation material onto previously unaffected parts of the pipe surface consideration should be given to introducing an air gap at the interface between the pipe surface and insulation material using suitable standoff supports.

8.0 References

Ahluwalia, H. S., 2006. *CUI: An In Depth Analysis.* [Online]
Available at: https://insulation.org/io/articles/cui-an-in-depth-analysis/
[Accessed 16th January 2021].

Ahmad, Z., 2006. *Principles of Corrosion Engineering and Corrosion Control.* 1st ed. Oxford: Elservier.

Anderson, S. A., 2010. *Out of sight, out of mind?.* [Online]
Available at: https://www.intertek.com/articles/2010-08-corrosion-under-insulation/
[Accessed 20th September 2020].

API, 2011. *Damage Mechanisms Affecting fixed Equipment in the Refining Industry.* 2nd ed. Washington: API.

API, 2016. *Piping Inspection Code: In-service Inspection, Rating, Repair, and Alteration of Piping Systems.* 4th ed. Washington: API.

API, 2019. *Corrosion Under Insulation and Fireproofing.* 2nd ed. Washington: API.

Arduino, 2020. *What is Arduino?.* [Online]
Available at: https://www.arduino.cc/

Ashrafizadeh, H., Fisher, G. & McDonald, A., 2016. Thermal Spray Coatings for the Oil and Gas Industry. *Journal of Thermal Spray Technology,* Volume 25, pp. 1376-1440.

ASTM, 1995. *ASTM G4 - Standard Guide for Conducting Corrosion Tests in Field Applications.* Philadelphia: ASTM.

ASTM, 2013. *ASTM G189 - Standard Guide for Laboratory Simulation of Corrosion Under Insulation.* Philadelphia: ASTM.

Bahadori, A., 2014. *Thermal Insulation Handbook for Oil Gas, and Petrochemical Industries.* 1st ed. Oxford: Gulf Professional Publishing.

Baorong, H. et al., 2017. *The cost of corrosion in China.* [Online]
Available at: https://www.nature.com/articles/s41529-017-0005-2
[Accessed 20th September 2020].

Begg, H., 2018. *A new Corrosion Under Insualtion Test Method 1097/2018.* [Online]
Available at: https://www.twi-global.com/what-we-do/research-and-technology/research-reports/industrial-member-reports/evaluation-of-a-new-corrosion-under-insulation-test-method-1097-2018
[Accessed 7th October 2020].

Bock, P., 2015. *Preventing CUI with thermal spray metal coating new use for a traditional process,* Hooksett: Advanced Polymerics Inc..

BoilerRock, 2017. *What Do I need to know about Corrosion Under Insulation- part II.* [Online]
Available at: https://boilerrockllc.com/2017/11/28/what-do-i-need-to-know-about-corrosion-under-insulation-part-ii/
[Accessed 3rd December 2020].

Burhani, N. R. A., Muhammad, M., Ismail, M. C. & Mahed, M. A., 2016. An experimental analysis using Taguchi method in resolving the significant factors subject to corrosion under insulation. *APRN Journal of Engineering and Applied Sciences,* 11(20), pp. 11966-11970.

Burhani, N. R. A., Muhammad, M. & Rosli, N. S., 2019. Combined Experimental and Field Data Sources in aPrediction Model for Corrosion Rate under Insulation. *Sustainability,* 11(23), p. 6853.

Caines, S., Khan, F., Shirokoff, J. & Qiu, W., 2015. Experimental design to study corrosion under insulation in harsh marine environments. *Journal of Loss Prevention in the Process Industries,* Volume 33, pp. 39-51.

Climate-Data.org, 2020. *Swansea climate.* [Online]
Available at: https://en.climate-data.org/europe/united-kingdom/wales/swansea-91/
[Accessed 3rd August 2020].

Cosham, A., Hopkins, P. & Macdonald, K. A., 2007. Best Practice for the assessment of defects in pipelines - Corrosion. *Engineering Failure Analysis,* 14(7), pp. 1245-1265.

DBK, 2020. *PTC Heating Technology.* [Online]
Available at: https://www.dbk-group.co.uk/ptc-heating

Department for Environment Food & Rural Affairs, 2020. *UKEAP: Precip-Net.* [Online]
Available at: https://uk-air.defra.gov.uk/networks/network-info?view=precipnet
[Accessed 20th December 2020].

Department of Enery and Climate Change, 2009. *Offshore Energy SEA APPENDIX 3f - CLIMATE AND METEOROLOGY.* [Online]
Available at:
https://assets.publishing.service.gov.uk/government/uploads/system/uploads/attachment_data/file/194346/OES_A3f_Climate_Meteorology.pdf
[Accessed 20th December 2020].

DuBose, B., 2020. *Water Repellency Technology Mitigates Corrosion Under Insulation Risk.* [Online]
Available at: https://www.materialsperformance.com/articles/material-selection-design/2019/05/water-repellency-technology-mitigates-corrosion-under-insulation-risk
[Accessed 10th January 2021].

Edwards, R., 2013. *Aqueous Corrosion of Steel.* [Online]
Available at: https://www.corrosionengineering.co.uk/downloads/knowledge-library/aqueous-corrosion-rev0.pdf
[Accessed 18th December 2020].

Eltai, E. et al., 2016. Investigating the corrosion under insulation (CUI) on steel pipe exposed to Arabian Gulf sea water drops. *Key Engineering Materials,* Volume 689, pp. 148-153.

Fitzgerald, B. J. & Winnik, S., 2005. *A strategy for preventing corrosion under insulation on pipeline in the petrochemical industry.* [Online]
Available at:
https://www.researchgate.net/publication/293478325_A_strategy_for_preventing_corrosion_under_insulation_on_pipeline_in_the_petrochemical_industry
[Accessed 21st September 2020].

Fitzgerald, B., Winnik, S., Lazar, P. & Kay, R., 2003. *Strategies to Prevent Corrosion Under Insulation in Petrochemical Industry Piping.* [Online]
Available at:
https://www.researchgate.net/publication/254545229_Strategies_to_Prevent_Corrosion_Under_Insulation_in_Petrochemical_Industry_Piping
[Accessed 20th September 2020].

Geary, W., 2013. *Analysis of a corrosion under insulation faulire in a carbon steel refinery line,* Buxton: Health and Safety Laboratory.

Groysman, A., 2010. *Corrosion for Everybody.* New York: Springer.

Haraldsen, K., 2010. *Corrosion Under Insulation-Testing of Protective Systems at High Temperatures.* Houston, NACE.

HSE, 2013. *Corrosion under insulation of plant and pipework.* [Online]
Available at:
https://www.hse.gov.uk/foi/internalops/hid_circs/technical_general/spc_tech_gen_18.htm
[Accessed 20th September 2020].

Ifezue, D., Tobins, F. H. & Nettikaden, V. C., 2014. CUI Failure of a Hot Oil Line Due to Intermittent Operations. *Journal of Failure Analysis and Prevention,* Volume 14, pp. 13-16.

Kane, R. D., Chauviere, M. & Chustz, K., 2008. *Evaluation Of Steel And Tsa Coating In A Corrosion Under Insulation (Cui) Environment.* Louisiana, NACE.

Landolt, D., 2007. *Corrosion and Surface Chamistry of Metals.* 1st ed. Lausanne: EPFL Press.

NACE, 2010. *Control of Corrosion Under Insualtion and Fireproofing Materials - A systems Approach,* Houston: NACE International.

NACE, 2010. *Corrosion control in the refining industry.* Houston: NACE International.

NACE, 2016. *International Measures of Prevention, Application, and Economics of corrosion Technologies Study.* [Online]
Available at: http://impact.nace.org/documents/Nace-International-Report.pdf
[Accessed 20th September 2020].

NACE-Jubail, 2015. *Corrosion Under Insulation (CUI) and the Insulation System.* [Online]
Available at: http://www.nace-jubail.org/Meetings/CUI_2015/7-ROOKWOOL.pdf
[Accessed 12 October 2020].

Pojtanabuntoeng, T. et al., 2015. Influence of Drain Holes in Jacketing on Corrosion Under Thermal Insulation. *Corrosion the Journal of Science and Engineering,* 71(12), pp. 1511-1520.

Praxair, 2010. *Thermal Sprayed Aluminium (TSA) Corrosion Protection Systems for the Offshore Oil and Gas Industry.* [Online]
Available at: https://www.praxairsurfacetechnologies.com/-/media/corporate/praxairsurface/us/documents/brochures/thermal-sprayed-aluminum-coatings-for-oil-and-gas.pdf?la=en&rev=32d6b73fadde41a6b70e13660d40637e
[Accessed 28th October 2020].

Rasmussen, S., 2017. *Cyclic CUI Testing of Insulation Materials.* Houston, NACE.

Reichert, D., 1998. Corrosion of carbon steel under wet insulation. *Materials Performance,* 37(5), p. 73.

Schmitz, K. S., 2017. *Phyical Chemistry Concepts and Theory.* Oxford: Elservier.

Tang, J. Q., Gong, J. M. & Jiang, Y. J., 2012. Studies on CUI of Carbon Steel in Simulation Environment Containing Chloride and Sulfur at 80°C. *Advanced Material Research,* Volume 509, pp. 166-170.

U.S. Department of Energy , 2012. *Insulate Steam Distribution and Condensate Return Lines.* [Online]
Available at: https://www.energy.gov/sites/prod/files/2014/05/f16/steam2_insulate.pdf
[Accessed 20th September 2020].

Uhlig, H. H., 1949. *The Cost of Corrosion to The United States.* [Online]
Available at: https://corrosionjournal.org/doi/10.5006/0010-9312-6.1.29
[Accessed 20th September 2020].

Welsh Water, 2020. *In Your Area.* [Online]
Available at: https://inyourarea.digdat.co.uk/dwrcymru#
[Accessed 20th September 2020].

Winnik, S., 2008. *Corrosion-under-insulation (CUI) guidelines.* 1st ed. Cambridge: Woodhead Publishing Material.

Zwaag, C. & Rasmussen, S. N., 2018. *Mineral wool and water repellency.* s.l., Nace International.

9.0 Appendices

9.1 Appendix 1 – Project Plan (Gantt Chart)

Major Project M7X01373 - Project Plan

James Milling 1503259

Project Start Date 05/05/2020

	TASK	START	END	DAYS	%DONE
1	**Project Proposal**		-		
1.1	Project meeting	Tue 5/05/20	Tue 5/05/20	1	100%
1.2	Project topic research	Sat 5/09/20	Thu 5/28/20	20	100%
1.3	Submit project proposal	Tue 6/02/20	Tue 6/02/20	1	100%
2	**Project Development**		-		
2.1	Literature Review (1)	Sun 5/10/20	Thu 11/05/20	180	100%
2.2	Draft problem definition, aim, objectives and reasons	Sat 6/27/20	Sun 6/28/20	2	100%
2.3	Project Meeting	Thu 7/02/20	Thu 7/02/20	1	100%
2.4	Finalise problem definition, aim, objectives and reasons	Sat 7/11/20	Sun 7/12/20	2	100%
2.5	Project meeting	Thu 7/30/20	Thu 7/30/20	1	100%
3	**Project Implementation**				-
3.1	Draw up experimentation design	Sat 8/01/20	Sun 8/30/20	30	100%
3.2	Source sample materials	Sat 9/12/20	Fri 10/02/20	21	100%
3.3	Source experiment apparatus	Sat 8/29/20	Fri 10/02/20	35	100%
3.4	Design and test Arduino scripts	Sat 8/15/20	Wed 9/23/20	40	100%
3.5	Prepare experiment samples	Sat 10/03/20	Sun 10/04/20	2	100%
3.6	Prepare experiment apparatus	Sat 9/19/20	Sun 10/04/20	16	100%
3.7	Project meeting	Wed 9/23/20	Wed 9/23/20	1	100%
4	**Experimentation Period**				-
4.1	12 week experiment period	Mon 10/05/20	Mon 12/28/20	85	100%
5	**Interim Report**		-		
5.1	Project meeting	Wed 10/28/20	Wed 10/28/20	1	100%
5.2	Draft interim report	Sat 10/31/20	Sun 11/29/20	30	100%
5.3	Draft interim presentation	Wed 11/28/20	Wed 11/29/20	2	100%
5.4	project meeting	Wed 11/25/20	Wed 11/25/20	1	100%
5.5	Finalise interim report	Mon 11/30/20	Thu 12/10/20	11	100%
5.6	Finalise interim presentation	Sat 12/05/20	Sun 12/06/20	2	100%
5.7	Present interim viva	Wed 12/09/20	Wed 12/09/20	1	100%
5.8	Submit interim report	Fri 12/11/20	Fri 12/11/20	1	100%
6	**Sample Analysis**		-		
6.1	Remove experiment samples	Tue 12/29/20	Tue 12/29/20	1	100%
6.2	Record observations	Tue 12/29/20	Wed 12/30/20	2	100%
6.3	Prepare for laboratory analysis	Tue 12/29/20	Sun 1/03/21	6	100%
6.4	Undertake laboratory analysis	Mon 02/15/21	TFri 04/02/21	15	100%
7	**Final Report**		-		
7.1	Literature Review (2)	Mon 1/04/21	Sat 4/03/21	90	100%
7.2	Project meeting	Fri 03/05/21	Fri 03/05/21	1	100%
7.3	Draft final report	Sat 1/23/21	Tue 3/23/21	60	100%
7.4	Draft final presentation	Sat 3/20/21	Tue 3/23/21	4	100%
7.5	project meeting		-	1	0%
7.6	Finalise final report	Sat 3/20/21	Tue 4/13/21	25	100%
7.7	Finalise final presentation	Sat 4/10/21	Tue 4/13/21	4	100%
7.8	Submit final report	Fri 4/16/21	Fri 4/16/21	1	100%
7.9	Present final viva	tbc	-	1	0%

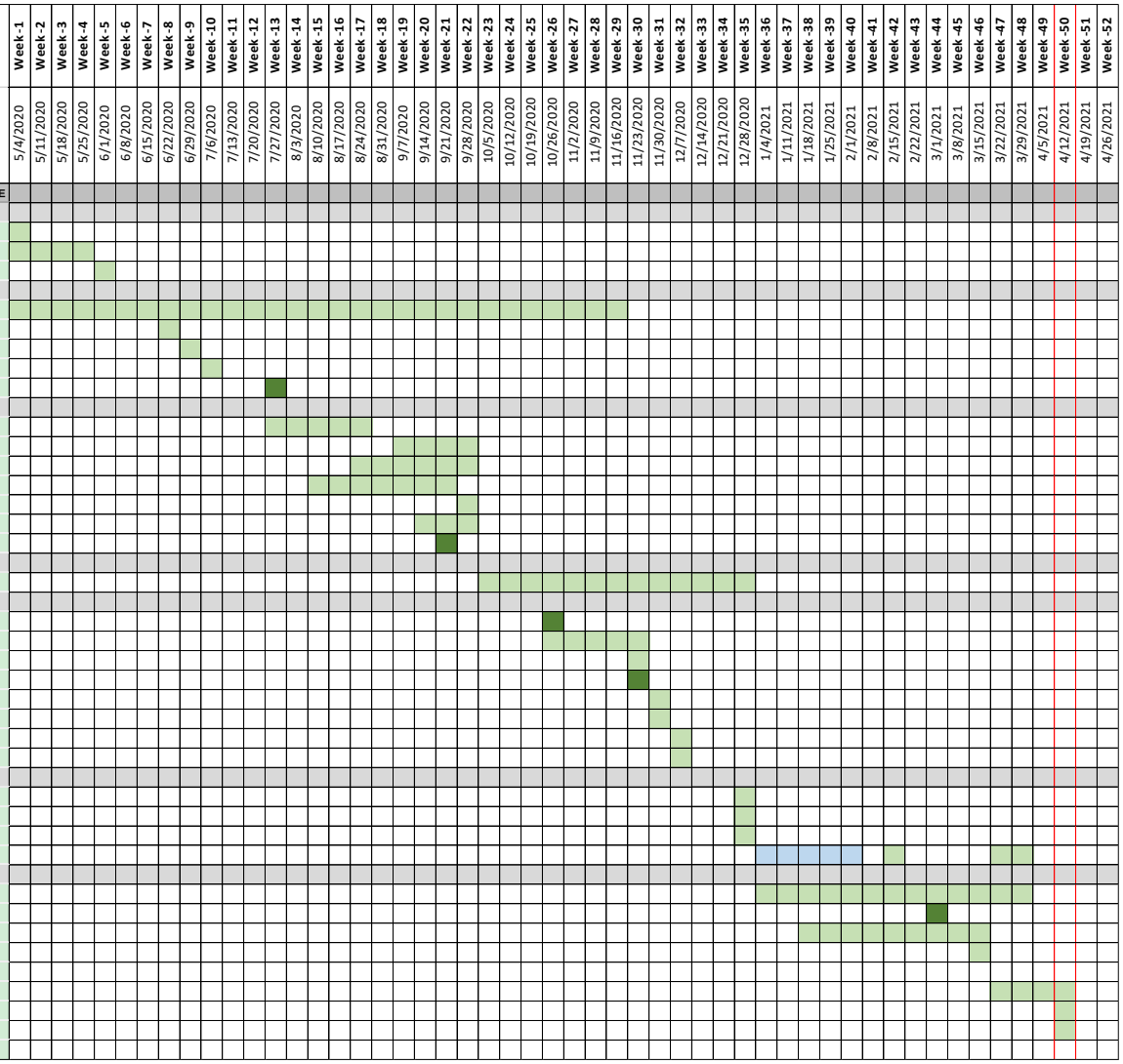

9.2 Appendix 2 – Steel tube: Tata Steel Install Plus S235GT

TATA STEEL

TATA

Install® Plus: Technical delivery conditions

S235GT multi-certified, hot-finished tube

Install® Plus multi-certified, hot-finished tube has been specifically developed to satisfy a wider range of building, engineering and industrial pipework applications.

Install® Plus is the perfect replacement for BS1387, which is now a withdrawn, unsupported standard that does not allow CE marking or satisfy the Construction Products Regulations (CPR).

Maximum flexibility

Tata Steel now satisfy the requirements of the new EN10255 S235GT grade, as well as EN10217-2 P235GH and many other applicable standards.

This provides maximum flexibility in meeting a wider range of customer pipework requirements (please refer to the relevant technical datasheet for full details).

Many advantages

- Hot-finished for consistent mechanical performance and improved ductility.
- Suitable for welding, threading, bending, grooving or flaring.
- Suitable from -20 to 300°C.
- CPR-CE marked CAT3 & 4.
- New Tata Steel red paint for enhanced corrosion protection.
- Covers a wider range of applicable industrial standards.

Table 1

Summary of chemical composition (ladle analysis) and mechanical properties

Steel Grade	Chemical Composition %				Mechanical Properties		
Steel Name	C max	Mn max	P max	S max	Upper Yield Strength R_{eH} min (MPa)	Tensile Strength R_m (MPa)	Elongation A min %
S235GT/P235GH	0.16	1.2	0.025	0.020	235	360 to 500	27

Table 2

Install® Plus tube data

OD	Nominal bore		Outside diameter		Wall thickness	Heavy weight Weight per metre		Wall thickness	Medium weight Weight per metre	
	NB		OD		T	Plain end/ grooved tube	Screwed & socketed	T	Plain end/ grooved tube	Screwed & socketed
	(mm)	(inch)	Max (mm)	Min (mm)	(mm)	(kg/m)	(kg/m)	(mm)	(kg/m)	(kg/m)
21.3	15	½	21.8	21.0	3.2	1.44	1.45	2.6	1.21	1.22
26.9	20	¾	27.3	26.5	3.2	1.87	1.88	2.6	1.56	1.57
33.7	25	1	34.2	33.3	4.0	2.93	2.95	3.2	2.41	2.43
42.4	32	1¼	42.9	42.0	4.0	3.79	3.82	3.2	3.10	3.13
48.3	40	1½	48.8	47.9	4.0	4.37	4.41	3.2	3.56	3.60
60.3	50	2	60.8	59.7	4.5	6.19	6.26	3.6	5.03	5.10
76.1	65	2½	76.6	75.3	4.5	7.93	8.05	3.6	6.42	6.54
88.9	80	3	89.5	88.0	5.0	10.30	10.50	4.0	8.36	8.53
114.3	100	4	115.0	113.1	5.4	14.50	14.80	4.5	12.20	12.50
139.7	125	5	140.8	138.5	5.4	17.90	18.40	5.0	16.60	17.10
165.1	150	6	166.5	163.9	5.4	21.30	21.90	5.0	19.80	20.40

For larger Install® Plus XL EN10255 sizes, please refer to our Inline® product literature for full details.

www.tatasteelconstruction.com

Withdrawal of BS1387

Please ensure that any pipework specifications are updated to reference the correct standard, EN10255. Otherwise, there is a risk that you may be exposed to poor quality, non-compliant material.

Tubes to BS1387 were typically made to a strength level of 195MPa. Our multi-certified 'gaslist' tube has always been produced to a 235MPa minimum strength. Therefore, we are fully aligned with the new EN10255 S235GT grade.

Weld seam integrity

Install® Plus tube is subjected to a standard regime of non destructive and destructive testing to ensure specified properties are achieved.

For sizes ≤ OD165.1mm weld seam integrity is demonstrated by both Eddy Current (EC to EN ISO10893-2) and Ultrasonic Test (UT to EN ISO10893-11).

Hydrostatic testing is used for sizes ≥ OD 219.1mm (please refer to our manufacturing technical data sheet for full details).

Coating options

Install® Plus can be supplied coated with a new and improved Tata Steel Red paint, which delivers an enhanced corrosion resistance performance compared to previous transit protection coatings.

Galvanized tubes are supplied to EN10240 (qualities B.2 or A.1) or EN ISO1461 (please refer to the relevant technical datasheet for full details).

Extruded polymer and epoxy coatings are also available; please reference the relevant data sheet or contact us for additional details.

End finishes

Install® Plus tube is available with plain, grooved or screwed & socketed (taper/parallel joints) ends. All ends are square, and free from excessive burrs or projections.

Pressure ratings

The higher 235MPa strength of Install® Plus compared to the traditional 'gaslist' 195MPa provides greater pressure integrity and mechanical performance (please refer to our pressure ratings technical datasheet for full details).

Weight & cost savings

Our fully traceable 235MPa steel also provides the opportunity for cost and weight savings through using a stronger medium weight instead of a traditional 195MPa heavy thickness.

Application compatibility

Install® Plus tube is suitable for pipework conveying a wide range of gases and fluids etc. Please refer to our tube compatibility technical data sheet or contact one of our Customer Technical Services experts for additional information.

Tube mechanical suitability

Unlike some cold formed tube, Install® Plus hot-finished tube is suitable for threading, grooving, bending and flaring and is fully compatible with commercially available fittings.

Hot-finished advantages

These have no Heat Affected Zone (HAZ) at the weldline, are fully normalised, stress free, deliver improved ductility and have consistent mechanical properties when compared to cold formed tubes. Please refer to our mechanical suitability technical datasheet.

European Directives

Install® Plus products to EN10255 have been prepared in accordance with the Construction Products Regulations (CPR) (Regulation (EU) 305/11).

CE marking and DOP

Install® Plus tube is CPR-CE marked to both CAT3 (fuel, gas and air) and CAT4 (water), and has a Declaration of Performance (DOP) thereby satisfying the requirements of the CPR in full.

To obtain a copy of the DOP, please refer to our website, or contact one of our Customer Technical Services (CTS) experts.

Test certification

Install® Plus tube is subject to non-specific inspection and testing in accordance with EN10204 and can be supplied with either a 2.1 type Certificate of Compliance or a 2.2 test report if requested prior to manufacture.

A Tata Steel 2.2 test report shows the chemical composition (ladle analysis) of the steel supplied together with a tensile test result (yield strength, tensile strength and elongation) representative of the product.

Multi-certification

Install® Plus is manufactured in accordance with the new EN10255 S235GT requirements and also EN10217-2 P235GH, enabling harmonisation with the requirements of both the CPR and the PED.

As a result of our manufacturing and testing regimes we are therefore also able to refer to additional tube standards which are directly or generally equivalent, please refer to the relevant technical datasheet for full details.

Quality Assurance

Tata Steel operates a Quality Assurance system conforming to EN ISO9001 and Annex I clause 4.3 of Directive 2014/68/EC (the Pressure Equipment Directive, or PED).

Temperature range

Install® Plus tube is suitable for use from -20 to +300°C, and is supplied in accordance with EN10217-2, with guaranteed mechanical properties in accordance with Table 5 up to and including 300°C.

www.tatasteelconstruction.com

Tata Steel
P. O. Box 101, Weldon Road,
Corby, Northants, NN17 5UA
United Kingdom
T: +44 (0) 1536 402121

Tubes Technical Helpline
T: +44 (0) 1536 404561
F: +44 (0) 1536 404111
E: technicalmarketing@tatasteel.com

Trademarks of Tata Steel
Install is a registered trademark of Tata Steel.

While care has been taken to ensure that the information contained in this publication is accurate, neither Tata Steel Europe Limited, nor its subsidiaries, accept responsibility or liability for errors or for information that is found to be misleading.

Copyright 2014 Tata Steel Europe Limited

Tata Steel Europe Limited is registered under number 05957565 with registered office at 30 Millbank, London, SW1P 4WY.

Language English TST61:PDF:ENG:0914

9.3 Appendix 3 – Rock Mineral Fibre Insulation: Knauf HPS 035 AluR

KNAUF INSULATION
Technical Solutions

December 2014

Pipe section HPS 035 AluR

Description

The mineral fibre pipe sections HPS 035 AluR are wound and ground, non-flammable pipe sections made from Rock Mineral Wool.

The product has a jacket made from glass-fibre reinforced aluminium and is equipped with a self-adhesive closure in the longitudinal direction.

Optimum insulating properties due to especially low thermal conductivity and high-precision shape as well as optimised concentricity are ensured by the modern production method with minimum production tolerances.

Purpose of use

HPS 035 AluR pipe sections are especially suitable for thermal insulation and also have positive characteristics with regard to diminution of unwanted noise.

Due to the optimised thermal conductivity, if properly dimensioned by the user, the product meets the requirements of the German energy-saving ordinance (EnEV, Deutschland).

This makes it easy to use in a legally compliant manner in domestic installations.

Certification

As the basis for the CE labelling, the HPS 035 AluR pipe sections fulfill all criteria of the harmonised product standard EN 14303. In particular the thermal conductivity and the characteristics of the product in case of fire are therefore tested and certified according to the latest standards.

Characteristics

Fire behaviour

HPS 035 AluR pipe sections are non-flammable, class A2 or A2L according to DIN EN 13501-1

Thermal conductivity

HPS 035 AluR have excellent thermal insulation characteristics.

For the core field of application in heating and plumbing installations, the product provides a thermal conductivity (as per EnEV) of 0.035 W/mK at a mean temperature of 40°C

(see table on page 2).

Advantages

- Very good thermal insulation
- Non-flammable
- Easy to install
- Can be subjected to point loads and is inherently stable
- Tear-resistant tough surface
- Attractive aluminium appearance
- Water-repellant
- Resistant to ageing
- Marine certified

Pipe Section HPS 035 AluR

Values tested and declared according to DIN 14303										CE
Property	Symbol	Description / Data							Unit	Test method / Standard
Thermal conductivity	ϑ_m	10	50	100	150	200	250		°C	EN ISO 8497
	λ_ϑ	0,033	0,037	0,044	0,052	0,062	0,073		W/(m·K)	
Reaction to fire*	--	A2-s1, d0 $D_a \leq 300$mm	A2-s1, d0 $D_a > 300$mm						--	EN 13501-1
Water vapour diffusion resistance value	μ	100							m	EN 13469
ASQuality (part of water soluble chloride ions)	--	≤ 10							mg/kg	EN 13468 AGI Q132
Maximum service temperature	ST(+)	fibre side ≤500, aluminium side ≤80							°C	EN 14707
Silicone free	--	Produced without addition of silicone oil							--	--
Hydrophobizing	W_p	water absorption ≤ 1,0 kg/m²							--	EN 13472

* depending on outside diameters

Product range

Internal diameter:	15 – 324 mm
Insulation thickness:	20 – 120 mm
Length:	1200 mm
Transport volume:	0.192 m³ per carton

For information about the packaging sizes for each dimension please refer to the current price list. Special sizes or packages on request.

Processing and storage

The packaging has been optimised for handling in the usual construction site environments. Ergonomically positioned carrying handles and a re-closable cover facilitate processing on site.

Cutting to length, fitting and assembly can be easily carried out with the usual equipment.

Note: Do not store outdoors!

KTS TDS HPS035AluR WS3-1015AUX

Knauf Insulation Ltd
PO Box 10
Stafford Road
St Helens
Merseyside
WA10 3NS

Customer Service (sales)
Tel: 0844 800 0135

Technical Advice and Support Centre
Tel: 01744 766 666

Literature
Tel: 08700 668 660

Headoffice Technical Solutions Europe
Knauf Insulation GmbH
Parkring 15-17
D-85748 Garching bei München

Production plant
Knauf Insulation d.o.o.
Novi Marof
Croatia

EC Certificate of Conformity: 0751-CPD.2-005.0-02

MW-EN14303-T8-ST(+)500-WS1-MV1-CL10
(outside diameter < 150 mm)
MW-EN14303-T9-ST(+)500-WS1-MV1-CL10
(outside diameter ≥ 150 mm)

www.knaufinsulation-ts.com

All rights reserved, including those of photomechanical reproduction and storage in electronic media. Commercial use of the processes and work activities presented in this document is not permitted. Extreme caution was observed when putting together the information, texts and illustrations in this document. Nevertheless, errors cannot quite be ruled out. The publisher and editors cannot assume legal responsibility or any liability whatever for incorrect information and the consequences thereof. The publisher and editors will be grateful for improvement suggestions and details of errors pointed out.

9.4 Appendix 4 – Glass Wool Insulation: Isover CLIMPIPE Section Alu2

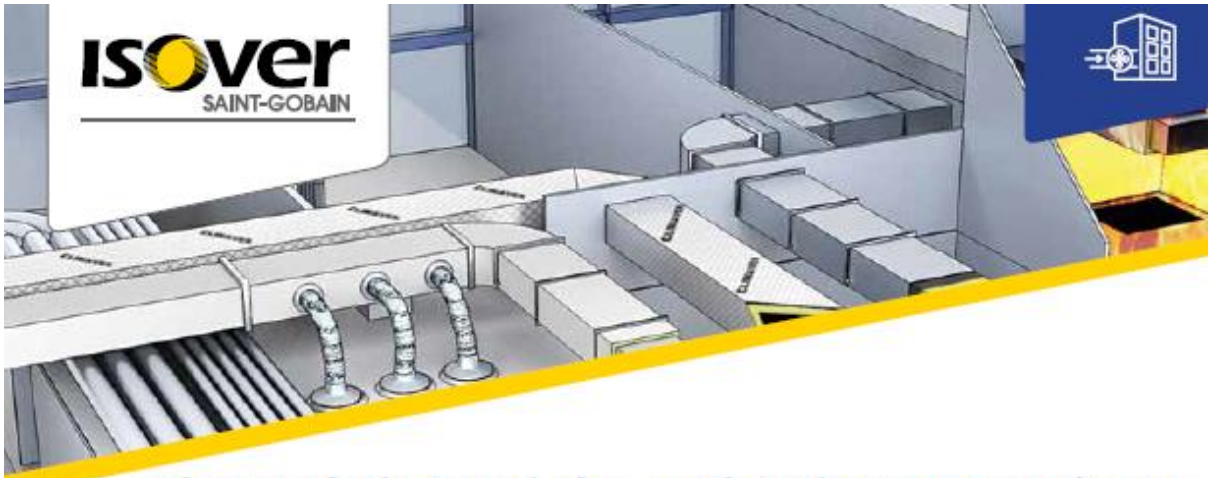

CLIMPIPE Section Alu2

Glasswool Alu-Faced pipe sections for HVAC, Marine or Industry applications

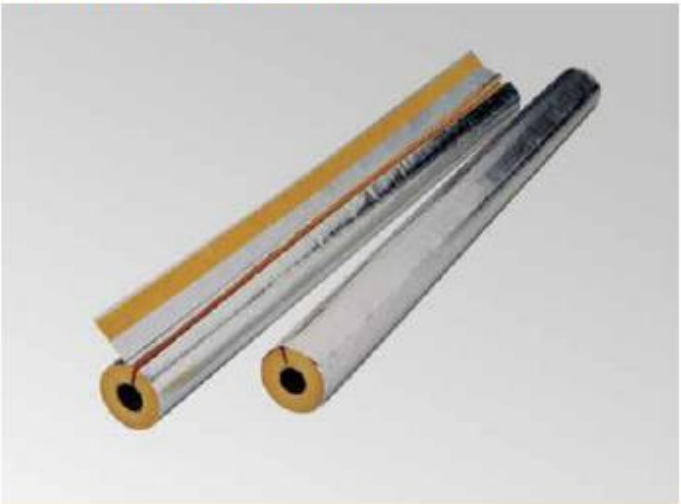

CLIMPIPE pipe solutions provides an easy to install, lightweight and efficient solution for thermal and acoustic insulation in HVAC pipe systems.

ISOVER CLIMPIPES provides topclass thermal insuLation for hot water and heating pipes. Alufacing provides efficient water vapour barrier when intact and seems carefully taped.

CLIMPIPE Sections are manufactured from inorganic chemically biosoluble materials and do not include anything that would have effect on corrosion and shall not facilitate microbial growth.

THERMAL INSULATION
High class insulation keeps the medium temperature as designed and secures system operating with minimal losses

SOUND ABSORPTION
Superior acoustic protection to reduce noise transmission through the duct- or pipework system

FAST INSTALLATION
Thanks to its light weight and high flexibility, it can be installed by one person without any special equipment

CLIMPIPE Section Alu2

Characteristic	Symbol	Unit	Quantities and declared values						Standard
Thermal conductivity	T	[°C]	10	50	100	200	300	400	EN 12667
	λ	[W/(m·K)]	0.033	0.036	0.043	0.062	0.092	0.130	
Thermal behaviour	T	[°C]	< 550 °C (tape and alu-facing 80 °C)						EN 14706

Characteristic	Symbol	Unit	Quantities and declared values	Standard
Reaction to fire	-	-	Non-combustible, Euroclass $A2_L$-s1,d0	EN 13501-1
Application field	-	-	ISOVER CLIMPIPE Section provides topclass thermal insuLation for hot water and heating pipes Alufacing provides efficient watervapour barrier when intact and seams carefully taped	-
Water behaviour	-	-	Hydrophobic	EN 12086
CE marking			MW-EN14303-T8-ST(+)500-MV2 MW-EN14303-T9-ST(+)500-MV2	EN 14303
Quality management	-	-	ISOVER is certified according to EN ISO 9001 and EN ISO 14001	EN ISO 9001 EN ISO 14001

www.isover-technical-insulation.com

The technical information corresponds to our present state of knowledge and experience at the date of printing (see imprint). But no legal guarantee can be given, unless it has been explicitly agreed. The state of experience and knowledge is developing continuously. Please see to it that you always use the latest edition of this information. The described product applications do not take special circumstances in consideration. Please verify whether our products are appropriate for the concrete application. For further information please contact our Isover sales offices. We deliver only according to our terms of trade and terms of delivery.

SAINT-GOBAIN ISOVER · "Les Miroirs" · 18, avenue d'Alsace · 92400 Courbevoie · France

9.5 Appendix 5 – Closed-Cell Elastomer Foam Insulation: Union foam Eutobatex AT

TECHNICAL DATA SHEET nº 03 - Rev. 06

EUROBATEX® AT

Type of material:	Black closed-cell flexible elastomeric foam (FEF).
Product range:	Tubes in pipe sections and coils with thicknesses from 6 to 32 mm and diameters from 10 to 114 mm. Sheets in rolls (also in a self-adhesive version) with thicknesses from 6 to 32 mm. Tapes with a thickness of 3 mm.
Fields of application:	Thermal insulation of refrigeration, air-conditioning and heating & plumbing services in commercial, industrial and domestic applications, and solar thermal systems working at high temperatures.
Dimensional tolerances:	In accordance with the European Standard EN 14304.
Environmental Information:	CFC, HCFC-free flexible and expanded rubber foam. It does not damage the ozone layer (ODP zero) and does not contribute to the greenhouse effect (GWP zero).
Additional information:	Self-adhesive material: the self-adhesive coating is based on modified acrylate; available plain or reinforced with mesh structure. Protection liner made of polytethylene or paper foil. Traces of silicon can be found on the foil protecting the self-adhesive coating.
Storage conditions/shelf life:	Store the material in a dry and clean environment at a temperature between 0 °C and 35 °C, and a RH between 50% and 70%. Do not expose the material to heat or direct sunlight before installing. Tapes and self-adhesive sheets should not be kept in storage for more than one year.

PHYSICAL PROPERTIES	RESULT OBTAINED	TEST METHOD
Operating temperature range*	Tubes -45 °C +150 °C	EN 14706/EN 14707
Thermal conductivity λ At a mean temperature of + 40 °C	≤0.042 W/m·K	EN 12667/EN ISO 8497
Water absorption	<0,1 kg/m^2	EN 13472/EN 1609
Fire performance European standard	E	EN 13501-1
Ozone resistance	Excellent	ISO 7326
UV resistance	Excellent	UNI ISO 4892-2
Antimicrobial behaviour	Meets test requirements	AATCC test method 30-2004
Corrosion risk	Meets test requirements	EN 13468

* NB: for applications at lower temperatures please contact our technical department.
For information regarding the chemical resistance of the product please consult the specific technical documentation.
For self-adhesive sheets and tapes are available adhesives with operating temperatures up to +100°C and +140°C.

System 3 CE Marking in accordance with the European Standard EN 14304.

All the normatives quoted in this document are updated to the latest issued versions.
Union Foam S.p.A. reserves the right to modify any information at any time without prior notice.

UNION FOAM

advanced elastomeric thermal and acoustic insulation materials

9.6 Appendix 6 – Portable Water Quality Reference Readings

9.6.1 Portable Water Reference Tests during Experimentation

Date	pH	Temperature (°C)	tds (mg/l)	Conductivity (µS/cm)
04/10/2020	7	13.6	70	120
11/10/2020	7	12.4	74	134
18/10/2020	7	11.8	72	144
25/10/2020	7	11.6	64	144
01/11/2020	7	11.6	66	132
08/11/2020	7	10.4	64	126
15/11/2020	7	9	63	124
22/11/2020	7	9.8	61	122
29/11/2020	7	8.2	58	116
06/12/2020	7	7.2	55	114
13/12/2020	7	6.4	57	114
20/12/2020	7	7	57	114
27/12/2020	7	6.8	53	108
Average	7	9.68	62.62	124
Median	7	9.8	63	122

Table 9.1 Portable Water Reference Tests

9.6.2 Published Portable Water Quality Data

DWR CYMRU / WELSH WATER

Drinking Water Compliance Summary

Water Quality Zone 1034 G16 Swansea / Morriston (Bryngwyn /F From 01/01/2019 To 31/12/2019

Parameter	Unit of Measurement	No. Samples Taken	Average Value	Max Value	Limit	% Compliance
Colour	Pt/Co mg/l	76	1.4539	6.30	20.00	100.00
Odour	Dilution number	76	0.0658	5.00	0.00	98.68
Taste	Dilution number	76	0.00	0.00	0.00	100.00
Hydrogen Ion Lower Minimum	pH Unit	76	7.7816	8.00	6.50	100.00
Hydrogen ion - Upper maximum	pH units	76	7.7816	8.00	9.50	100.00
Sulphate	mg/l	8	14.875	19.00	250.00	100.00
Nitrite (mg/l NO2)	mg/l	8	0.0144	0.0148	0.50	100.00
Sodium	mg/l	8	6.25	6.80	200.00	100.00
Nitrate (mg/l NO3)	mg/l	8	4.8686	12.3928	50.00	100.00
Ammonium	mg/l	8	0.0039	0.0039	0.50	100.00
Aluminium	ug/l	75	11.2627	23.00	200.00	100.00
TOTAL IRON UG/L	ug/l	76	14.1868	87.00	200.00	100.00
Manganese	ug/l	76	1.7395	5.70	50.00	100.00
Copper	mg/l	8	0.0266	0.065	2.00	100.00
Phosphorus	ug/l	8	478.75	520.00	2200.00	100.00
Fluoride	mg/l	8	0.0299	0.031	1.50	100.00
Arsenic	ug/l	8	0.1438	0.18	10.00	100.00
Cadmium	ug/l	8	0.0138	0.02	5.00	100.00
Cyanide	ug/l	8	1.90	1.90	50.00	100.00
Chromium	ug/l	8	0.115	0.13	50.00	100.00
Mercury	ug/l	8	0.0163	0.02	1000.00	100.00
Nickel	ug/l	8	0.4388	0.57	20.00	100.00
Lead	ug/l	8	0.1725	0.76	5.00	100.00
Antimony	ug/l	8	0.0488	0.05	5.00	100.00
Selenium	ug/l	8	0.0975	0.12	10.00	100.00
Enterococci	/100ml	10	0.00	0.00	0.00	100.00
Turbidity	Turbidity units	76	0.0563	0.18	4.00	100.00
Total Coliforms	/100ml	204	0.0098	2.00	0.00	99.51
Faecal Coliforms	/100ml	204	0.00	0.00	0.00	100.00
Temperature	Degrees C	204	13.3358	23.50	25.00	100.00
Conductivity	us/cm	76	124.8684	140.00	2500.00	100.00
Chloride	mg/l	8	8.25	9.00	250.00	100.00
Boron	mg/l	8	0.0229	0.041	1.00	100.00
Benzo (a) Pyrene	ug/l	8	0.0008	0.0008	0.01	100.00
Tetrachloromethane	ug/l	32	0.042	0.073	3.00	100.00
Trichloroethene	ug/l	32	0.041	0.041	10.00	100.00
Tetrachloroethene	ug/l	33	0.06	0.06	10.00	100.00
Bromate	ug/l	8	0.1375	0.32	10.00	100.00
Benzene	ug/l	9	0.03	0.03	1.00	100.00
1,2 Dichloroethane	ug/l	8	0.054	0.054	3.00	100.00
Pesticides :						
Aldrin	ug/l	30	0.002	0.002	0.03	100.00
Dieldrin	ug/l	32	0.0021	0.0021	0.03	100.00
Heptachlor	ug/l	8	0.0025	0.0025	0.03	100.00
Heptachlor Epoxide	ug/l	8	0.0057	0.0057	0.03	100.00
Mecoprop	ug/l	32	0.0026	0.0034	0.10	100.00
2-4,D	ug/l	32	0.0033	0.011	0.10	100.00
MCPA	ug/l	32	0.0063	0.032	0.10	100.00
Asulam	ug/l	33	0.0033	0.0033	0.10	100.00
Glyphosate	ug/l	32	0.0024	0.011	0.10	100.00
**Total Pesticides*	*ug/l*	*38*	*0.006*	*0.04*	*0.50*	*100.00*

Page 1 of 2

DWR CYMRU / WELSH WATER

Drinking Water Compliance Summary

Water Quality Zone 1034 G16 Swansea / Morriston (Bryngwyn /F From 01/01/2019 To 31/12/2019

Parameter	Unit of Measurement	No. Samples Taken	Average Value	Max Value	Limit	% Compliance	
Polycyclic aromatic hydrocarbons :							
Benzo 1,12 perylene	ug/l	8	0.0025	0.0025			
Benzo 3, 4 fluoranthene	ug/l	8	0.0017	0.0017			
Benzo 11,12 fluoranthene	ug/l	8	0.002	0.002			
Indeno 1,2,3-CD pyrene	ug/l	8	0.0038	0.0038			
**Total PAH*	*ug/l*	*8*	*0.000*	*0.00*	*0.20*	*100.00*	
Trihalomethanes :							
Trichloromethane	ug/l	8	10.80	17.00			
Dichlorobromomethane	ug/l	8	7.9125	11.00			
Tribromomethane	ug/l	8	0.56	0.71			
Dibromochloromethane	ug/l	8	4.65	5.40			
**Total trihalomethanes*	*ug/l*	*8*	*23.923*	*34.00*	*100.00*	*100.00*	
Total Organic Carbon	mg/l	8	0.8563	1.00			
Colony Count (2 days, 37 C)	Number per ml	1	0.00	0.00			
CHLORINE FREE (MGL)	mg/l	204	0.462	0.80			
Total chlorine	mg/l	204	0.5183	0.81			
Colony Count (3 days,22 C)	Number per ml	76	5.4737	300.00			
Trihalomethanes	ug/l	8	24.00	34.00			
Total Samples Taken		*234*					

Notes:

Where the final column contains the letters RE this indicates that an Authorisation to exceed the statutory limit has been granted.

Where the final column contains the letters UN this indicates that an Undertaking has been given by Dwr Cymru to carry out improvement work.

* When calculating these parameters in this report any result which is 'less than' the limit of analytical detection is treated as zero.

Date 10/02/2020